# Nonlinear Analysis of Rectangular Laminated Plates

Osama Mohammed Elmardi Suleiman

Professor of Mechanical Engineering, Nile Valley University, Atbara, Sudan

بسم الله الرحمن الرحيم

# Dedication

To the memory of my father, my first teacher in life.

To the memory of my mother, whose prayers and supplications to Allah were and will always be the thrust that boosts me through the thorny road of research.

To my wife, my beautiful three daughters, whose patience and silence is my shelter whenever it gets hard.

To my homeland, Sudan, hoping to contribute in its development and superiority.

# *Acknowledgement*

I am grateful and deeply indebted to professor Dr/Mahmoud Yassin Osman for close supervision, constructive criticism, and provision of useful parts of his papers and/or other relevant materials during his stay in china, and also the valuable recommendations during the various stages of building up the present book, without which this work would not have been accomplished.

I am also indebted to many people. Published texts in mechanics of materials , numerical techniques analysis have been contributed to the author's thinking. Members of mechanical engineering department at Nile valley university have served to sharpen and refine the treatment of my topics. The author is extremely grateful to them for constructive criticisms and suggestions.

Special appreciation is due to the British Council's Library for its quick response in ordering the requested reviews and papers.

Also thanks are extended to the Faculty of Engineering and Technology for enabling me to utilize its facilities in accessing the internet and printing out some papers, reviews and conference minutes concerning the present book.

Special gratitude is due to associate professor Dr/ Mohamed Ibrahim Shukri for the valuable gift 'How to write a research ' which assisted a lot in writing sequentially the present book. Thanks are also due to associate professor/Izz Eldin Ahmed Abdullah for helping with the internet.

Thanks are also due to Faculty of engineering and technology/ Nile Valley University administration for funding this research in spite of its financial hardships.

# ABSTRACT

Dynamic Relaxation (DR) method is presented for the geometrically linear and nonlinear laterally loaded, rectangular laminated plates. The analysis uses the Mindlin plate theory which accounts for transverse shear deformation. A computer program has been compiled. The convergence and accuracy of the DR solutions for elastic small and large deflection response are established by comparison with various exact and approximate solutions. New numerical results are generated for uniformly loaded square laminated plates which serve to quantify the effects of shear deformation, material anisotropy, fiber orientation, and coupling between bending and stretching.

It was found that linear analysis seriously over-predicts deflections of plates. The shear deflection depends greatly on a number of factors such as length/ thickness ratio, degree of anisotropy and number of layers. It was also found that coupling between bending and stretching can increase or decrease the bending stiffness of a laminate depending on whether it is positive or negative.

# ملخّــص


في هذا الكتاب تم استخدام اسلوب الاسترخاء الديناميكي (**DR**) للتحليل الخطي واللا خطي للألواح الشرائحية المستطيلة المسلط عليها حمل عرضي موزّع بانتظام. يستخدم التحليل نظرية مندلين للألواح ( **Mindlin plate theory**) التي تتضمن تأثيرات تشوه القص المستعرض. تمّ عمل برنامج حاسوب للحل الرقمي للمعادلات الرئيسية. وقد تم التحقق من تقارب ودقة البرنامج بتحليل طيف واسع من الالواح ذات الانحرافات الصغيرة والكبيرة ومقارنتها بحلول بديلة وقد اعطى البرنامج نتائج جيدة موافقة لتلك الموجودة في الحلول البديلة. تم الحصول على نتائج رقمية جديدة لشرائح مستطيلة مسلّط عليها حمل عرضي ساكن موزّع بانتظام وذلك للتحقق من تأثير تشوهات القص المستعرض، تباين الخواص للمادة، اتجاه الالياف، والازدواج بين الانحناء والاستطالة.

وجد في هذه الدراسة ان التحليل الخطي يعطي تقديراً زائداً لانحرافات الالواح مقارنة بالتحليل اللاخطي . كما تمّ التوصل الى انّ انحراف القص يعتمد كثيراً على عدد من العوامل من بينها نسبة طول اللوح الى سمكه، درجة تباين خواص المادة وعدد الطبقات . كما وُجِد ايضاً انّ تأثير الازدواج بين الانحناء والاستطالة يمكن ان يزيد او يقلّل كزازة الانحناء للشرائح اعتماداً على ما إذا كان الازدواج موجباً ام سالباً.

# Contents

# List of figures

# List of tables

# List of abbreviations

| | |
|---|---|
| DR | Dynamic Relaxation |
| CLPT | Classical Laminated Plate Theory |
| FSDT | First order Shear Deformation Theory |
| HSDT | Higher order Shear Deformation Theory |
| L | Linear |
| NL | Non-Linear |
| GFRP | Glass Fiber Reinforced Plate |
| SCF | Shear Correction Factor |
| NOL | Number Of Layers |

# Notations

| | |
|---|---|
| $a$ | Plate length. |
| $A_{ij}(i,j=1,2,6)$ | Plate in-plane stiffnesses. |
| $A_{ij}(i,j=4,5)$ | Plate transverse shear stiffnesses. |
| $b$ | Plate breadth. |
| $B_{ij}(i,j=1,2,6)$ | Plate coupling stiffnesses. |
| $D_{ij}(i,j=1,2,6)$ | Plate flexural stiffnesses. |
| $E_1,E_2,G_{12}$ | Longitudinal, transverse, and in-plane shear moduli of a lamina. |
| $G_{13},G_{23}$ | Transverse shear moduli in the x – z and y – z planes, respectively. |
| $Z_k$ , $Z_{k+1}$ | Distance of upper and lower surfaces of the lamina from the plate mid-plane. |
| $h$ | Plate thickness. |
| $k$ | Lamina number. |
| $K_4^2, K_5^2$ | Shear correction factors. |
| $M_1, M_2, M_6$ | Stress couples. |
| $\overline{M}_1\left(=M_1a^2E_2^{-1}h^{-4}\right), \overline{M}_2, \overline{M}_6$ | Dimensionless stress couples. |
| $n$ | Number of layers. |
| $N_1, N_2, N_6$ | Stress resultants. |
| $\overline{N}_1\left(=N_1a^2E_2^{-1}h^{-3}\right), \overline{N}_2, \overline{N}_6$ | Dimensionless stress resultants. |
| $q$ | Transverse pressure. |
| $\overline{q}\left(=qa^2E_2^{-1}h^{-4}\right)$ | Dimensionless Transverse pressure. |
| $Q_1, Q_2$ | Transverse shear resultants. |
| $u$ ,$v$ | In-plane displacements. |
| $w$ | Deflections. |
| $\overline{w}\left(=wh^{-1}\right)$ | Dimensionless deflections. |
| $x$ ,$y$ ,$z$ | Cartesian co-ordinates. |
| $\delta t$ | Time increment. |
| $\varepsilon_1^o, \varepsilon_2^o, \varepsilon_6^o$ | Extensional and shear strain components of plate mid-plane. |
| $\varepsilon_5^o, \varepsilon_4^o$ | Transverse shear strain components of plate mid-plane. |
| $\phi, \psi$ | Rotations of the original normal to the plate mid-plane. |
| $\nu_{12}$ | Poisson's ratio. |
| $\rho_u, \rho_v, \rho_w, \rho_\phi, \rho_\psi$ | In-plane, out-of-plane and rotational fictitious densities. |
| $\chi_1^o, \chi_2^o, \chi_6^o$ | Curvature and twist components of plate mid-plane. |
| Subscripts 1,2,3,4,5,6 | Denote *x*, *y*, *z*, *yz*, *xz*, *xy*. |

# Preface

The objective of this book is to present a complete and up to date treatment of rectangular laminated plates with uniform cross sections. Dynamic relaxation (DR) method coupled with finite differences procedures is used for solving governing equations of small and large deflection composite plates and their solutions using first order shear deformation (FSDT) theory. Plates are common structural elements of most engineering structures, including aerospace, automotive, and civil engineering structures, and their study from theoretical and analysis points of view is fundamental to the understanding of the behavior of such structures.

The motivation that led to the writing of the present book has come from many years of studying first order shear deformation theory and its analysis by the finite differences and dynamic relaxation methods, and also from the fact that there does not exist a book that contains a detailed coverage of shear deformation plate theory, and finite differences mixed with dynamic relaxation model in one volume. The present book fulfills the need for a complete treatment of first order shear deformation theory of plates and its solution by a numerical method.

The material presented is intended to serve as a basis for a critical study of the fundamental of elasticity and several branches of solid mechanics including advanced mechanics of materials, theories of plates, composite materials and numerical methods. Chapter one includes certain properties of laminated plates, and at the end of this chapter the most important objectives of the book are cited, this subject may be used either as a required reading or as a reference subject. The mathematical modeling of the plates for both linear and nonlinear theories is presented in chapter two. In chapter three a powerful numerical technique which could be applied for all types of analysis i.e. linear and nonlinear, various number and angle of plies, different boundary conditions and uniform transverse loading is presented. The present DR results are validated with similar results generated by DR and/or other numerical and approximate analytical solutions in chapter four. In chapter five, the effects of transverse shear deformation, material anisotropy, orientation, and coupling between

stretching and bending on the deflections of laminated plates are investigated. Chapter six is dedicated to the conclusions and suggestions for further research.

The book is suitable as a textbook for a first course on theory of plates and dynamic relaxation technique in civil and mechanical engineering curricula. It can be used as a reference by engineers and scientists working in industry and academic institutions.

Osama Mohammed Elmardi
Mechanical Engineering Department,
Nile valley university, Atbara, Sudan

# CHAPTER (1)

# Introduction

## 1.1 General Introduction

Composites were first considered as structural materials a little more than half a century ago. And from that time to now, they have received increasing attention in all aspects of material science, manufacturing technology, and theoretical analysis.

The term composite could mean almost anything if taken at face value, since all materials are composites of dissimilar subunits if examined at close enough details. But in modern materials engineering, the term usually refers to a matrix material that is reinforced with fibers. For instance, the term "FRP" which refers to Fiber Reinforced Plastic usually indicates a thermosetting polyester matrix containing glass fibers, and this particular composite has the lion's share of today commercial market.

Many composites used today are at the leading edge of materials technology, with performance and costs appropriate to ultra-demanding applications such as space craft. But heterogeneous materials combining the best aspects of dissimilar constituents have been used by nature for millions of years. Ancient societies, imitating nature, used this approach as well: The book of Exodus speaks of using straw to reinforce mud in brick making, without which the bricks would have almost no strength. Here in Sudan, people from ancient times dated back to Merowe civilization, and up to now used *zibala* mixed with mud as a strong building material.

As seen in Table 1.1 below, which is cited by David Roylance [54], the fibers used in modern composites have strengths and stiffnesses far above those of traditional structural materials. The high strengths of the glass fibers are due to processing that avoids the internal or surface flaws which normally weaken glass, and the strength and stiffness of polymeric aramid fiber is a consequence of the nearly perfect alignment of the molecular chains with the fiber axis.

Table 1.1 Properties of composite reinforcing fibers

| Material | E ($GN/m^2$) | $\sigma_b$ ($GN/m^2$) | $\varepsilon_b$ (%) | $\rho$ ($Mg/m^3$) | $E/\rho$ (MN.m/kg) | $\sigma_b/\rho$ (MN.m/kg) |
|---|---|---|---|---|---|---|
| E-glass | 72.4 | 2.4 | 2.6 | 2.54 | 28.5 | 0.95 |
| S-glass | 85.5 | 4.5 | 2.0 | 2.49 | 34.3 | 1.8 |
| Aramid | 124 | 3.6 | 2.3 | 1.45 | 86 | 2.5 |
| Boron | 400 | 3.5 | 1.0 | 2.45 | 163 | 1.43 |
| H S graphite | 253 | 4.5 | 1.1 | 1.80 | 140 | 2.5 |
| H M graphite | 520 | 2.4 | 0.6 | 1.85 | 281 | 1.3 |

Where E is Young's modulus, $\sigma_b$ is the breaking stress, $\varepsilon_b$ is the breaking strain, and $\rho$ is the mass density.

Of course, these materials are not generally usable as fibers alone, and typically they are impregnated by a matrix material that acts to transfer loads to the fibers, and also to protect the fibers from abrasion and environmental attack. The matrix dilutes the properties to some degree, but even so very high specific (weight – adjusted) properties are available from these materials. Polymers are much more commonly used, with unsaturated Styrene – hardened polyesters having the majority of low – to – medium performance applications and Epoxy or more sophisticated thermosets having the higher end of the market. Thermoplastic matrix composites are increasingly attractive materials, with processing difficulties being perhaps their principal limitation.

Composites possess two desirable features: the first one is high strength to weight ratio, and the second is their properties that can be tailored through variation of the fiber orientation and stacking sequence which gives the designers a wide spectrum of flexibility. The incorporation of high strength, high modulus and low-

density filaments in a low strength and a low modulus matrix material is known to result in a structural composite material with a high strength / weight ratio. Thus, the potential of a two-material composite for use in aerospace, under-water, and automotive structures has stimulated considerable research activities in the theoretical prediction of the behaviour of these materials. One commonly used composite structure consists of many layers bonded one on top of another to form a high-strength laminated composite plate. Each lamina is fiber- reinforced along a single direction, with adjacent layers usually having different filament orientations. For these reasons, composites are continuing to replace other materials used in structures such as those mentioned earlier. In fact composites are the potential structural materials of the future as their cost continues to decrease due to the continuous improvements in production techniques and the expanding rate of sales.

## 1.2 Structure of composites:

There are many situations in engineering where no single material will be suitable to meet a particular design requirement. However, two materials in combination may possess the desired properties and provide a feasible solution to the materials selection problem. A composite can be defined as a material that is composed of two or more distinct phases, usually a reinforced material supported in a compatible matrix, assembled in prescribed amounts to achieve specific physical and chemical properties.

In order to classify and characterize composite materials, distinction between the following two types is commonly accepted; see Vernon [1], Jan Stegmann and Erik Lund [5], and David Roylance [54].

1. Fibrous composite materials: Which consist of high strength fibers embedded in a matrix. The functions of the matrix are to bond the fibers together to protect them from damage, and to transmit the load from one fiber to another. See Fig.1.1.

2. Particulate composite materials: This composed of particles encased within a tough matrix, e.g. powders or particles in a matrix like ceramics.

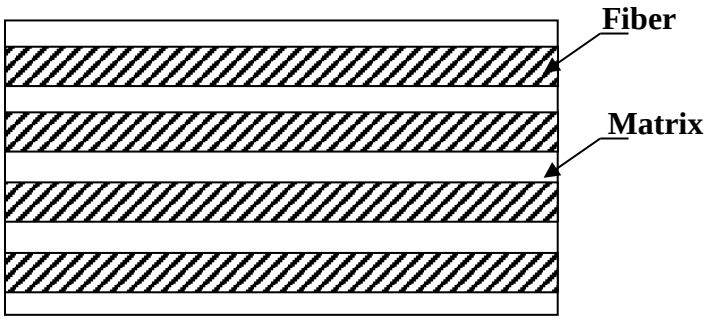


**Fig. 1.1 Structure of a fibrous composite**

In this thesis the focus will be on fiber-reinforced composite materials, as they are the basic building element of a rectangular laminated plate structure. Typically, such a material consists of stacks of bonded-together layers (i.e. laminas or plies) made from fiber-reinforced material. The layers will often be oriented in different directions to provide specific and directed strengths and stiffnesses of the laminate. Thus, the strengths and stiffnesses of the laminated fiber-reinforced composite material can be tailored to the specific design requirements of the structural element being built.

### 1.2.1 Mechanical properties of a fiber-reinforced lamina

Composite materials have many mechanical characteristics, which are different from those of conventional engineering materials such as metals. More precisely, composite materials are often both inhomogeneous and non-isotropic. Therefore, and due to the inherent heterogeneous nature of composite materials, they can be studied from a micromechanical or a macro-mechanical point of view. In micromechanics, the behaviour of the inhomogeneous lamina is defined in terms of the constituent materials; whereas in macro-mechanics the material is presumed homogeneous and the effects of the constituent materials are detected only as averaged apparent macroscopic properties of the composite material. This approach is generally accepted when modeling gross response of composite structures. The

micromechanics approach is more convenient for the analysis of the composite material because it studies the volumetric percentages of the constituent materials for the desired lamina stiffnesses and strengths, i.e. the aim of micromechanics is to determine the moduli of elasticity and strength of a lamina in terms of the moduli of elasticity, and volumetric percentage of the fibers and the matrix. To explain further, both the fibers and the matrix are assumed homogeneous, isotropic and linearly elastic.

The fibers may be oriented randomly within the material, but it is also possible to arrange for them to be oriented preferentially in the direction expected to have the highest stresses. Such a material is said to be anisotropic (i.e. different properties in different directions), and control of the anisotropy is an important means of optimizing the material for specific applications. At a microscopic level, the properties of these composites are determined by the orientation and distribution of the fibers, as well as by the properties of the fiber and matrix materials.

Consider a typical region of material of unit dimensions, containing a volume fraction, $V_f$ of fibers all oriented in a single direction. The matrix volume fraction is then, $V_m = 1 - V_f$ . This region can be idealized by gathering all the fibers together, leaving the matrix to occupy the remaining volume. If a stress $\sigma_l$ is applied along the fiber direction, the fiber and matrix phases act in parallel to support the load. In these parallel connections the strains in each phase must be the same, so the strain $\varepsilon_l$ in the fiber direction can be written as:

$$\varepsilon_l = \varepsilon_f = \varepsilon_m \tag{1.1}$$

Where the subscripts *L, f* and *m* denote the lamina, fibers and matrix respectively.

The forces in each phase must add to balance the total load on the material. Since the forces in each phase are the phase stresses times the area (here numerically equal to the volume fraction), we have

$$\sigma_l = \sigma_f V_f + \sigma_m V_m = E_f \varepsilon_l V_f + E_m \varepsilon_l V_m \tag{1.2}$$

The stiffness in the fiber direction is found by dividing the strain:

$$E_l = \frac{\sigma_l}{\varepsilon_l} = E_f V_f + E_m V_m \qquad (1.3)$$

(Where E is the longitudinal Young's modulus)

This relation is known as a rule of mixtures prediction of the overall modulus in terms of the moduli of the constituent phases and their volume fractions.

Rule of mixtures estimates for strength proceed along lines similar to those for stiffness. For instance consider a unidirectional reinforced composite that is strained up to the value at which the fiber begins to fracture. If the matrix is more ductile than the fibers, then the ultimate tensile strength of the lamina in Eqn. (1.2) will be transformed to:

$$\sigma_l^u = \sigma_f^u V_f + \sigma_m^f \left(1 - V_f\right) \qquad (1.4)$$

Where the superscript *u* denotes an ultimate value, and $\sigma_m^f$ is the matrix stress when the fibers fracture as shown in fig.1.2.

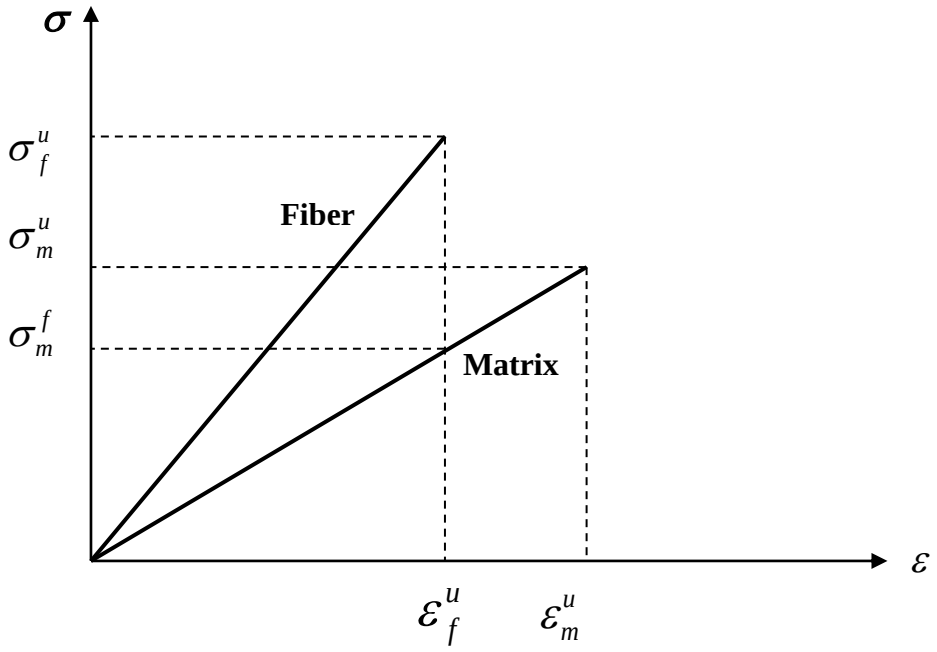


**Fig .1.2 Stress-strain relationships for fiber and matrix**

It is clear that if the fiber volume fraction is very small, the behaviour of the lamina is controlled by the matrix.

This can be expressed mathematically as follows:

$$\sigma_l^u = \sigma_m^u \left(1 - V_f\right) \qquad (1.5)$$

If the lamina is assumed to be useful in practical applications, then there is a minimum fiber volume fraction that must be added to the matrix. This value is obtained by equating equations (1.4) and (1.5) i.e.

$$V_{min} = \frac{\sigma_m^u - \sigma_m^f}{\sigma_f^u + \sigma_m^u - \sigma_m^f} \tag{1.6}$$

The variation of the strength of the lamina with the fiber volume fraction is illustrated in Fig.1.3. It is obvious that when $0 < V_f < V_{min}$ the strength of the lamina is dominated by the matrix deformation which is less than the matrix strength. But when the fiber volume fraction exceeds a critical value (i.e. $V_f > V_{Critical}$ ), Then The lamina gains some strength due to the fiber reinforcement.

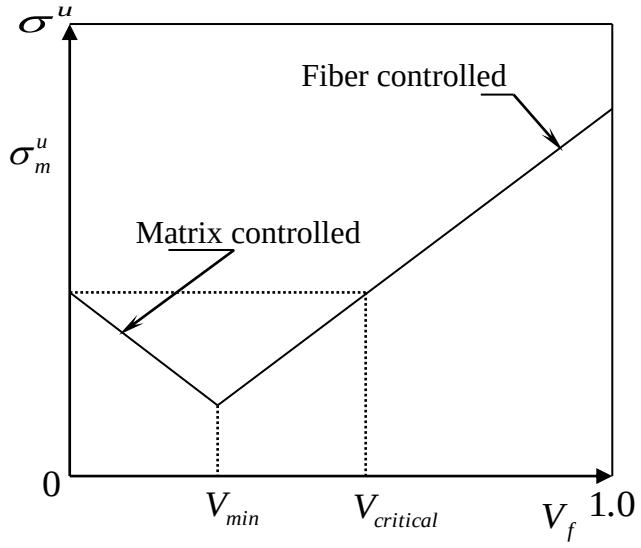


**Fig. 1.3 Variation of unidirectional lamina strength with the fiber volume fraction**

The micromechanical approach is not responsible for the many defects which may arise in fibers, matrix, or lamina due to their manufacturing. These defects, if they exist include misalignment of fibers, cracks in matrix, non-uniform distribution of the fibers in the matrix, voids in fibers and matrix, delaminated regions, and initial stresses in the lamina as a result of it's manufacture and further treatment. The above mentioned defects tend to propagate as the lamina is loaded causing an accelerated rate of failure. The experimental and theoretical results in this case tend to differ.

Hence, due to the limitations necessary in the idealization of the lamina components, the properties estimated on the basis of micromechanics should be proved experimentally. The proof includes a very simple physical test in which the lamina is considered homogeneous and orthotropic. In this test, the ultimate strength and modulus of elasticity in a direction parallel to the fiber direction can be determined experimentally by loading the lamina longitudinally. When the test results are plotted, as in Fig.1.4 below, the required properties may be evaluated as follows: -

$$E_1 = \sigma_1 / \varepsilon_1 \quad ; \quad \sigma^u = P^u / A \quad ; \quad \nu_{12} = -\varepsilon_2 / \varepsilon_1$$

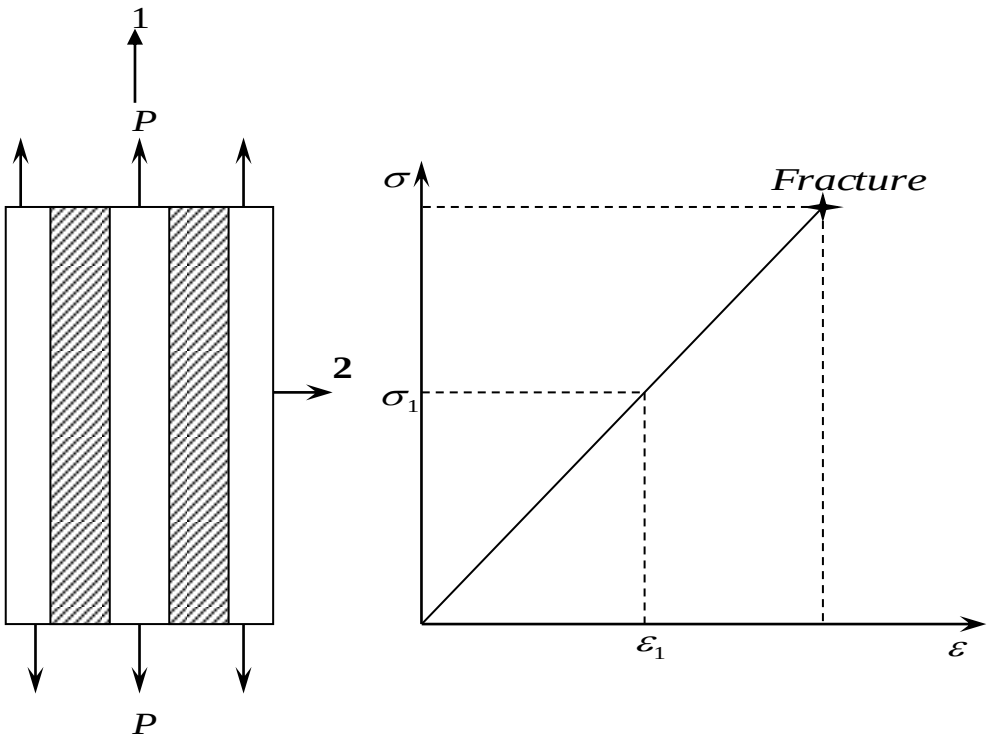


**Fig.1.4 Unidirectional lamina loaded in the fiber-direction**

Similarly, the properties of the lamina in a direction perpendicular to the fiber-direction can be evaluated in the same procedure.

### 1.2.2 Analytical modeling of composite laminates

The properties of a composite laminate depend on the geometrical arrangement and the properties of its constituents. The exact analysis of such structure – property relationship is rather complex because of many variables involved. Therefore, a few

simplifying assumptions regarding the structural details and the state of stress within the composite have been introduced.

It has been observed, that the concept of representative volume element and the selection of appropriate boundary conditions are very important in the discussion of micromechanics. The composite stress and strain are defined as the volume averages of the stress and strain fields, respectively, within the representative volume element. By finding relations between the composite stresses and the composite strains in terms of the constituent properties expressions for the composite moduli could be derived. In addition, it has been shown that, the results of advanced methods can be put in a form similar to the rule of mixtures equations.

Prediction of composite strengths is rather difficult because there are many unknown variables and also because failure critically depends on defects. However, the effects of constituents including fiber – matrix interface on composite strengths can be qualitatively explained. Certainly, failure modes can change depending on the material combinations. Thus, an analytical model developed for one material combination cannot be expected to work for a different one. Ideally a truly analytical model will be applicable to material combination. However, such an analytical model is not available at present. Therefore, it has been chosen to provide models each of which is applicable only to a known failure mode. Yet, they can explain many of the effects of the constituents. (refer to Ref. [2]).

### 1.3 Developments in the theories of laminated plates

From the point of view of solid mechanics, the deformation of a plate subjected to transverse loading consists of two components: flexural deformation due to rotation of cross-sections, and shear deformation due to sliding of sections or layers. The resulting deformation depends on two parameters: the thickness to length ratio and the ratio of elastic to shear moduli. When the thickness to length ratio is small, the plate is considered thin, and it deforms mainly by flexure or bending; whereas when the thickness to length and the modular ratios are both large, the plate deforms mainly through shear. Due to the high ratio of in-plane modulus to

transverse shear modulus, the shear deformation effects are more pronounced in the composite laminates subjected to transverse loads than in the isotropic plates under similar loading conditions.

The three-dimensional theories of laminates in which each layer is treated as homogeneous anisotropic medium (see Reddy [17]) are intractable as the number of layers becomes moderately large. Thus, a simple two-dimensional theory of plates that accurately describes the global behaviour of laminated plates seems to be a compromise between accuracy and ease of analysis.

Putcha and Reddy [10] classified the two-dimensional analyses of laminated composite plates into two categories: (1) the classical lamination theory, and (2) shear deformation theories. In both theories it is assumed that the laminate is in a state of plane stress, the individual lamina is linearly elastic, and there is perfect bonding between layers. The classical laminate theory (CLPT), which is an extension of the classical plate theory (CPT) applied to laminated plates was the first theory formulated for the analysis of laminated plates by Reissner and Stavsky [37] in 1961, in which the Kirchhoff-Love assumption that normal to the mid-surface before deformation remain straight and normal to the mid-surface after deformation is used (see Fig. 1.5), but it is not adequate for the flexural analysis of moderately thick laminates. However, it gives reasonably accurate results for many engineering problems i.e. thin composite plates, as stated by Srinivas and Rao [11] and Reissner and Stavsky [37].

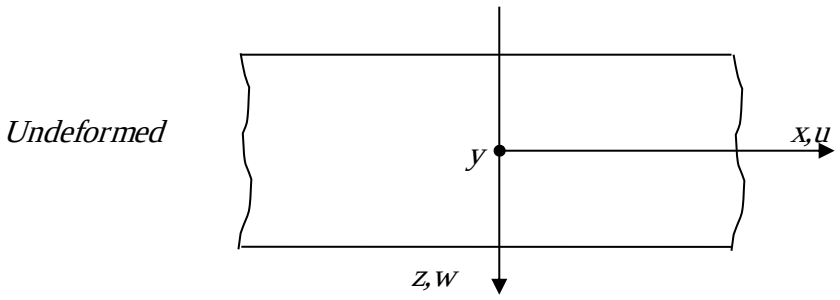


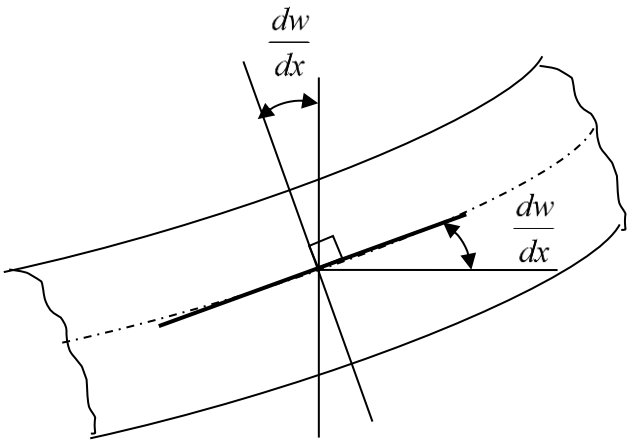


*Assumed deformation of normal (CLPT) (Shear stress neglected )*

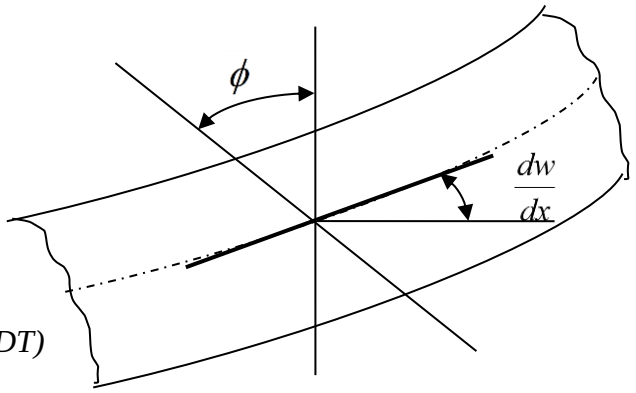


*Assumed deformation of normal (FSDT) (shear stress assumed uniform)*

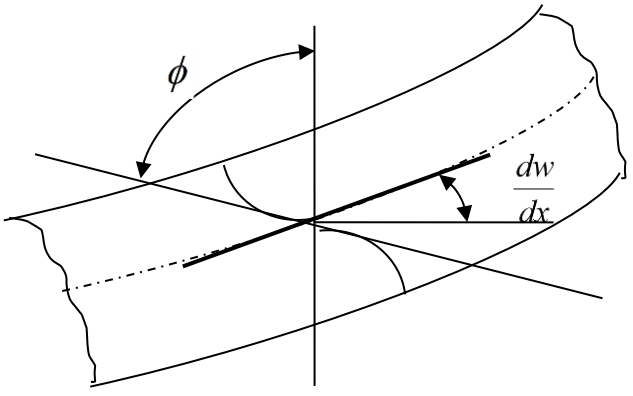


*Assumed deformation of normal (HSDT) (parabolic shear stress distribution)*

**Fig. 1.5 Assumed deformation of the transverse normal in various displacement base plate theories.**

This theory ignores the transverse shear stress components and models a laminate as an equivalent single layer. The classical laminated plate theory (CLPT) under-predicts deflections as proved by Turvey and Osman [6, 7, 8] and Reddy [17] due to the neglect of transverse shear strain. The errors in deflections are even higher for plates made of advanced filamentary composite materials like graphite -epoxy and boron-epoxy, whose elastic modulus to shear modulus ratios are very large (i.e. of the order of 25 to 40, instead of 2.6 for typical isotropic materials). However, these composites are susceptible to thickness effects because their effective transverse shear moduli are significantly smaller than the effective elastic modulus along the fiber direction. This effect has been confirmed by Pagano [40] who obtained analytical solutions of laminated plates in bending based on the three-dimensional theory of elasticity. He proved that classical laminated plate theory (CLPT) becomes of less accuracy as the side to thickness ratio decreases. In particular, the deflection of a plate predicted by CLPT is considerably smaller than the analytical value for side to thickness ratio less than 10. These high ratios of elastic modulus to shear modulus render classical laminate theory as inadequate for the analysis of composite plates.

Many theories which account for the transverse shear and normal stresses are available in the literature (see, for example Mindlin [43]) .These are too numerous to review here. Only some classical papers and those which constitute a background for the present thesis will be considered. These theories are classified according to Phan and Reddy [9] into two major classes on the basis of the assumed fields as :( 1) stress based theories, and (2) displacement based theories. The stress-based theories are derived from stress fields, which are assumed to vary linearly over the thickness of the plate:

$$\sigma_i = \frac{M_i}{\left(h^2/6\right)} \cdot \frac{z}{\left(h/2\right)} \qquad \left(i = 1,2,6\right) \tag{1.7}$$

(Where $M_i$ is the stress couples, $h$ is the plate thickness, and $z$ is the distance of the lamina from the plate mid-plane)

The displacement-based theories are derived from an assumed displacement field as:

$$u = u_o + zu_1 + z^2u_2 + z^3u_3 + ...$$
$$v = v_o + zv_1 + z^2v_2 + z^3v_3 + ... \quad (1.8)$$
$$w = w_o + zw_1 + z^2w_2 + z^3w_3 + ...$$

Where $u_o$ , $v_o$ and $w_o$ are the displacements of the middle plane of the plate.

The governing equations are derived using the principle of minimum total potential energy. The theory used in the present work comes under the class of displacement-based theories. Extensions of these theories which include the linear terms in $z$ in $u$ and $v$ and only the constant term in $w$, to account for higher -order variations and to laminated plates, can be found in the work of Yang, Norris and Stavsky [38], Whitney and Pagano [44] and Phan and Reddy [9]. In this theory which is called first-order shear deformation theory (FSDT), the transverse planes, which are originally normal and straight to the mid-plane of the plate, are assumed to remain straight but not necessarily normal after deformation, and consequently shear correction factor are employed in this theory to adjust the transverse shear stress, which is constant through thickness (see Fig. 1.5). Recently Reddy [17] and Phan and Reddy [9] presented refined plate theories that use the idea of expanding displacements in the powers of thickness co-ordinate. The main novelty of these works is to expand the in-plane displacements as cubic functions of the thickness co-ordinate, treat the transverse deflection as a function of the $x$ and $y$ co-ordinates, and eliminate the functions $u_2$ ,$u_3$ ,$v_2$ and $v_3$ from equation (1.8) by requiring that the transverse shear stresses be zero on the bounding planes of the plate. Numerous studies involving the application of the first-order theory to bending analysis can be found in the works of Reddy [22], and Reddy and Chao [23].

In order to include the curvature of the normal after deformation, a number of theories known as Higher-order Shear Deformation Theories (HSDT) have been devised in which the displacements are assumed quadratic or cubic through the thickness of the plate. In this aspect, a variationally consistent higher-order theory which not only accounts for the transverse shear deformation but also satisfies the zero transverse shear stress conditions on the top and bottom faces of the plate and

does not require shear correction factors was suggested by Reddy [17]. Reddy's modifications consist of a more systematic derivation of displacement field and variationally consistent derivation of the equilibrium equations. The refined laminate plate theory predicts a parabolic distribution of the transverse shear stresses through the thickness, and requires no shear correction coefficients.

In the non-linear analysis of plates considering higher-order theory (HSDT), shear deformation has received considerably less attention compared with linear analysis. This is due to the geometric non-linearity which arises from finite deformations of an elastic body and which causes more complications in the analysis of composite plates. Therefore fiber-reinforced material properties and lamination geometry have to be taken into account. In the case of anti-symmetric and unsymmetrical laminates, the existence of coupling between bending and stretching complicates the problem further.

Non-linear solutions of laminated plates using higher-order theories have been obtained through several techniques, i.e. perturbation method as in Ref. [45], finite element method as in Ref. [10], the increment of lateral displacement method as in Ref. [18], and the small parameter method as in Ref. [29].

In the present work, a numerical method known as Dynamic Relaxation (DR) coupled with finite differences is used. The DR method was first proposed in 1960s; see Rushton [13], Cassell and Hobbs [52], Day [53]. In this method, the equations of equilibrium are converted to dynamic equation by adding damping and inertia terms. These are then expressed in finite difference form and the solution is obtained through iterations. The optimum damping coefficient  and time increment used to stabilize the solution depend on a number of factors including the stiffness matrix of the structure, the applied load, the boundary conditions and the size of the mesh used, etc…

Numerical techniques other than the DR include finite element method, which is widely used in the literature. In a comparison between the DR and the finite element method, Aalami [56] found that the computer time required for finite element

method is eight times greater than for DR analysis, whereas the storage capacity for finite element analysis is ten times or more than that for DR analysis. This fact is supported by Putcha and Reddy [10] who noted that some of the finite element formulations require large storage capacity and computer time. Hence, due to less computations and computer time involved in the present study, the DR method is considered more efficient than the finite element method. In another comparison Aalami [56] found that the difference in accuracy between one version of finite element and another may reach a value of 10% or more, whereas a comparison between one version of finite element method and DR showed a difference of more than 15%. Therefore, the DR method can be considered of acceptable accuracy. The only apparent limitation of DR method is that it can only be applied to limited geometries. However, this limitation is irrelevant to rectangular plates which are widely used in engineering applications.

**1.4 The objectives of the present study: -**

The present work involves a comprehensive study of the following objectives, which have been achieved over a period of three years:

1. A survey of various plate theories and techniques used to predict the response of composite plates to static lateral loading.
2. The development of a theoretical model capable of predicting stresses and deformations in a laminated plate in which the shear deformation is considered for both linear and non-linear deflections.
3. The development and application of the dynamic relaxation technique for the analysis of rectangular laminated plates subjected to uniform lateral loading.
4. Investigation of the accuracy of the theoretical model through a wide range of theoretical comparisons.
5. Generation of results based on first order shear deformation theory (FSDT) for the comparison between linear and non-linear analyses.
6. Study the factors affecting the deflection of a laminated plate.

# CHAPTER (2)

# Mathematical modeling of plates

There are two main theories of laminated plates depending on the magnitude of deformation resulting from loading a plate and these are known as the linear and nonlinear theories of plates. The difference between the two theories is that the deformations are small in the linear theory, whereas they are finite or large in the nonlinear theory.

## 2.1 Linear theory:

### 2.1.1 Assumptions

1- The plate shown in Fig 2.1 is constructed of an arbitrary number of orthotropic layers bonded together as in Fig 2.2. However, the orthotropic axes of material symmetry of an individual layer need not coincide with the axes of the plate.

2- The displacements *u, v,* and *w* are small compared to the plate thickness.

3- In-plane displacements *u* and *v* are linear functions of the z-coordinate.

4- Each ply obeys Hook's law.

5- The plate is flat and has constant thickness.

6- There are no body forces such as gravity force.

7- The transverse normal stress is small compared with the other stresses and is therefore neglected.

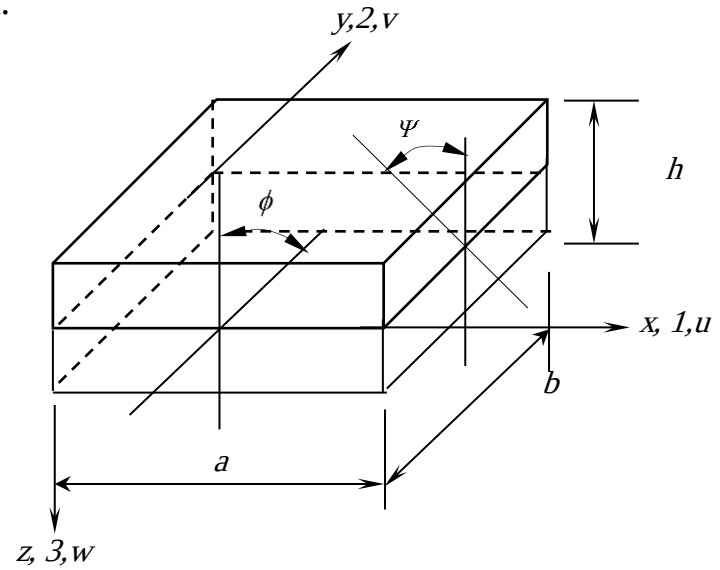


**Fig. 2.1 A plate showing dimensions and deformations**

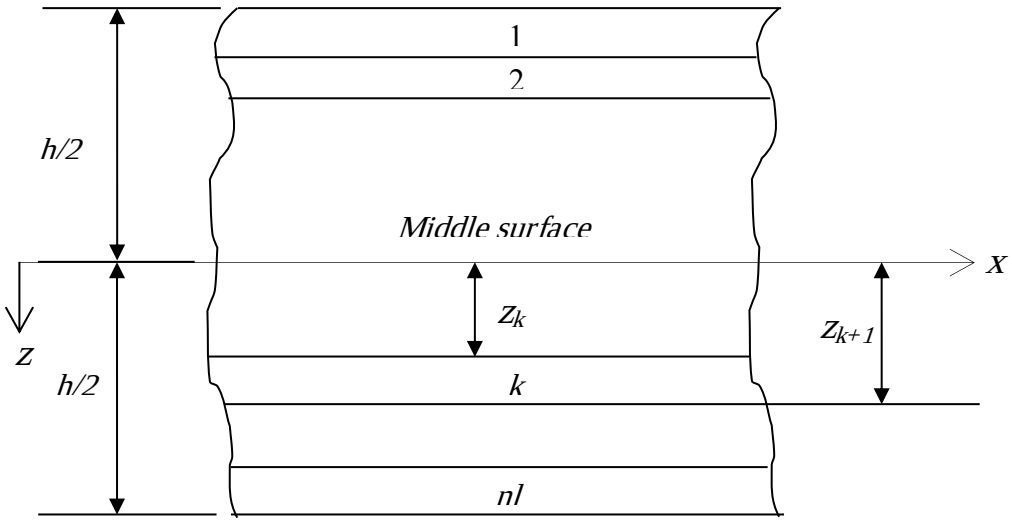


**Fig. 2.2 Geometry of an *n*-Layered laminate**

## 2.1.2 Equations of equilibrium

The stresses within a body vary from point to point. The equations governing the distribution of the stresses are known as the equations of equilibrium. Consider the static equilibrium state of an infinitesimal parallel piped with surfaces parallel to the co-ordinate planes. The resultants stresses acting on the various surfaces are shown in Fig.2.3. Equilibrium of the body requires the vanishing of the resultant forces and moments.

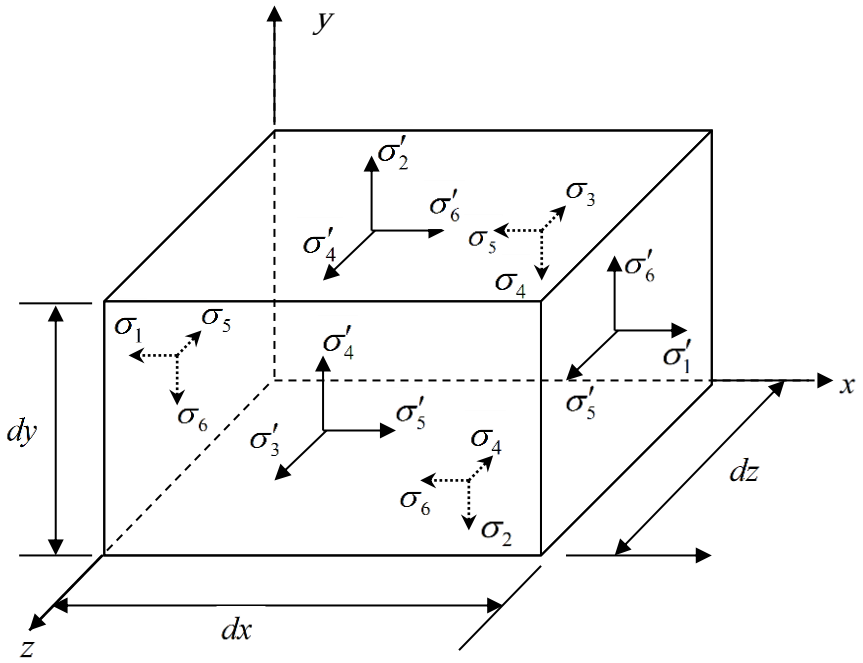


**Fig.2.3 Stresses acting on an infinitesimal element**

Where the dash indicates a small increment of stress e.g. $\sigma_1' = \sigma_1 + \frac{\partial \sigma_1}{\partial x} dx$

The forces in the direction of *x* are shown in Fig.2.4. The sum of these forces gives the following equation.

$$\frac{\partial \sigma_1}{\partial x} + \frac{\partial \sigma_6}{\partial y} + \frac{\partial \sigma_5}{\partial z} = 0 \qquad (2.1)$$

By summing forces in the directions y and z, the following two equations are obtained:

$$\frac{\partial \sigma_6}{\partial x} + \frac{\partial \sigma_2}{\partial y} + \frac{\partial \sigma_4}{\partial z} = 0 \qquad (2.2)$$

$$\frac{\partial \sigma_5}{\partial x} + \frac{\partial \sigma_4}{\partial y} + \frac{\partial \sigma_3}{\partial z} = 0 \qquad (2.3)$$

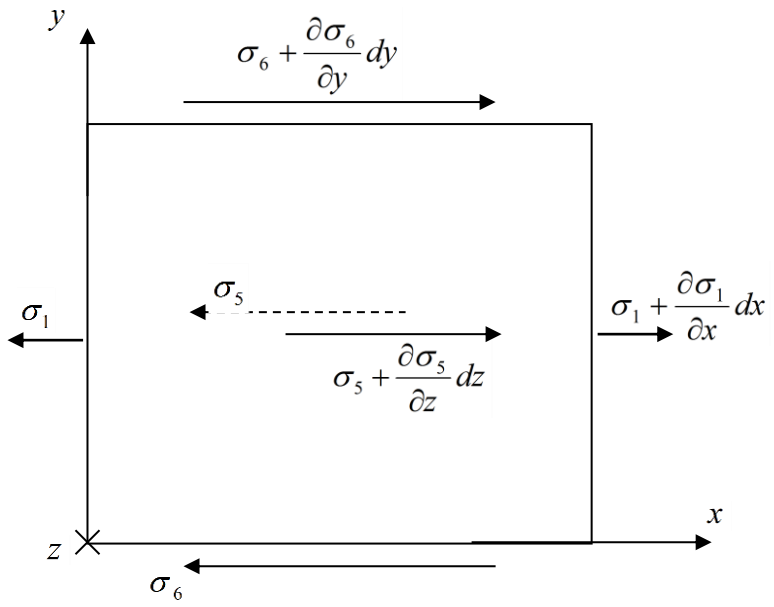


**Fig.2.4 Stresses acting in the *x*–direction.**

In order to facilitate the analysis of a multi-layered plate as a single layer plate, stress resultants and stress couples are introduced and defined as follows:

$$[N_i, M_i] = \sum_{k=1}^{n} \int_{z_k}^{z_{k+1}} \sigma_i [1, z] dz \qquad (\mathrm{i} = 1,2,6) \qquad (2.4)$$

$$[Q_1, Q_2] = \sum_{k=1}^{n} \int_{z_k}^{z_{k+1}} (\sigma_5, \sigma_4) dz \qquad (2.5)$$

Where $z_k$ and $z_{k+1}$ are the distances of top and bottom surfaces of the $k^{th}$ ply from the middle plane of the plate as shown in Fig. 2.2 . The stress resultants and stress couples are clearly shown in Fig. 2.5 and 2.6 respectively.

When integrating Eqn. (2.1) term by term across each ply, and summing over the plate thickness, it will be converted to:

$$\sum_{k=1}^{n}\int_{Z_k}^{Z_{k+1}}\frac{\partial\sigma_1}{\partial x}dz+\sum_{k=1}^{n}\int_{Z_k}^{Z_{k+1}}\frac{\partial\sigma_6}{\partial y}dz+\sum_{k=1}^{n}\int_{Z_k}^{Z_{k+1}}\frac{\partial\sigma_5}{\partial z}dz=0$$

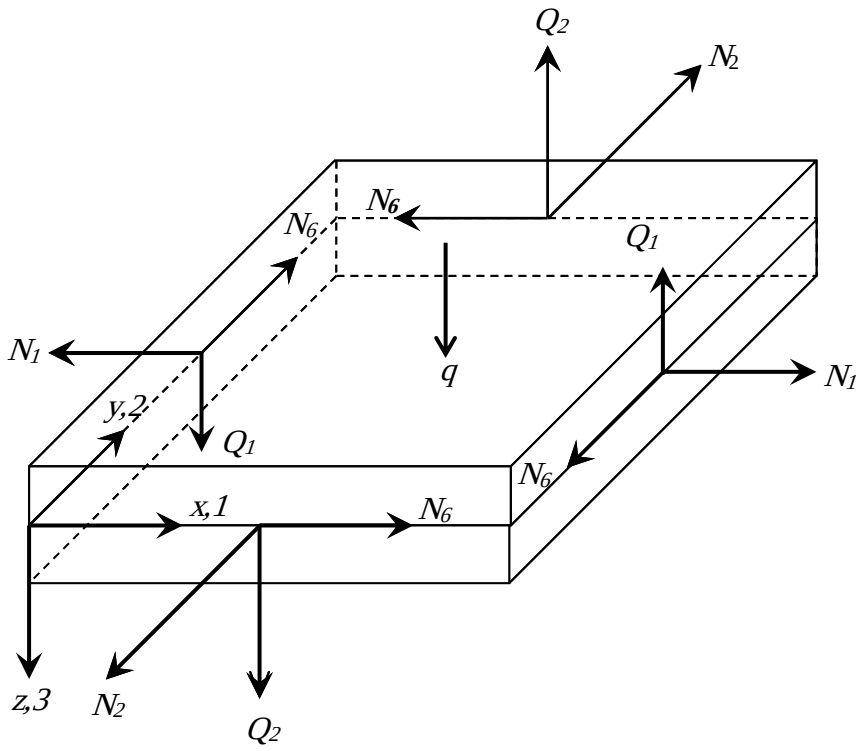


Fig. 2.5 Nomenclature for stress resultants

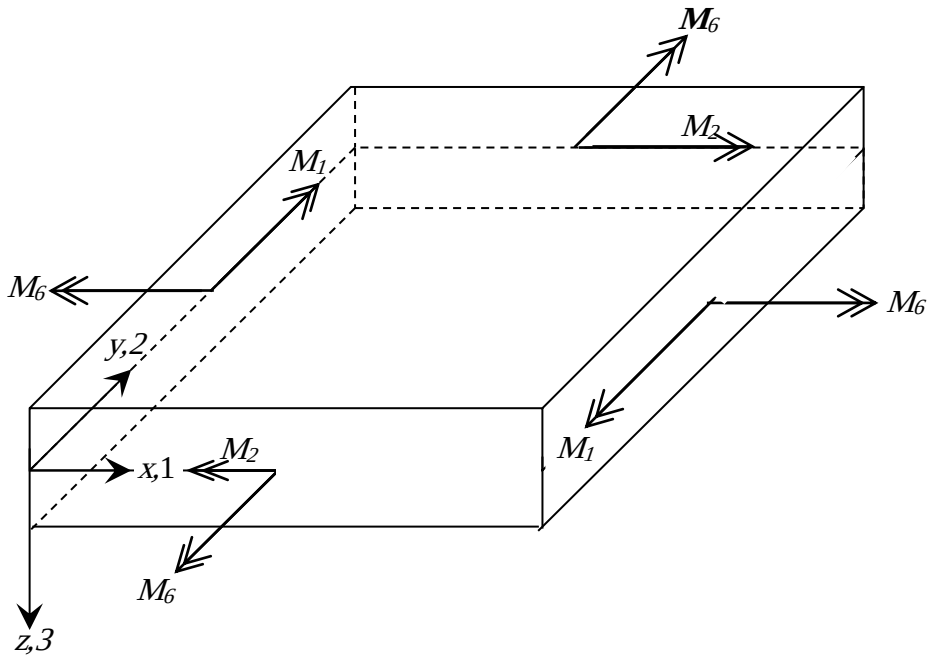


Fig. 2.6 Nomenclature for stress couples

In order to introduce the stress resultants given in Eqn. (2.4), summation can be interchanged with differentiation in the first two terms.

$$\frac{\partial}{\partial x}\left[\sum_{k=1}^{n}\int_{Z_k}^{Z_{k+1}}\sigma_1 dz\right]+\frac{\partial}{\partial y}\left[\sum_{k=1}^{n}\int_{Z_k}^{Z_{k+1}}\sigma_6 dz\right]+\left[\sum_{k=1}^{n}\sigma_5\right]_{Z_k}^{Z_{k+1}}=0$$

The first and second bracketed terms, according to Eqn. (2.4), are $N_1$ and $N_6$ receptively. The last term must vanish because between all plies the inter-laminar shear stresses cancel each other out, and the top and bottom surfaces of the plate are assumed shear stress free.

The first integrated equation of equilibrium can then be written in the following form:

$$\frac{\partial N_1}{\partial x}+\frac{\partial N_6}{\partial y}=0 \qquad (2.6)$$

Similarly Eqn. (2.2) and (2.3) can be integrated to give:

$$\frac{\partial N_6}{\partial x}+\frac{\partial N_2}{\partial y}=0 \qquad (2.7)$$

$$\frac{\partial Q_1}{\partial x}+\frac{\partial Q_2}{\partial y}+q=0 \qquad (2.8)$$

*where* $\mathrm{q}=\sigma_3\left(-\frac{h}{2}\right)-\sigma_3\left(\frac{h}{2}\right)$

The equations of moment equilibrium can be obtained by multiplying Eqn.(2.1) by *z* and integrating with respect to *z* over plate thickness which yields the following equation:

$$\sum_{k=1}^{n}\int_{z_k}^{Z_{k+1}}\frac{\partial\sigma_1}{\partial x}zdz+\sum_{k=1}^{n}\int_{z_k}^{Z_{k+1}}\frac{\partial\sigma_6}{\partial y}zdz+\sum_{k=1}^{n}\int_{z_k}^{Z_{k+1}}\frac{\partial\sigma_5}{\partial z}zdz=0$$

When integration and summation are interchanged with differentiation and the stress couples given in Eqn. (2.4) are introduced, the first two terms become $\left(\frac{\partial M_1}{\partial x}+\frac{\partial M_6}{\partial y}\right)$. The third term must be integrated by parts as follows: -

$$\sum_{k=1}^{n}\int_{z_k}^{Z_{k+1}}\frac{\partial\sigma_5}{\partial z}zdz=\sum_{k=1}^{n}\int_{z_k}^{Z_{k+1}}\left\{\left[z\sigma_5\right]_{Z_k}^{Z_{k+1}}-\int_{z_k}^{Z_{k+1}}\sigma_5 dz\right\}$$

The first term on the right hand side of the above equation represents the moments of all inter-lamina stresses between plies which again must cancel each other out. The last term, according to Eqn. (2.5), is $-Q_1$. Hence the integrated moment equilibrium equation is:

$$\frac{\partial M_1}{\partial x}+\frac{\partial M_6}{\partial y}-Q_1=0 \qquad (2.9)$$

When Eqn. (2.2) is treated similarly, it yields the following equation:

$$\frac{\partial M_6}{\partial x}+\frac{\partial M_2}{\partial y}-Q_2=0 \qquad (2.10)$$

Hence, the equilibrium equations of the plate are the five equations, i.e. Eqns. (2.6) to (2.10).

### 2.1.3 The strain-displacement equations:

Fig.2.7 shows a small element *ABCD* in the Cartesian co-ordinates *x*, *y* which deforms to $A'B'C'D'$ . The deformations can be described in terms of extensions of lines and distortion of angles between lines. From Fig.2.7, it is possible to write expressions for linear and shear strains as follows:

$$\varepsilon_1 = \left\{ \frac{\left[u + (\partial u / \partial x)dx\right] - u}{dx} \right\} = \frac{\partial u}{\partial x} \tag{2.11}$$

Similarly: $$\varepsilon_2 = \frac{\partial v}{\partial y} \tag{2.12}$$

If $\theta$ is very small, then,

$$\theta_x = tan\theta_x = \frac{\partial v}{\partial x}$$

$$\theta_y = tan\theta_y = \frac{\partial u}{\partial y}$$

Hence, the shear strain which is the change in the right angle $\angle$ *BAD* is:

$$\varepsilon_6 = \theta_x + \theta_y = \frac{\partial v}{\partial x} + \frac{\partial u}{\partial y} \tag{2.13}$$

For a three-dimensional problem, the following strains may be added:

$$\varepsilon_3 = \frac{\partial w}{\partial z} \tag{2.14}$$

$$\varepsilon_4 = \frac{\partial w}{\partial y} + \frac{\partial v}{\partial z} \tag{2.15}$$

$$\varepsilon_5 = \frac{\partial w}{\partial x} + \frac{\partial u}{\partial z} \tag{2.16}$$

The displacements, which comply with assumption (3), are: -

$$\begin{aligned} u &= u^o(x,y) + z\Phi^o(x,y) \\ v &= v^o(x,y) + z\Psi^o(x,y) \\ w &= w^o(x,y) \end{aligned} \tag{2.17}$$

Where $u^o$ ,$v^o$ ,and $w^o$ are the displacements of the middle surface of the plate. When Eqn. (2.17) is differentiated and substituted in Eqns (2.11 – 2.16), the following strain displacement relations are obtained.

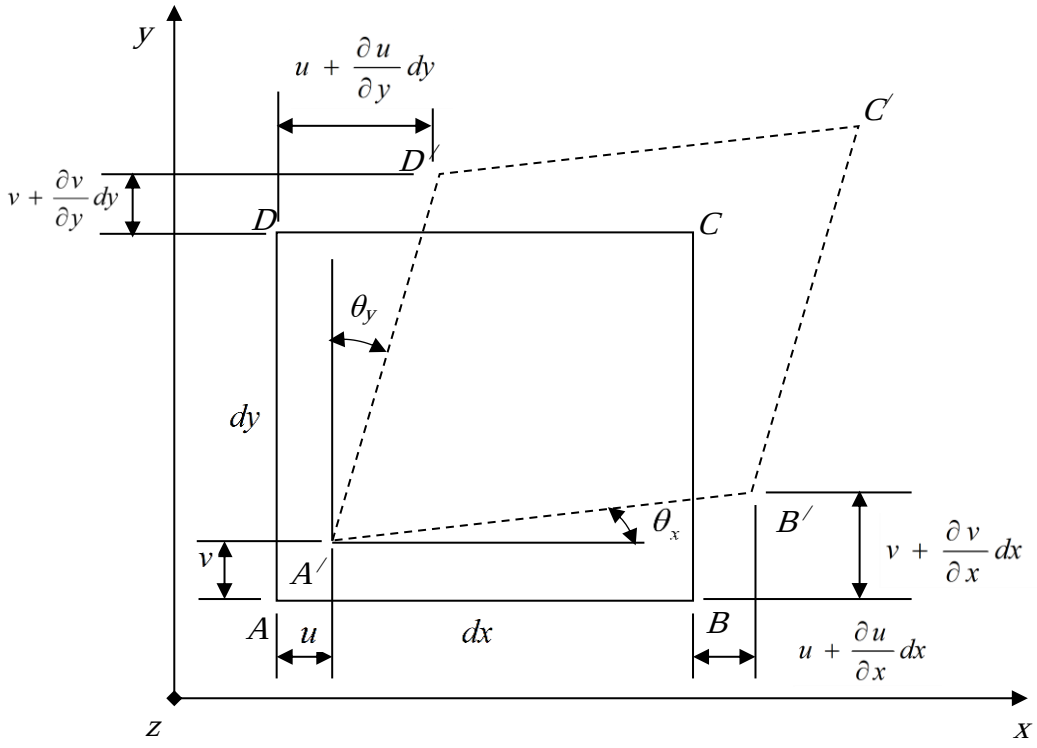


**Fig.2.7 Small deformation of an elastic element**

$$\varepsilon_1 = \frac{\partial u^o}{\partial x} + z\frac{\partial \Phi}{\partial x}$$

$$\varepsilon_2 = \frac{\partial v^o}{\partial y} + z\frac{\partial \Psi}{\partial y}$$

$$\varepsilon_6 = \frac{\partial u^o}{\partial y} + \frac{\partial v^o}{\partial x} + z\left\{\frac{\partial \Phi}{\partial y} + \frac{\partial \Psi}{\partial x}\right\} \qquad (2.18)$$

$$\varepsilon_4 = \frac{\partial w}{\partial y} + \Psi$$

$$\varepsilon_5 = \frac{\partial w}{\partial x} + \Phi$$

## 2.1.4 The constitutive equations:

The constitutive equations of an individual lamina, k, are of the form:

$$\sigma_i^{(k)} = C_{ij}^{(k)} \varepsilon_j^{(k)} \qquad (i, j = 1,2,6) \qquad (2.19)$$

Where $\sigma_i^{(k)}$ and $\varepsilon_j^{(k)}$ are the stresses and strains in the lamina referred to the plate axes .Using Eqn. (2.18) in the form $\varepsilon_i = \varepsilon_i^o + z\chi_i^o$ ( $i$ =1,2,6)

$$where\, \varepsilon_1^o = \frac{\partial u^o}{\partial x} \;,\; \varepsilon_2^0 = \frac{\partial v^o}{\partial y} \;,\; \varepsilon_6^0 = \frac{\partial u^o}{\partial y} + \frac{\partial v^o}{\partial x}$$

$$\chi_1^o = \frac{\partial \Phi}{\partial x} \;,\; \chi_2^0 = \frac{\partial \Psi}{\partial y} \;,\; \chi_6^0 = \frac{\partial \Phi}{\partial y} + \frac{\partial \Psi}{\partial x}$$

Then Eqn.(2.19) becomes:-

$$\sigma_i = C_{ij}\left(\varepsilon_j^o + z\chi_j^o\right) \tag{2.20}$$

Substitute Eqn. (2.20) in Eqn. (2.4) to give:

$$N_i = \sum_{k=1}^{nl} \int_{z_k}^{z_{k+1}} C_{ij}\left(\varepsilon_j^o + z\chi_j^o\right) dz \tag{2.21}$$

Eqn. (2.21) can be written in the form:-

$$N_i = A_{ij}\varepsilon_j^o + B_{ij}\chi_j^o \quad (i = 1,2,6) \tag{2.22}$$

Similarly using Eqn. (2.20) in Eqn. (2. 4) gives: -

$$M_i = \sum_{k=1}^{n} \int_{z_k}^{z_{k+1}} C_{ij}\left(\varepsilon_j^o + z\chi_j^o\right) z\, dz \tag{2.23}$$

Eqn. (2.23) can be written in the form:

$$M_i = B_{ij}\varepsilon_j^o + D_{ij}\chi_j^o \quad (i = 1,2,6) \tag{2.24}$$

Where $A_{ij}$ ,$B_{ij}$ , and $D_{ij}$ ,($i, j$=1, 2,3) are respectively the membrane rigidities, coupling rigidities and flexural rigidities of the plate . The rigidities $B_{ij}$ display coupling between transverse bending and in-plane stretching. The coupling will disappear when the reference plane is taken as the plate mid-plane for symmetric laminate .The rigidities are calculated as follows:-

$$\left(A_{ij}, B_{ij}, D_{ij}\right) = \sum_{k=1}^{n} \int_{z_k}^{z_{k+1}} C_{ij}\left(1, z, z^2\right) dz \tag{2.25}$$

Hence, the laminate constitutive equations can be represented in the form:

$$\begin{Bmatrix} N_i \\ M_i \end{Bmatrix} = \begin{bmatrix} A_{ij} & B_{ij} \\ B_{ij} & D_{ij} \end{bmatrix} \begin{Bmatrix} \varepsilon_j^o \\ \chi_j^o \end{Bmatrix} \tag{2.26}$$

$$\begin{Bmatrix} Q_2 \\ Q_1 \end{Bmatrix} = \begin{bmatrix} A_{44} & A_{45} \\ A_{45} & A_{55} \end{bmatrix} \begin{Bmatrix} \varepsilon_4 \\ \varepsilon_5 \end{Bmatrix} \tag{2.27}$$

Where $A_{ij}$ ($i,j$ =4,5) denote the stiffness coefficients , and are calculated as follows:-

$$A_{ij} = \sum_{k=1}^{n} K_i K_j \int_{z_k}^{z_{k+1}} C_{ij}^{(k)} dz\,, \quad (i, j = 4,5) \tag{2.28}$$

Where $K_i$ ,$K_j$ are the shear correction factors.

### 2.1.5 Boundary conditions:

The proper boundary conditions are those which are sufficient to guarantee a unique solution of the governing equations. To achieve that goal, one term of each of the following five pairs must be prescribed along the boundary.

$$N_n \text{ or } u_n \;;\; N_{ns} \text{ or } u_s \;;\; M_n \text{ or } \phi_n \;;\; M_s \text{ or } \phi_s \;;\; Q \text{ or } w \tag{2.29}$$

Where the subscripts *n* and *s* indicate the normal and tangential directions respectively. The boundary conditions used in this thesis are given in Appendix C.

## 2.2 Nonlinear theory:

### 2.2.1 Assumptions:-

The assumptions made in the nonlinear theory of laminated plates are the same as those listed for linear analysis, section 2.1.1, except for assumption (2), which is concerned with the magnitude of deformations. In the nonlinear theory, in-plane displacements are again small compared to the thickness of the plate, but the out-of-plane displacement is not.

### 2.2.2 Equations of equilibrium:

The derivation of the equilibrium equations for finite deformations can be found in Refs.[3,6,7,8] and can be written in the following form:

$$\frac{\partial}{\partial x}\left[\sigma_1\left(1+\frac{\partial u}{\partial x}\right)+\sigma_6\frac{\partial u}{\partial y}+\sigma_5\frac{\partial u}{\partial z}\right]+\frac{\partial}{\partial y}\left[\sigma_6\left(1+\frac{\partial u}{\partial x}\right)+\sigma_2\frac{\partial u}{\partial y}+\sigma_4\frac{\partial u}{\partial z}\right]$$
$$+\frac{\partial}{\partial z}\left[\sigma_5\left(1+\frac{\partial u}{\partial x}\right)+\sigma_4\frac{\partial u}{\partial y}+\sigma_3\frac{\partial u}{\partial z}\right]=0 \tag{2.30}$$

$$\frac{\partial}{\partial x}\left[\sigma_1\frac{\partial v}{\partial x}+\sigma_6\left(1+\frac{\partial v}{\partial y}\right)+\sigma_5\frac{\partial v}{\partial z}\right]+\frac{\partial}{\partial y}\left[\sigma_6\frac{\partial v}{\partial x}+\sigma_2\left(1+\frac{\partial v}{\partial y}\right)+\sigma_4\frac{\partial v}{\partial z}\right]$$
$$+\frac{\partial}{\partial z}\left[\sigma_5\frac{\partial v}{\partial x}+\sigma_4\left(1+\frac{\partial v}{\partial y}\right)+\sigma_3\frac{\partial v}{\partial z}\right]=0 \qquad (2.31)$$
$$\frac{\partial}{\partial x}\left[\sigma_1\frac{\partial w}{\partial x}+\sigma_6\frac{\partial w}{\partial y}+\sigma_5\left(1+\frac{\partial w}{\partial z}\right)\right]+\frac{\partial}{\partial y}\left[\sigma_6\frac{\partial w}{\partial x}+\sigma_2\frac{\partial w}{\partial y}+\sigma_4\left(1+\frac{\partial w}{\partial z}\right)\right]$$
$$+\frac{\partial}{\partial z}\left[\sigma_5\frac{\partial w}{\partial x}+\sigma_4\frac{\partial w}{\partial y}+\sigma_3\left(1+\frac{\partial w}{\partial z}\right)\right]=0 \qquad (2.32)$$

The equilibrium equations of a body undergoing large deformations are given in Eqns. (2.30) – (2.32) .Assuming the in-plane displacement gradients are small compared to unity and neglecting the transverse normal stress $\sigma_3$, Eqns. (2.30) – (2.32) can be written in a simpler form as follows:

$$\frac{\partial\sigma_1}{\partial x}+\frac{\partial\sigma_6}{\partial y}+\frac{\partial\sigma_5}{\partial z}=0 \qquad (2.33)$$

$$\frac{\partial\sigma_6}{\partial x}+\frac{\partial\sigma_2}{\partial y}+\frac{\partial\sigma_4}{\partial z}=0 \qquad (2.34)$$

$$\frac{\partial}{\partial x}\left[\sigma_5+\sigma_1\frac{\partial w}{\partial x}+\sigma_6\frac{\partial w}{\partial y}\right]+\frac{\partial}{\partial y}\left[\sigma_4+\sigma_6\frac{\partial w}{\partial x}+\sigma_2\frac{\partial w}{\partial y}\right]+\frac{\partial}{\partial z}\left[\sigma_5\frac{\partial w}{\partial x}+\sigma_4\frac{\partial w}{\partial y}+\sigma_3\right]=0 \qquad (2.35)$$

Integrating Eqns. (2.33) and (2.34) over the thickness of the plate as in section 2.1.2 gives Eqns. (2.6) and (2.7) as before. When Eqn. (2.35) is integrated, it gives:-

$$\frac{\partial}{\partial x}\left[Q_1+N_1\frac{\partial w}{\partial x}+N_6\frac{\partial w}{\partial y}\right]+\frac{\partial}{\partial y}\left[Q_2+N_6\frac{\partial w}{\partial x}+N_2\frac{\partial w}{\partial y}\right]+\frac{\partial}{\partial z}\left[Q_1\frac{\partial w}{\partial x}+Q_2\frac{\partial w}{\partial y}\right]+q=0 \qquad (2.36)$$

This can be rewritten in the following form:

$$N_1\frac{\partial^2 w}{\partial x^2}+2N_6\frac{\partial^2 w}{\partial x\partial y}+N_2\frac{\partial^2 w}{\partial y^2}+\frac{\partial Q_1}{\partial x}+\frac{\partial Q_2}{\partial y}+q+\frac{\partial w}{\partial x}\left(\frac{\partial N_1}{\partial x}+\frac{\partial N_6}{\partial y}\right)+\frac{\partial w}{\partial y}\left(\frac{\partial N_6}{\partial x}+\frac{\partial N_2}{\partial y}\right)=0 \qquad (2.37)$$

$$where\ q=\sigma_3\left(-\frac{h}{2}\right)-\sigma_3\left(\frac{h}{2}\right)$$

However, similar to Eqns. (2.6) and (2.7), the last two terms in Eqn. (2.37) must be zero, and so the above equation reduces to:

$$N_1\frac{\partial^2 w}{\partial x^2}+2N_6\frac{\partial^2 w}{\partial x\partial y}+N_2\frac{\partial^2 w}{\partial y^2}+\frac{\partial Q_1}{\partial x}+\frac{\partial Q_2}{\partial y}+q=0 \qquad (2.38)$$

Multiplying Eqns. (2.33) and (2.34) by *z* and again integrating over the thickness of the plate to obtain Eqns. (2.9) and (2.10).

Hence, the governing equations of the plate are the following five Eqns. (2.6), (2.7), (2.38), (2.9), and (2.10). It should be noted that the shear deformation theory derived above reduces to classical laminated theory when the transverse shear strains are eliminated by setting:

$$\phi = -\frac{\partial w}{\partial x} \quad , and \quad \psi = -\frac{\partial w}{\partial y}$$

### 2.2.3 The strain-displacement equations:

The in-plane displacements *u* and *v* are small, whereas the deflection *w* is of the order of half the plate thickness or more. This assumption implies that:

$$\frac{\partial(u,v)}{\partial(x,y)} << \frac{\partial w}{\partial(x,y)} \tag{2.39}$$

Consequently, the expressions for finite strains can be simplified as follows:-

$$\begin{aligned}
\varepsilon_1 &= \frac{\partial u}{\partial x} + \frac{1}{2}\left(\frac{\partial w}{\partial x}\right)^2 \\
\varepsilon_2 &= \frac{\partial v}{\partial y} + \frac{1}{2}\left(\frac{\partial w}{\partial y}\right)^2 \\
\varepsilon_3 &= 0 \\
\varepsilon_4 &= \frac{\partial w}{\partial y} + \frac{\partial v}{\partial z} \\
\varepsilon_5 &= \frac{\partial w}{\partial x} + \frac{\partial u}{\partial z} \\
\varepsilon_6 &= \frac{\partial v}{\partial x} + \frac{\partial u}{\partial y} + \frac{\partial w}{\partial x}.\frac{\partial w}{\partial y}
\end{aligned} \tag{2.40}$$

The in-plane displacements are again assumed to vary linearly through the thickness of the plate as described for linear analysis i.e.:-

$$\begin{aligned}
u &= u^o(x,y) + z\phi^o(x.y) \\
v &= v^o(x,y) + z\psi^o(x.y) \\
w &= w^o(x,y)
\end{aligned} \tag{2.41}$$

When these displacements are substituted into Eqn. (2.40), the following relations are obtained:-

$$\varepsilon_i = \varepsilon_i^o + z\chi_i^o \qquad (i = 1,2,6)$$
$$\varepsilon_4 = \frac{\partial w}{\partial y} + \psi \tag{2.42}$$
$$\varepsilon_5 = \frac{\partial w}{\partial x} + \phi$$

$$where\ \varepsilon_1^o = \frac{\partial u^o}{\partial x} + \frac{1}{2}\left(\frac{\partial w}{\partial x}\right)^2$$
$$\varepsilon_2^o = \frac{\partial v^o}{\partial y} + \frac{1}{2}\left(\frac{\partial w}{\partial y}\right)^2$$
$$\varepsilon_6^o = \frac{\partial u^o}{\partial y} + \frac{\partial v^o}{\partial x} + \frac{\partial w}{\partial x}.\frac{\partial w}{\partial y}$$
$$\chi_1^o = \frac{\partial \phi}{\partial x}$$
$$\chi_2^o = \frac{\partial \psi}{\partial y}$$
$$\chi_6^o = \frac{\partial \phi}{\partial y} + \frac{\partial \psi}{\partial x}$$

$$\varepsilon_1 = \frac{\partial u^o}{\partial x} + \frac{1}{2}\left(\frac{\partial w}{\partial x}\right)^2 + z\frac{\partial \phi}{\partial x}$$
$$\varepsilon_2 = \frac{\partial v^o}{\partial y} + \frac{1}{2}\left(\frac{\partial w}{\partial y}\right)^2 + z\frac{\partial \psi}{\partial y}$$
$$\varepsilon_6 = \frac{\partial u^o}{\partial y} + \frac{\partial v^o}{\partial x} + \frac{\partial w}{\partial x}.\frac{\partial w}{\partial y} + z\left(\frac{\partial \phi}{\partial y} + \frac{\partial \psi}{\partial x}\right) \tag{2.43}$$
$$\varepsilon_4 = \frac{\partial w}{\partial y} + \psi$$
$$\varepsilon_5 = \frac{\partial w}{\partial x} + \phi$$

### 2.2.4 The constitutive equations:

These are the same as Eqns. (2.26), and (2.27) of sections 2.1.4.

### 2.2.5 Boundary conditions:

These are the same as Eqn. (2.29) of sections 2.1.5.

## 2.3 Transformation equations

### 2.3.1 Stress-strain equations

For linear elastic materials, the relation between the stress and strain is as follows:

$$\sigma_i' = C_{ij}' \varepsilon_j' \qquad (ij=1,2,.. \tag{2.44}$$

Where the first subscript i refers to the direction of the normal to the face on which the stress component acts, and the second subscript j corresponds to the direction of the stress.

When an orthotropic body is in a state of plane stress, the non-zero components of the stiffness tensors $C_{ij}'$ are:

$$C_{11}' = \frac{E_1}{1-\nu_{12}\nu_{21}}$$

$$C_{12}' = \frac{\nu_{21}E_1}{1-\nu_{12}\nu_{21}} = \frac{\nu_{12}E_2}{1-\nu_{12}\nu_{21}}$$

$$C_{22}' = \frac{E_2}{1-\nu_{12}\nu_{21}}$$

$$C_{44}' = G_{23}, \quad C_{55}' = G_{13}, \quad C_{66}' = G_{12} \tag{2.45}$$

Where $E_1$ and $E_2$ are Young's moduli in directions 1 and 2 respectively. $\nu_{ij}$ is Poisson's ratio of transverse strain in the j-direction when stressed in the *i*-direction i.e. $\nu_{ij} = -\varepsilon_j' / \varepsilon_i$ When $\sigma_i' = \sigma$ and all other stress are zero.

### 2.3.2 Transformation of stresses and strains

Consider a co-ordinate system rotated anticlockwise through an angle θ, the rotated axes are denoted by $1'$, $2'$ as in Fig.2.8. Consider the equilibrium of the small element ABC shown. Resolving forces parallel to $1'$ axis gives:

$$\sigma_{11}' ds = \sigma_{11} dy \cos\theta + \sigma_{22} dx \sin\theta + \sigma_{12} dx \cos\theta + \sigma_{12} dy \sin\theta \tag{2.46}$$

On rearranging, the expression reduces to:

$$\sigma_{11}' = \sigma_{11} \cos^2\theta + \sigma_{22} \sin^2\theta + 2\sigma_{12} \sin\theta\cos\theta + \sigma_{12} dy \sin\theta \tag{2.47}$$

Resolving forces parallel to $2'$ axis gives:

$$\sigma_{12}' ds = -\sigma_{11} dy \sin\theta + \sigma_{22} dx \cos\theta + \sigma_{12} dy \cos\theta - \sigma_{12} dx \sin\theta \tag{2.48}$$

This can then be written in the form:

$$\sigma_{12}' = -\sigma_{11} \sin\theta\cos\theta + \sigma_{22} \sin\theta\cos\theta + \sigma_{12}\left(\cos^2\theta - \sin^2\theta\right) \tag{2.49}$$

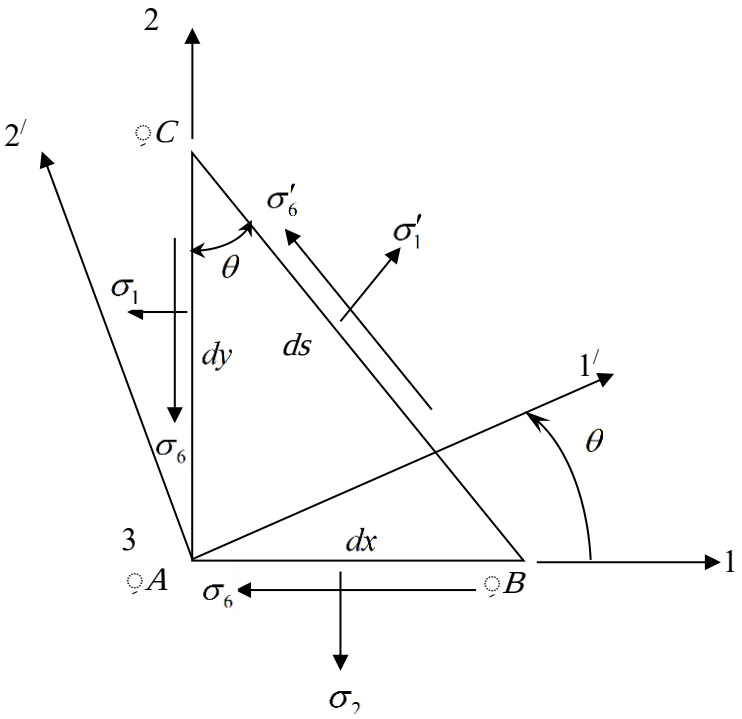


**Fig.2.8 Stresses on a triangular element**

The same procedure is applied to obtain the other transformed stresses which may be written in a matrix form as:

$$\{\sigma_i'\} = [M]\{\sigma_i\} \tag{2.50}$$

Where $[M] = \begin{bmatrix} m^2 & n^2 & 0 & 0 & 0 & 2mn \\ n^2 & m^2 & 0 & 0 & 0 & -2mn \\ 0 & 0 & 1 & 0 & 0 & 0 \\ 0 & 0 & 0 & m & -n & 0 \\ 0 & 0 & 0 & n & m & 0 \\ -mn & mn & 0 & 0 & 0 & (m^2 - n^2) \end{bmatrix}$

The strains are transformed similarly:

$$\{\varepsilon_i'\} = [N]\{\varepsilon_j\} \tag{2.51}$$

Where $[N] = \begin{bmatrix} m^2 & n^2 & 0 & 0 & 0 & mn \\ n^2 & m^2 & 0 & 0 & 0 & -mn \\ 0 & 0 & 1 & 0 & 0 & 0 \\ 0 & 0 & 0 & m & -n & 0 \\ 0 & 0 & 0 & n & m & 0 \\ -2mn & 2mn & 0 & 0 & 0 & (m^2 - n^2) \end{bmatrix}$

### 2.3.3 Transformation of the elastic moduli

In general the principle material axes ($1^{/}$, $2^{/}$, $3^{/}$) are not aligned with the geometric axes (1, 2, 3) as shown in Fig.2.9 for a unidirectional continuous fiber composite. It is necessary to be able to relate the stresses and strains in both co-ordinate systems. This is achieved by multiplying Eqn. (2.50) by $[M]^{-1}$ i.e.:

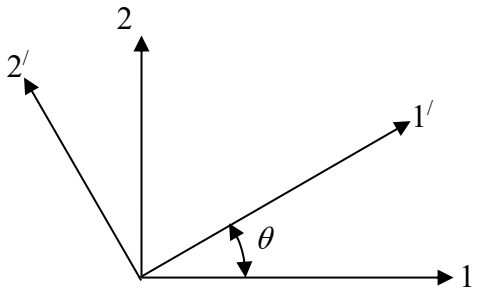


**Fig.2.9 A generally orthotropic plate**

$$\{\sigma_i\} = [M]^{-1}\{\sigma_i'\} \tag{2.52}$$

Substitute Eqn. (2.44) in Eqn. (2.52) to obtain:

$$\{\sigma_i\} = [M]^{-1}[C_{ij}']\{\varepsilon_j'\} \tag{2.53}$$

Then, substitute Eqn. (2.51) in Eqn. (2.53)

$$\{\sigma_i\} = [M]^{-1}[C_{ij}'][N]\{\varepsilon_j\} \tag{2.54}$$

This equation can be written as:

$$\{\sigma_i\} = \lfloor C_{ij} \rfloor \{\varepsilon_j\} \tag{2.55}$$

Where $\{C_{ij}\} = [M]^{-1}[N][C_{ij}']$

Eqn. (2.55) gives the constitutive equation for a generally orthotropic lamina in which the material axes and geometric axes are not aligned. The constants $C_{ij}$ are as follows:

$$C_{11} = C_{11}'m^4 + 2m^2n^2(C_{12}' + 2C_{66}') - 4mn(C_{16}'m^2 + C_{26}'n^2) + C_{22}'n^4$$
$$C_{12} = m^2n^2(C_{11}' + C_{22}' - 4C_{66}') + 2mn(m^2 - n^2)(C_{16}' + C_{26}') + (m^4 + n^4)C_{12}'$$
$$C_{13} = C_{13}'m^2 + C_{23}'n^2$$

$$C_{16} = m^2 n^2 \left[ C'_{11} m^2 - C'_{22} n^2 - \left( C'_{12} + 2C'_{66} \right) \left( m^2 - n^2 \right) \right] + m^2 \left( m^2 - 3n^2 \right) C'_{16} + n^2 \left( 3m^2 - n^2 \right) C'_{26}$$

$$C_{22} = C'_{11} n^4 + 2m^2 n^2 \left( C'_{12} + 2C'_{66} \right) + 4mn \left( C'_{26} m^2 + C'_{16} n^2 \right) + C'_{22} m^4$$

$$C_{23} = C'_{13} n^2 + C'_{23} m^2$$

$$C_{26} = m^2 \left( m^2 - 3n^2 \right) C'_{26} + mn \left[ C'_{11} n^2 - C'_{22} m^2 + \left( C'_{12} + 2C'_{66} \right) \left( m^2 - n^2 \right) \right] + n^2 \left( 3m^2 - n^2 \right) C'_{16}$$

$$C_{33} = C'_{33}$$

$$C_{36} = \left( C'_{23} - C'_{13} \right) mn$$

$$C_{44} = C'_{44} m^2 + 2mnC'_{45} + C'_{55} n^2$$

$$C_{45} = \left( m^2 - n^2 \right) C'_{45} - mn \left( C'_{44} - C'_{55} \right)$$

$$C_{55} = C'_{55} m^2 - 2mnC'_{45} + C'_{44} n^2$$

$$C_{66} = m^2 n^2 \left( C'_{11} + C'_{22} - 2C'_{12} \right) - 2mn \left( m^2 - n^2 \right) \left( C'_{26} - C'_{16} \right) + \left( m^2 - n^2 \right)^2 C'_{66}$$

$$C_{14} = C_{15} = C_{24} = C_{25} = C_{34} = C_{35} = C_{46} = C_{56} = 0 \qquad (2.56)$$

Where $m=\cos\theta$ and $n=\sin\theta$

# CHAPTER (3)

# Numerical technique

In the present work, finite differences coupled with dynamic relaxation (DR) Method, which is a numerical technique, is used. The DR method was first proposed and developed in 1960, see Refs. [13], [52], and [53]. In this method, the equations of equilibrium are converted to dynamic equations by adding damping and inertia terms. These are then expressed in finite difference form and the solution is obtained by an iterative procedure as explained below.

## 3.1 DR Formulation:

The DR formulae begin with the dynamic equation, which can be written as:

$$f = \rho \frac{\partial^2 u}{\partial t^2} + k \frac{\partial u}{\partial t} \tag{3.1}$$

Where f is a function of the stress resultants and couples, u is referred to as a displacement, $\partial u / \partial t$ and $\partial^2 u / \partial t^2$ are the velocity and acceleration respectively, $\rho$ and k are the inertia and damping coefficients respectively, and t is time.

If the velocities before and after a period $\Delta t$ at an arbitrary node in the finite difference mesh are denoted by $\left\{\partial u / \partial t\right\}_{n-1}$ and $\left\{\partial u / \partial t\right\}_{n}$ respectively, then using finite differences in time, and specifying the value of the function at $\left(n-\frac{1}{2}\right)$, it is possible to write equation (3.1) in the following form:

$$f_{n-\frac{1}{2}} = \frac{\rho}{\Delta t}\left[\left\{\frac{\partial u}{\partial t}\right\}_{n} - \left\{\frac{\partial u}{\partial t}\right\}_{n-1}\right] + k\left\{\frac{\partial u}{\partial t}\right\}_{n-\frac{1}{2}} \tag{3.2}$$

$\left\{\partial u / \partial t\right\}_{n-\frac{1}{2}}$ is the velocity at the middle of the time increment, which can be approximated by the mean of the velocities before and after the time increment $\Delta t$, i.e.

$$\left\{\frac{\partial u}{\partial t}\right\}_{n-\frac{1}{2}} = \frac{1}{2}\left[\left\{\frac{\partial u}{\partial t}\right\}_{n} + \left\{\frac{\partial u}{\partial t}\right\}_{n-1}\right]$$

Hence equation (3.2) can be expressed as:

$$f_{n-\frac{1}{2}} = \frac{\rho}{\Delta t}\left[\left\{\frac{\partial u}{\partial t}\right\}_{n} - \left\{\frac{\partial u}{\partial t}\right\}_{n-1}\right] + \frac{k}{2}\left[\left\{\frac{\partial u}{\partial t}\right\}_{n} + \left\{\frac{\partial u}{\partial t}\right\}_{n-1}\right] \tag{3.3}$$

Equation (3.3) can then be arranged to give the velocity after the time interval, $\Delta t$ :

$$\left\{\frac{\partial u}{\partial t}\right\}_{n} = \left(1+k^{*}\right)^{-1}\left[\frac{\Delta t}{\rho} f_{n-\frac{1}{2}} + \left(1-k^{*}\right)\left\{\frac{\partial u}{\partial t}\right\}_{n-1}\right] \tag{3.4}$$

Where $k^{*} = \dfrac{k\Delta t}{2\rho}$

The displacement at the middle of the next time increment can be determined by integrating the velocity, so that:

$$u_{n+\frac{1}{2}} = u_{n-\frac{1}{2}} + \left\{\frac{\partial u}{\partial t}\right\}_{n} \Delta t \tag{3.5}$$

The formulation is completed by computing the stress resultants and stress couples from the known displacement field. The iterative procedure begins at time t=0 with all initial values of the velocities, displacements, and stresses equal to zero or any suitable values. In the first iteration, the velocities are obtained from equation (3.4), and the displacements from equation (3.5). After the satisfaction of the displacement boundary conditions, the stress resultants and stress couples are computed and the appropriate boundary conditions for stresses are applied. Subsequent iterations follow the same steps. The iterations continue until the desired accuracy is achieved.

## 3.2 The plate equations

### 3.2.1 Dimensional plate equations

The equations concerning the analysis of plates in bending (i.e. Eqns. (2.6) , (2.7), (2.9) ,(2.10), and (2.38) are derived in chapter 2.

### 3.2.2 Non-dimensional plate equations

The plate equations can be written in non-dimensionalized form as follows:

$$[x', y', b'] = \frac{1}{a}[x, y, b] , \quad \mathrm{h}' = \frac{\mathrm{h}}{\mathrm{h}} = 1 , \ \mathrm{w}' = \frac{\mathrm{w}}{\mathrm{h}}$$

$$[u', v'] = \left(\frac{a}{h^2}\right)[u, v] \ , [\phi', \psi'] = \left(\frac{a}{h}\right)[\phi, \psi]$$

$$\varepsilon_i' = \left(\frac{a}{h}\right)^2 \varepsilon_i \ , \ \chi_{\mathrm{i}}{}' = \left(\frac{a^2}{h}\right)\chi_i , \ (\mathrm{i} = 1,2,6)$$

$$A_{ij}' = \left(\frac{1}{E_2 h}\right)A_{ij} \ , B_{ij} = \left(\frac{1}{E_2 h^2}\right)B_{ij} , \tag{3.6}$$

$$D_{ij}' = \left(\frac{1}{E_2 h^3}\right)D_{ij} , (\mathrm{i, j} = 1,2,6)$$

$$N_i' = \left(\frac{a^2}{E_2 h^3}\right)N_i , \quad M_i' = \left(\frac{a^2}{E_2 h^4}\right)M_i , (\mathrm{i} = 1,2,6)$$

$$Q_i' = \left(\frac{a}{E_2 h^2}\right)Q_i , (\mathrm{i} = 1,2) \ , \mathrm{q}' = \left(\frac{a^4}{\mathrm{E}_2 h^4}\right)q$$

Substituting Eqn. (3.6) into Eqns. (2.6),(2.7), (2.9),(2.10), (2.38) the non-dimensionalized dynamic plate equations are obtained.

In the following equations, the primes are omitted:

$$\frac{\partial N_1}{\partial x} + \frac{\partial N_6}{\partial y} = \rho_u \frac{\partial^2 u}{\partial t^2} + k_u \frac{\partial u}{\partial t} \tag{3.7}$$

$$\frac{\partial N_6}{\partial x} + \frac{\partial N_2}{\partial y} = \rho_v \frac{\partial^2 v}{\partial t^2} + k_v \frac{\partial v}{\partial t} \tag{3.8}$$

$$N_1 \frac{\partial^2 w}{\partial x^2} + 2N_6 \frac{\partial^2 w}{\partial x \partial y} + N_2 \frac{\partial^2 w}{\partial y^2} + \left(\frac{a}{h}\right)^2 \left[\frac{\partial Q_1}{\partial x} + \frac{\partial Q_2}{\partial y}\right] + q = \rho_w \frac{\partial^2 w}{\partial t^2} + k_w \frac{\partial w}{\partial t} \tag{3.9}$$

$$\frac{\partial M_1}{\partial x} + \frac{\partial M_6}{\partial y} - \left(\frac{a}{h}\right)^2 Q_1 = \rho_\phi \frac{\partial^2 \phi}{\partial t^2} + k_\phi \frac{\partial \phi}{\partial t} \tag{3.10}$$

$$\frac{\partial M_6}{\partial x} + \frac{\partial M_2}{\partial y} - \left(\frac{a}{h}\right)^2 Q_2 = \rho_\psi \frac{\partial^2 \psi}{\partial t^2} + k_\psi \frac{\partial \psi}{\partial t} \tag{3.11}$$

The next step is to transform the differential equations into finite difference equations.

## 3.3 The finite difference approximation

### 3.3.1 Interpolating function *F (x, y)*

It can be shown by using Taylor's series that the first and second derivatives of a function $F(x, y)$ at an arbitrary node $i, j$ shown in figure (3.1) can be written as follows:

$$\frac{\partial F}{\partial x}(i,j)=\frac{1}{2\Delta x}\left[F(i+1,j)-F(i-1,j)\right] \tag{3.12}$$

$$\frac{\partial^2 F}{\partial x^2}(i,j)=\frac{1}{\Delta x^2}\left[F(i+1,j)-2F(i,j)+F(i-1,j)\right] \tag{3.13}$$

$$\frac{\partial^2 F}{\partial x\partial y}(i,j)=\frac{1}{4\Delta x\Delta y}\left[F(i+1,j+1)+F(i+1,j-1)-F(i-1,j+1)+\mathrm{F(i-1,j-1)}\right] \tag{3.14}$$

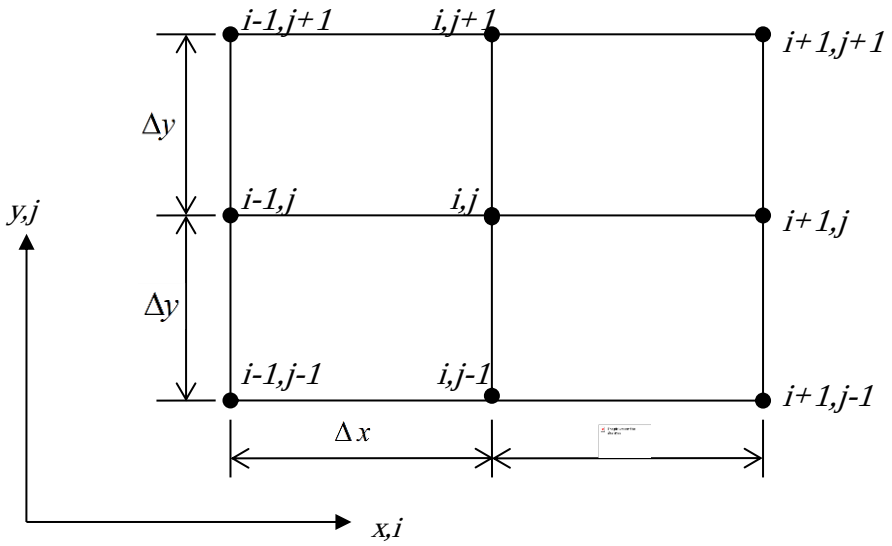


**Fig.3.1 Finite difference mesh for an interpolating function** $F(x,y)$ **with two independent variables** $x,y$

Also $\partial F(i,j)/\partial y$ And $\partial^2 F(i,j)/\partial y^2$ can be obtained similarly.

# 3.4 Finite difference form of plate equations

## 3.4.1 The velocity equations

According to equation (3.4) and from the equations of motion of the plate, i.e. Eqns. (3.7) – (3.11) , the velocities are determined as follows :-

$$\frac{du}{dt}(i,j)_n=\left(1+k_u^*\right)^{-1}\left[\left(1-k_u^*\right)\frac{du}{dt}(i,j)_{n-1}+\frac{\Delta t}{\rho_u(i,j)}F_u(i,j)\right] \tag{3.15}$$

$$\frac{dv}{dt}(i,j)_n=\left(1+k_v^*\right)^{-1}\left[\left(1-k_v^*\right)\frac{dv}{dt}(i,j)_{n-1}+\frac{\Delta t}{\rho_v(i,j)}F_v(i,j)\right] \tag{3.16}$$

$$\frac{dw}{dt}(i,j)_n = \left(1+k_w^*\right)^{-1}\left[\left(1-k_w^*\right)\frac{dw}{dt}(i,j)_{n-1} + \frac{\Delta t}{\rho_w(i,j)}F_w(i,j)\right] \tag{3.17}$$

$$\frac{d\phi}{dt}(i,j)_n = \left(1+k_\phi^*\right)^{-1}\left[\left(1-k_\phi^*\right)\frac{d\phi}{dt}(i,j)_{n-1} + \frac{\Delta t}{\rho_\phi(i,j)}F_\phi(i,j)\right] \tag{3.18}$$

$$\frac{d\psi}{dt}(i,j)_n = \left(1+k_\psi^*\right)^{-1}\left[\left(1-k_\psi^*\right)\frac{d\psi}{dt}(i,j)_{n-1} + \frac{\Delta t}{\rho_\psi(i,j)}F_\psi(i,j)\right] \tag{3.19}$$

Where $k_f^* = \dfrac{k_f \Delta t}{2\rho_f(i,j)}$ and $f$ is denoted by $u$, $v$, $w$, $\frac{dw}{dx}$ or $\psi$.

In Eqns. (3.15) – (3.19), $F_1(i,j)$ , $F_2(i,j)$, $F_3(i,j)$, $F_4(i,j)$ and $F_5(i,j)$ are the finite difference approximations of the terms on the left hand side of the dynamic Eqns. (3.7) – (3.11), i.e.

$$F_u(i,j) = \frac{1}{2\Delta x}\left[N_1(i+1,j) - N_1(i-1,j)\right] + \frac{1}{2\Delta y}\left[N_6(i,j+1) - N_6(i,j-1)\right]$$

$$F_v(i,j) = \frac{1}{2\Delta x}\left[N_6(i+1,j) - N_6(i-1,j)\right] + \frac{1}{2\Delta y}\left[N_2(i,j+1) - N_2(i,j-1)\right]$$

$$\begin{aligned} F_w(i,j) = {} & \frac{N_1(i,j)}{\Delta x^2}\left[w(i+1,j) - 2w(i,j) + w(i-1,j)\right] \\ & + \frac{N_6(i,j)}{2\Delta x\Delta y}\left[w(i+1,j+1) - w(i+1,j-1) - w(i-1,j+1) + w(i-1,j-1)\right] \\ & + \frac{N_2(i,j)}{\Delta y^2}\left[w(i,j+1) - 2w(i,j) + w(i,j-1)\right] + \left(\frac{a}{h}\right)^2 \frac{1}{2\Delta x}\left[Q_1(i+1,j) - Q_1(i-1,j)\right] \\ & + \left(\frac{a}{h}\right)^2 \frac{1}{2\Delta y}\left[Q_2(i,j+1) - Q_2(i,j-1)\right] + q(i,j) \end{aligned}$$

$$F_\phi(i,j) = \frac{1}{2\Delta x}\left[M_1(i+1,j) - M_1(i-1,j)\right] + \frac{1}{2\Delta y}\left[M_6(i,j+1) - M_6(i,j-1)\right] - \left(\frac{a}{h}\right)^2 Q_1(i,j)$$

$$F_\psi(i,j) = \frac{1}{2\Delta x}\left[M_6(i+1,j) - M_6(i-1,j)\right] + \frac{1}{2\Delta y}\left[M_2(i,j+1) - M_2(i,j-1)\right] - \left(\frac{a}{h}\right)^2 Q_2(i,j) \tag{3.20}$$

### 3.4.2 The displacement equations:

The displacements are obtained using the velocities that are explained in Eqns. (3.15) to (3.19) as follows:

$$f(i,j)_{n+\frac{1}{2}} = f(i,j)_{n-\frac{1}{2}} + \frac{d\alpha}{dt}(i,j)_n \Delta t \qquad (3.21)$$

Where $\alpha$ can be denoted by $u, v, w, \frac{dw}{dx}$ or $\psi$.

### 3.4.3 The stress resultants and couples equations:

The finite difference approximations of the stress resultants and stress couples can be obtained using Eqns. (2.26) and (2.27) in chapter 2 as stated below

$$N_1(i,j) = A_{11}\varepsilon_1^o(i,j) + A_{12}\varepsilon_2^o(i,j) + A_{16}\varepsilon_6^o(i,j) + B_{11}\chi_1^o(i,j) + B_{12}\chi_2^o(i,j) + B_{16}\chi_6^o(i,j) \qquad (3.22)$$

$$N_2(i,j) = A_{12}\varepsilon_1^o(i,j) + A_{22}\varepsilon_2^o(i,j) + A_{26}\varepsilon_6^o(i,j) + B_{12}\chi_1^o(i,j) + B_{22}\chi_2^o(i,j) + B_{26}\chi_6^o(i,j) \qquad (3.23)$$

$$N_6(i,j) = A_{16}\varepsilon_1^o(i,j) + A_{26}\varepsilon_2^o(i,j) + A_{66}\varepsilon_6^o(i,j) + B_{16}\chi_1^o(i,j) + B_{26}\chi_2^o(i,j) + B_{66}\chi_6^o(i,j) \qquad (3.24)$$

$$M_1(i,j) = B_{11}\varepsilon_1^o(i,j) + B_{12}\varepsilon_2^o(i,j) + B_{16}\varepsilon_6^o(i,j) + D_{11}\chi_1^o(i,j) + D_{12}\chi_2^o(i,j) + D_{16}\chi_6^o(i,j) \qquad (3.25)$$

$$M_2(i,j) = B_{12}\varepsilon_1^o(i,j) + B_{22}\varepsilon_2^o(i,j) + B_{26}\varepsilon_6^o(i,j) + D_{12}\chi_1^o(i,j) + D_{22}\chi_2^o(i,j) + D_{26}\chi_6^o(i,j) \qquad (3.26)$$

$$M_6(i,j) = B_{16}\varepsilon_1^o(i,j) + B_{26}\varepsilon_2^o(i,j) + B_{66}\varepsilon_6^o(i,j) + D_{16}\chi_1^o(i,j) + D_{26}\chi_2^o(i,j) + D_{66}\chi_6^o(i,j) \qquad (3.27)$$

$$Q_1(i,j) = A_{45}\varepsilon_4^o(i,j) + A_{55}\varepsilon_5^o(i,j) \qquad (3.28)$$

$$Q_2(i,j) = A_{44}\varepsilon_4^o(i,j) + A_{45}\varepsilon_5^o(i,j) \qquad (3.29)$$

### 3.4.4 Estimation of the fictitious variables:

To compute the derivatives of displacements, stress resultants and stress couples at the boundaries of a plate, fictitious nodes are considered by extending the finite difference mesh beyond the boundaries as shown in Fig.3.2. The values of the variables at the fictitious nodes are known as fictitious values. The fictitious values are estimated in order to eliminate the third derivative of the interpolating function, which is quadratic as explained in section 3.3.1.

Referring to Fig.3.3, the fictitious values at the points defined by (1,j) can be obtained by extrapolation as follows :

$$f(1,j) = 3f(2,j) - 3f(3,j) + f(4,j) \qquad (3.30)$$

Where *f* in Eqn. (3.34) can be replaced by *u, v, w,* $\phi$, and $\psi$.

## 3.5 The DR iterative procedure

In the DR technique, explained in the previous sections of this chapter, the static equations of the plate have been converted to dynamic equations i.e. Eqns. (3.7) – (3.11). Then the inertia and damping terms are added to all of these equations. The

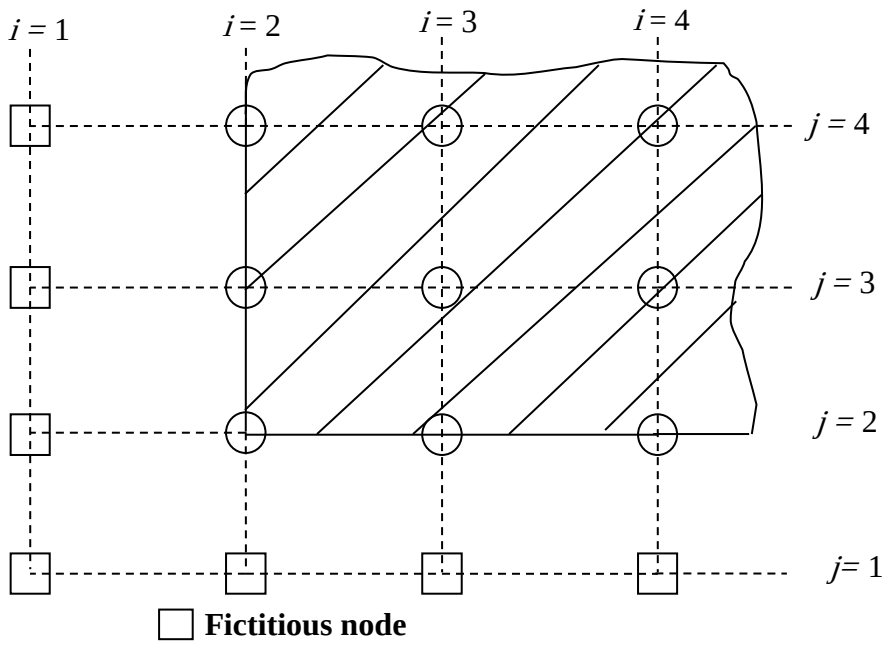


**Fig.3.2 Fictitious nodes outside the plate boundaries**.

iterations of the DR technique can then be carried out in following procedures:

1. Set all initial values of variables to zero.
2. Compute the velocities from Eqns. (3.15) – (3.19).
3. Compute the displacements from Eqn. (3.21).
4. Apply suitable boundary conditions for the displacements.
5. Compute the stress resultants and stress couples from Eqns. (3.22) to (3.29).
6. Apply the appropriate boundary conditions for the stress resultants and stress couples.
7. Check if the convergence criterion is satisfied, if it is not repeat the steps From 2 to 6.

It is obvious that this method requires five fictitious densities and a similar number of damping coefficients so as the solution will be converged correctly.

## 3.6 The fictitious densities:-

The computation of the fictitious densities based on the Gershgorin upper bound of the stiffness matrix of a plate is discussed in Ref.[52] . The fictitious densities vary from point to point over the plate as well as for each iteration, so as to improve the convergence of the numerical computations. The corresponding expressions for the computations of the fictitious densities are given in Appendix (D).

## 3.7 Remarks on the DR technique

The DR program is designed for the analysis of rectangular plates irrespective of material, geometry, edge conditions. The functions of the program are as follows: read the data file; compute the stiffness of the laminate, the fictitious densities, the velocities and displacements and the mid-plane deflections and stresses; check the stability of the numerical computations, the convergence of the solution, and the wrong convergence; compute through-thickness stresses in direction of plate axes; and transform through-thickness stresses in the lamina principal axes.

The convergence of the DR solution is checked, at the end of each itera-tion, by comparing the velocities over the plate domain with a predetermined value which ranges between $10^{-9}$ for small deflection and $10^{-6}$ for large deflection. When all velocities are smaller than the predetermined value, the solution is deemed converged and consequently the iterative procedure is terminated. Sometimes DR solution converges to invalid solution. To check for that the profile of variable is compared with the expected profile over the domain. For example when the value of the function on the boundaries is zero, and it is expected to increase from edge to center, then the solution should follow a similar profile. And when the computed profile is different from that expected, the solution is considered incorrect and can hardly be made to converge to the correct answer by altering the damping coefficients and time increment. Therefore, the boundary conditions should be examined and corrected if they are improper.

Time increment is a very important factor for speeding convergence and controlling numerical computations. When the increment is too small, the convergence becomes tediously slow; and when it is too large, the solution becomes unstable. The proper time increment in the present study it is taken as 0.8 for all boundary conditions.

The optimum damping coefficient is that which produces critical motion. When the damping coefficients are large, the motion is over damped and the convergence becomes very slow. And when the coefficients are small, the motion is under damped and can cause numerical instability. Therefore, the damping coefficients must be selected carefully to eliminate under damping and over damping.

The errors inherent in the DR technique include the discretization error which is due to the replacement of a continuous function with a discrete function, and an additional error because the discrete equations are not solved exactly due to the variations of the velocities from the edge of the plate to the center. Finer meshes reduce the discretization error, but increase the round-off error due to the large number of calculations involved. The last type of error is relative to the rank of the interpolating function employed i.e. quadratic, cubic, etc…

# CHAPTER (4)

# Verification of the computer program

The present DR results are compared with similar results generated by DR and/or alternative techniques including approximate analytical and exact solutions so as to validate the DR program. In the following discussion a wide spectrum of elastic comparison results of small and large deflections are dealt with including isotropic, orthotropic, and laminated plates subjected to static uniformly distributed loading.

## 4.1 Small deflection comparisons

Table A.1 (Appendix A) shows the variations in the center deflection of a moderately thick isotropic plate (h/a =0.1) with simply supported (SS5) conditions (see Appendix C) as the mesh size is progressively reduced. These results suggest that a 5×5 mesh over one quarter of the plate is adequate for the present work (i.e. less than 0.3% difference compared to the finest mesh result available). In Table A.2 comparisons of the DR deflections and stresses with Turvey and Osman [6] and Reddy [46] are presented for a uniformly loaded square and rectangular plates of thin (i.e. *h/a=0.01*), moderately thick (i.e. *h/a=0.1*), and thick laminates (i.e. *h/a=0.2*) with simply supported (SS5) conditions. In this analysis, the results provided are in good agreement with each other. Another comparison analysis for small deformation of thin and moderately thick Square simply supported isotropic plate (SS5) between the present DR, and Roufaeil [31] is shown in Table A.3. Again, these results provide further confirmation that a DR analysis based on a 5×5 quarter-plate mesh produces results of acceptable accuracy.

In the following analyses, several orthotropic materials were employed, and their properties are given in Table 4.1 below. Exact FSDT solutions are available for plates simply supported on all four edges (SS3).

**Table 4.1 Material properties used in the orthotropic plate comparison analysis**

| Material | $E_1/E_2$ | $G_2/E_2$ | $G_{13}/E_2$ | $G_{23}/E_2$ | $\nu_{12}$ | SCF $\left(k_4^2 = k_5^2\right)$ |
|---|---|---|---|---|---|---|
| I | 25.0 | 0.5 | 0.5 | 0.2 | 0.25 | 5/6 |
| II | 1.904 | 0.558 | 0.339 | 0.566 | 0.44 | 5/6 |
| III | 3.0 | 0.5 | 0.5 | 0.5 | 0.25 | 5/6 |
| IV | 2.345 | 0.289 | 0.289 | 0.289 | 0.32 | 5/6 |

By imposing only a small load on the plate, the DR program may be made to simulate these small deflection solutions. In Table A.4, the computations were made for uniform loads and for thickness/side ratio ranges between 0.2 to 0.01 of square simply supported in-plane free plates made of material I with ($\bar{q} = 1$) .In this case the center deflections of the present DR results are close to those of Turvey and Osman [7], and Reddy [46]. Another small deflection analysis comparison on Table A.5 was made for uniformly loaded plates with simply supported in-plane fixed (SS5) square and rectangular plates made of material II and subjected to uniform loading ($\bar{q} = 1$). In this instance the four sources of results agree on the central deflection, and the center stresses at upper and /or lower surface of the plate and corner mid-plane stresses. However the analytical solution of Srinivas and Rao [11] is not in good agreement with the others as far as stresses are concerned. These differences may be attributed to the different theory adopted in the analytical solution results of Ref. [11].

Most of the published literature on laminated plates are devoted to linear analysis and in particular to the development of higher-order shear deformation theories. Comparatively, there are few studies on the nonlinear behavior of laminated plates and even fewer are those, which include shear deformation. The elastic properties of the materials used in the analyses are given in Table 4.2 below. The shear correction factors are $k_4^2 = k_5^2 = 5/6$, unless otherwise stated.

**Table 4.2 Material properties used in the laminated plate comparison analysis**

| Material | $E_1/E_2$ | $G_2/E_2$ | $G_{13}/E_2$ | $G_{23}/E_2$ | $\nu_{12}$ | SCF $\left(k_4^2 = k_5^2\right)$ |
|---|---|---|---|---|---|---|
| I | 25.0 | 0.5 | 0.5 | 0.2 | 0.25 | 5/6 |
| V | 40.0 | 0.5 | 0.5 | 0.5 | 0.25 | 5/6 |
| VI | 14.3 | 0.5 | 0.5 | 0.5 | 0.3 | 5/6 |
| VII | 12.308 | 0.526 | 0.526 | 0.335 | 0.24 | 5/6 |
| VIII | 15.0 | 0.43 | 0.43 | 0.358 | 0.3 | 5/6 |

In Table A.6 which shows a comparison between the present DR, and finite element results Ref. [22] for a simply supported (SS4) four anti symmetric angle-ply plates made of material V and subjected to a small uniform load ($\bar{q} = 1.0$ ), the center deflections and stresses are recorded for different thickness ratios including thick, moderately thick and thin laminates which are compared with Reddy's finite element results [22]. There is a good agreement between the two sets of results in spite of the different theory adopted in latter case.

Another comparison analysis of central deflections between the present DR and Zenkour et al [29] using third order shear deformation theory with the help of the small parameter method and the results of Librescu and Khdeir [57] are illustrated in Table A.7. The three results showed a good agreement especially as the thickness ratio decreases.

## 4.2 Large deflection comparisons

Table A.8 shows deflections, stress resultants and stress couples in simply supported in-plane free (SS3) isotropic plate. The present results have been computed with 6×6 uniform meshes. These results are in a fairly good agreement with those of Aalami et al [12] using finite difference analysis (i.e. for deflections, the difference ranges between 0.35% at $\bar{q}$ =20.8 and 0 % as the pressure is increased to 97). A similar

comparison between the two results is shown in Table A.9 for simply supported (SS4) conditions. It is apparent that the center deflections, stress couples, and stress resultants agree very well. The mid-side stress resultants do not show similar agreement whilst the corner stress resultants show considerable differences. This may be attributed to the type of mesh used in each analysis.

Table A.10 shows comparison between the present analysis and Aalami et al [12] for clamped (CC2) edge conditions. Again, it is clear that the center deflections and stress resultants and /or couples agree reasonably well, though for the edge stress couples it is rather less good. This latter observation may, possibly, be explained by the fact that in the present analysis the mesh employed is uniform, whereas it is graded in Ref. [12] giving finer mesh spacing at the plate edges. Table A.11 shows deflections, stress resultants and stress couples for clamped in-plane fixed (CC3) edge conditions. It can be seen that the agreement between the present results and Aalami and Chapman [12] is fairly good except for the mid-side and, more particularly, the corner stress resultants. A similar set of results for the clamped in-plane free (CC1) case are given in Table A.12. In this case the present center values for deflections, stress couples and the mid-side couples approach are close to those of Ref. [12], whereas the central and mid-side stress resultants differ considerably from those of Ref. [12].

The final set of thin plate results comparisons presented here are with Rushton [13], who employed the DR method coupled with finite differences. The present results for simply supported (SS5) square plates were computed for two thickness ratios using an $8\times8$ uniform mesh and are listed in Table A.13. In this instant, the present results differ slightly from those found in Ref. [13]. A similar comparison for plates with clamped edges (CC5) is shown in Table A.14. In this case it is observed that the center deflection; and the stress at the upper and /or lower side of the plate are slightly different compared to those of Ref. [13] as the load applied is increased. Also, the mid- side stress at the upper and/ or lower side of the plate shows a considerable difference compared to Ref. [13] with the increase of the applied load.

These significant differences may be attributed to the less well-converged solution of the latter.

Another comparison for simply-supported (SS5) square isotropic plates subjected to uniformly distributed loads are shown in Tables A.15 and A.16 respectively for large deflection analysis of thin and moderately thick plates . In this comparison, it is noted that, the center deflections of the present DR analysis, and those of Azizian and Dawe [16] who employed the finite strip method are fairly good (i.e. with a maximum error not exceeding 0.09%).

There are two large deflection comparisons for orthotropic plates were made with the same DR program. In the first case, the DR center deflections of a thin square plate made of material III with clamped in-plane fixed edges (CC5) and subjected to a uniform load were compared with DR results of Turvey and Osman [7] and Chia's [58] . The comparison is shown in Table A.17. The three sets of results show a good agreement for lower and intermediate loads, but they differ slightly as the load is increased further. These differences are due to the employment of the classical laminated plate theory (CLPT) in the analytical solution of Chia's values, which is less accurate than FSDT.

In the second case the present DR results are compared with DR Ref. [7], Reddy's [59], and Zaghloul et al results [42]. For a thin uniformly loaded square plate made of material IV and with simply supported in-plane free (SS3) edges. The center deflections are presented in Table A.18 where the DR showed a good agreement with the other three.

The small and large deflection analyses confirm the accuracy and versatility of the DR program based on FSDT.

In Table A.19, comparisons are made with Chia's perturbation results based on the Von Karman plate theory [60] for 4 and 2-layer antisymmetric angle-ply clamped (CC1) plates made of material V and subjected to uniform load for thickness/length ratio equivalent to 0.02 .For a 4-layer laminate the present DR center deflections are slightly higher than Chia's results. Whereas, the contrary applies to the 2-laminate

results. These changes are partially due to the different plate theories used in the present analysis and Chia's results and partially due to the approximation of Chia's values as it is taken from a graph.

Putcha and Reddy [10] presented finite element results for symmetric and anti-symmetric square moderately thick plates (h/a =0.1). These results are compared with the present DR results in Tables A.20 and A.21. Table A.20 shows a comparison of the center deflections for a laminated plate [$0^0$ / $45^o$ /$-45^o$ /$90^o$ ] with clamped (CC5) edges. It is observed that the present DR results are slightly higher than that of Ref. [10]. Whereas in Table A.21, comparisons are made between the present DR, and finite element results Ref. [10] for the center deflection of a 2 and 8-layer antisymmetric angles-ply laminates made of material I. The plates are square, clamped (CC5), thick, and uniformly loaded. For a 2-layer laminate the present DR results differ greatly from those of Ref. [10]. Whereas, for 8-layer laminate, the present results differ slightly from those of Ref. [10].

Another analysis of thin large deflection plates was made by recomputing Sun and Chin's results [12] for [ $90_4^o$ /$0_4^o$] using the DR program and material VI. The results were obtained for one quarter of a plate using a 5×5 rectangular mesh, with shear correction factors $k_4^2 = k_5^2 = 5/6$. The analysis was made for different boundary conditions and the results were shown in Tables A.22, A.23, A.24, and A.25 as follows: the present DR deflections of the two-layer antisymmetric cross-ply simply supported in-plane fixed (SS5) are compared with DR results of Turvey and Osman [8] and with Sun and Chin's values for a range of loads as shown in Table A.22. The good agreement found confirms that for simply supported (SS5) edge conditions, the deflection depends on the direction of the applied load or the arrangement of the layers. Table A.23 shows a comparison between the present DR, and DR Ref. [8] results, which are approximately identical. The difference between the center deflection of the laminates [$0^o$/$90^o$] and [$90^o$/$0^o$] at b/a =5 is 0.3 % whilst it is 0% when b/a =1. Also Tables A.24 and A.25 give central deflections, which are in good agreement with the DR results Ref. [8]. In Table A.26 which shows a comparison

between the present DR, Kolli and Chandrashekhara finite element method [28] large deformation results for simply supported (SS5) four-layer symmetric rectangular laminates of cross-ply [$0^o$ /$90^o$ /$90^o$ /$0^o$] and angle-ply [$45^o$/-$45^o$/-$45^o$/$45^o$] orientations of material VIII subjected to uniform pressure ($\bar{q} = 11.432$) .The center deflections are completely identical for cross-ply laminates and differ slightly for angle-ply laminates. The comparisons made between DR and alternative techniques show a good agreement and hence the present DR large deflection program using uniform finite differences meshes can be employed with confidence in the analysis of moderately thick and thin flat isotropic, orthotropic or laminated plates under uniform loads. The program can be used with the same confidence to generate small deflection results.

# CHAPTER (5)

# Case Studies

With confidence in the DR program proved through the various verification exercises undertaken, it was decided to undertake some study cases and generate new results for uniformly loaded laminated rectangular plates. The plates were assumed to be either simply supported or clamped on all edges.

The effects of transverse shear deformation, material anisotropy, orientation, and coupling between stretching and bending on the deflections of laminated plates are investigated.

The material chosen has the following properties:

$E_1 = 137.9\,\mathrm{kN/mm^2}$, $E_2 = 9.653\,\mathrm{kN/mm^2}$, $G_{12} = 4.8265\,\mathrm{kN/mm^2}$, $\nu_{12} = 0.3$. It is assumed that $G_{12} = G_{13} = G_{23}$.

## 5.1 Effect of load

The variations of the center deflections, $\bar{w}_C$ with load, $\bar{q}$ for thin (*h/a = 0.02*) and thick (*h/a=0.2*) isotropic plates of simply supported in-plane fixed (SS5) condition are given in Table A.27, and Fig. B.1. It is observed that, the center deflections of thin and thick plates increase with the applied load, and that the deflections of thick plates are greater than those of thin plates under the same loading conditions. The difference in linear deflection is due to shear deformation effects which are significant in thick plates. Whereas, the non-linear deflection of thin and thick plates, which are nearly coincident, implies that the shear deformation effect vanishes as the load is increased.

## 5.2 Effect of length to thickness ratio

Table A.28 and Fig.B.2 contain numerical results and plots of center deflection versus length to thickness ratio of anti-symmetric cross-ply [0º/90º/0º/90º] and angle-ply [45º/-45º/45º/-45º] square plates under uniform lateral load ($\bar{q} = 1.0$) for two boundary conditions (i.e. simply supported (SS1) and clamped (CC1)). The maximum percentage difference in deflections for a range of length / thickness ratio

between 10 and 100, fluctuates between 35% for simply supported (SS1) cross-ply laminate and 73.3% for angle-ply laminate as the length/thickness ratio increases to a value of a/h = 40.0, and then become fairly constant. It is evident that shear deformation effect is significant for a/h < 40.0. It is obvious that shear deformation reduces as the length/thickness ratio increases. The orientation effect is clearly noticeable when the plate is simply supported while it is not apparent when the plate is clamped.

As shown in Table A.29 and Fig.B.3, the maximum percentage difference in deflection ($\bar{q} = 200.0$) for a range of length/ thickness ratio between 10 and 100 fluctuates between 6.36% for simply supported (SS1) cross-ply laminate and 38.7% for clamped (CC1) angle-ply laminate. This means that the center deflections become independent on the length/thickness ratio as the load gets larger.

## 5.3 Effect of number of layers

Fig.B.4 shows a plot of the maximum deflection of a simply supported (SS5) anti-symmetric cross-ply $[(0^o/90^o)_n]$ ($n=1,2,3,4,8$) square plates under uniformly distributed load of a moderately thick plate ($h/a = 0.1$). The numerical results are given in Table A.30. Two, four, six, eight, and sixteen-layer laminates are considered. The results show that as the number of layers increases, the plate becomes stiffer and the deflection becomes smaller. This is mainly due to the existence of coupling between bending and stretching which generally increases the stiffness of the plate as the number of layers is increased. When the number of layers exceeds 8, the deflection becomes independent on the number of layers. This is because the effect of coupling between bending and stretching does not change as the number of layers increases beyond 8 layers.

In Table A.31 and Fig. B.5, the deflection of simply supported (SS5) angle-ply plates $[(45^o/-45^o)_n]$ is given. Similar features can be noted as in the case of cross-ply plates $[(0^o/90^o)_n]$ mentioned above.

## 5.4 Effect of material anisotropy

According to Whitney and Pagano [44], the severity of shear deformation effects depends on the material anisotropy, $E_1/E_2$ of the layers.

The exact maximum deflections of clamped (CC5) four-layer symmetric cross-ply [$0^o/90^o/90^o/0^o$] and angle-ply [$45^o/-45^o/-45^o/45^o$] laminates are compared in Table A.32 and Fig.B.6 for various degrees of anisotropy. It is observed that, when the degree of anisotropy is small the deflection is large. As the degree of the anisotropy increases, the plate becomes stiffer. This may be attributed to the shear deformation effects which increase as the material anisotropy is decreased. When the degree of anisotropy becomes greater than 40.0, the deflection becomes approximately independent on the degree of anisotropy. This is due to the diminishing of the shear deformation effects and the dominance of bending effects.

The results in Table A.33 and the plot in Fig. B.7 is for simply supported (SS5) laminates which follow a similar behaviour but the deflections are relatively smaller. The apparent difference between the non-linear deflections of both clamped (CC5) and simply supported (SS5) symmetric laminates, as shown in Figs. B.6 and B.7 may be attributed to the different boundary conditions used in each case which either permits edge rotation or prohibits it.

## 5.5 Effect of fiber orientation

The variation of the maximum deflection, $\overline{w}_C$ with fiber orientation of a square laminated plate is shown in Table A.34 and Fig.B.8 for $\overline{q} = 120.0$, and *h/a = 0.1*. Four simply supported boundary conditions SS2, SS3, SS4 and SS5 are considered in this case. The non-linear curves SS2 and SS3 conditions show minimum deflection at $\theta = 45^o$ . However, this trend is different for a plate under SS4 and SS5 conditions in which the non-linear deflection increases with $\theta$. This is due to the in-plane fixed edges in the latter case. Also, the non-linear curves for clamped boundary conditions CC1, CC3, CC4 and CC5 as shown in Table A.35 and Fig.B.9 indicate the same trend as in the simply supported SS4 and SS5. These differences indicate that the type of end support is a determinant factor in the deflections for different orientations.

Another set of results showing the variation of center deflections, $\overline{w}_C$ with Load, $\bar{q}$ for a range of orientations is given in Tables A.36 and A.37, and Fig. B.10 and B.11.Table A.36 and Fig. B.10 show the variations in the center deflection of thick laminates (*h/a=0.2*) with load ranges between $\bar{q} = 20.0$ and $\bar{q} = 200.0$ for a simply supported (SS4), 4 – layer anti-symmetric square plate of orientation [ $\theta^o / -\theta^o / \theta^o / -\theta^o$ ]**.** It is noticed from Fig. B.10 that the deflection of thick laminates increases with the applied load as the angle of orientation is decreased (i.e. from $45^o$ to $0^o$) to a point where $60 < \bar{q} \le 70$ and then increases as the angle of orientation is increased beyond that point. This results in the inflection of the deflection curves at a point where $60 < \bar{q} \le 70$. This behaviour is caused by coupling between bending and stretching which arises as the angle of orientation increases.

Similar behaviour is exhibited by thick anti-symmetric clamped (CC3) laminates as shown in Table A.37 and Fig. B.11 but with a low response due to the different boundary conditions used in each case.

## 5.6 Effect of reversing lamination order

The DR deflections of two-layer anti-symmetric cross-ply [$0^o$/$90^o$] simply supported in-plane fixed (SS5) rectangular laminates are given in Table A.38 and plotted in Fig. B.12. The deflection of the plate with coupling stiffness $(B_{ij} = 0)$ is also shown for the sake of comparison. The percentage difference between the center deflections $\overline{w}_1[0^o / 90^o]$ and $\overline{w}_2[90^o / 0^o]$ at $\bar{q} = 20.0$ is 146.5%.whilst when $\bar{q} = 200.0$, it is 54.1%. It is obvious that the deflection depends on the direction of the applied load or the arrangement of the layers. The coupling stiffness $(B_{ij} = 0)$ serves as the limit between positive and negative coupling. For a positive coupling, the deflection increases as the magnitude of coupling increases. In other words, the apparent laminate bending stiffness decreases as the bending – extension coupling increases. Whereas, negative coupling is seen to stiffen the laminate. This contradicts the common notion that the bending – extension coupling lowers the laminate bending stiffness.

In a similar analysis, the deflection of an anti-symmetric angle-ply $\overline{w}_1[45^o/-45^o]$ and $\overline{w}_2[-45^o/45^o]$ simply supported in-plane fixed (SS5) laminates are shown in Table A.39 and Fig. B.13. There is no difference in deflection between $[45^o/-45^o]$ and $[-45^o/45^o]$ as in the case of $[0^o/90^o]$ and $[90^o/0^o]$. This comparison with laminate $(B_{ij}=0)$ indicates that coupling between bending and twisting always lowers the laminate bending stiffness of angle-ply laminates.

## 5.7 Effect of aspect ratio

Table A.40 and correspondingly Fig.B.14 show the variations in the maximum deflection of a two-layer anti-symmetric cross-ply and angle-ply $[45^o/-45^o]$ simply supported in-plane fixed (SS5) rectangular laminate under uniform load and with different aspect ratios ($\bar{q}=200.0$, and h/a =0.1). It is noticeable that, when the aspect ratio is small the deflection is small, and as the aspect ratio increases further beyond 2.0, the deflection becomes independent on the aspect ratio. This is due to coupling between bending and stretching which becomes fairly constant beyond b/a=2.0 and therefore the plate behaves as a beam.

## 5.8 Effect of boundary conditions

The type of boundary support is an important factor in determining the deflections of a plate along with other factors such as the applied load, the length / thickness ratio, the fiber orientation, etc.

Three sets of boundary conditions ranging between extreme in-plane fixed to in-plane free of an isotropic plate were considered and the results are given in Table A.41 and shown graphically in Fig. B.15. the variations of center deflection, $\overline{w}_C$ with load**,** $\bar{q}$ for thin (h/a =0.02) isotropic simply supported (SS1) and (SS5) and clamped (CC5) plates are given. It is observed that, for all cases the deflections increase with the load but at different rates depending on whether the plate is simply supported in-plane free or clamped. The deflection is a maximum when the plate is simply supported in-plane free and a minimum when the plate is clamped.

## 5.9 Effect of lamination scheme

In the present analysis the lamination scheme of plates is either symmetric or anti-symmetric. The anti-symmetric arrangement involves coupling between bending and stretching which affects greatly the deflections of both cross-ply and angle-ply laminates.

The variations of center deflection, $\overline{w}_C$ with load, $\bar{q}$ varying between 0 and 100 are given in Tables A.42 and A.43 and shown graphically in Figs. B.16 and B.17. The transverse central deflection of 4- layered square laminated plates with simply supported (SS2) boundary condition subjected to uniformly distributed load is shown in Table A.42 and Fig.B.16. The thickness of all layers is assumed equal. The results indicate that the anti-symmetric angle-ply $\left[45^o/-45^o/45^o/-45^o\right]$ laminate is stiffer than the symmetric one, and that the symmetric cross-ply laminate is stiffer than the anti-symmetric one. This phenomenon is caused by coupling between bending and stretching which lowers the deflections of anti-symmetric angle-ply laminates, and raises the deflections of anti-symmetric cross-ply plates.

Similar behaviour is shown by angle-ply laminates for clamped (CC2) condition. In the case of cross-ply laminates as given in Table A.43 and shown in Fig. B.17 the anti-symmetric cross-ply is stiffer than the symmetric one. This is due to the restrained edge rotation in this case.

# CHAPTER (6)

# Conclusions and Suggestions for Further Research

## 6.1 Conclusions:

A Dynamic Relaxation (DR) program based on finite differences has been developed for small and large deflection analysis of rectangular laminated plates using first order shear deformation theory (FSDT). The plate, which is assumed to consist of a number of orthotropic layers, is replaced by a single anisotropic layer and the displacements are assumed linear through the thickness of the plate. A series of numerical comparisons have been undertaken to demonstrate the accuracy of the DR program. Finally, a series of new results for uniformly loaded thin, moderately thick, and thick plates with simply supported and clamped edges have been presented. These results show the following:

1. The linear theory seriously over-predicts the deflection of plates.
2. The deformations of a plate are dependent on bending and extension in the nonlinear theory, whereas they are dependent on bending alone in the linear theory.
3. Convergence of the DR solution depends on several factors including boundary conditions, mesh size, the fictitious densities, and load.
4. Deflection is greatly dependent on plate length/ thickness ratio at small loads, and it becomes almost independent on that when the load is large.
5. As the number of layers in a plate increases, the plate becomes increasingly stiffer.
6. As the degree of anisotropy increases, the plate becomes stiffer and when it is greater than 40.0, the deflection becomes virtually independent on the degree of anisotropy.
7. Deflection of plates depends on the angle of orientation of individual plies. An increase of angle of orientation results in a decrease in the deflection at small loads and an increase in deflection at large loads.

8. Coupling between bending and stretching increases the deflection of [$0^o/90^o$] and decreases the deflection of [$90^o/0^o$] plates depending on whether it is positive or negative. Whereas, it always decreases the deflection of [$45^o/-45^o$] and [$-45^o/45^o$] plates. It also lowers the deflection of anti-symmetric angle-ply laminate [$45^o/-45^o/45^o/-45^o$] and increases that of anti-symmetric cross-ply laminate [$0^o/90^o/0^o/90^o$].
9. Deflection depends on the aspect ratio of plate. When the aspect ratio becomes greater than 2.0, the plate behaves as a beam, and therefore the deflection becomes independent on the aspect ratio.
10. As the edges of a plate are more restrained, the deflection decreases.

## 6.2 Suggestions for Further Research:

The topics, which require further investigations in the future, are:

1. The DR iterations suffer from instability when a plate is in-plane free and the load is large. Further work could be directed towards investigating the sources of instability.
2. Further investigations on the influence of coupling between bending and extension and/ or twisting on the response of laminated plates could be carried out.
3. Analysis of plates under concentrated load is another area of research which requires further study.

# References:


[1] Vernon B.john, Introduction to Engineering Materials, second edition, (1972).

[2] Williams D.G and Aalami B, Thin Plate Design for In-plane Loading, John Wily and Sons, New York, (1979).

[3] Sadhu Singh, Theory of Elasticity, Khanna Publishers, Delhi, (1988).

[4] Valerie J.Calderbank, A course on Programming in FORTRAN, The University Press, Cambridge, (1983).

[5] Jan Stegmann and Erik Lund, Notes on Structural Analysis of Composite Shell Structures, Aalborg University, Denmark, (2001).

[6] Turvey G.J. and Osman M.Y.,'Elastic Large Deflection Analysis of Isotropic Rectangular Mindlin Plates', International Journal of Mech. Sciences, Vol. 22, (1990), PP. 1 – 14.

[7] Turvey G.J. and Osman M.Y.,' Large Deflection Analysis of orthotropic Mindlin Plates', Proceedings of the 12th Energy – Resources Tech. Conference and Exhibition, Houston, Texas, (1989), PP. 163 – 172.

[8] Turvey G.J. and Osman M.Y.,'Large Deflection Effects in Antisymmetric Cross-ply Laminated Strips and Plates', I.H. Marshall, Composite Structures , Vol. 6, Paisley College, Scotland, Elsevier Science Publishers, (1991), PP.397 – 413.

[9] Phan N.D. and Reddy J.N., 'Analysis of Laminated Composite Plate using Higher-Order Shear Deformation Theory', International Journal of Numerical Method in Engineering, Vol. 21, (1985),PP. 2201 – 2219 .

[10] Putcha N.S. and Reddy J.N. ,'A refined Mixed Shear Flexible Finite Element for the Non-linear Analysis of Laminated Plates', Computers and Structures, Vol. 22, No. 4 , (1986),PP.529 – 538 .

[11] Srinivas S. and Rao A.K., 'Bending, Vibration and Buckling of Simply Supported Thick Orthotropic Rectangular Plates and Laminates', Vol.6, (1970), PP. 1463 – 1481.

[12] Aalami B. and Chapman J.C., 'Large Deflection Behavior of Rectangular Orthotropic Plates under Transverse and In-plane Loads', Proceedings of The Institution of Civil Engineers, (1969), 42, PP. 347- 382 .

[13] Rushton K.R.,' Large Deflexion of Variable-thickness Plates', International Journal of Mech. Sciences, Vol. 10, (1968), PP. 723 – 735.

[14] Gajbir Singh and Sadasiva Rao Y.V.K., 'Large Deflection Behavior of Thick Composite Plates', Composite Structures, Vol.8, (1987), PP. 13 – 29.

[15] Sun C.T. and Chin H., 'On Large Deflection Effects in Unsymmetric Cross-ply Composite Laminates', Journal of Composite Materials, Vol. 22, (1988), PP.1045 – 1059.

[16] Azizian Z.G. and Dawe D.J., 'Geometrically Non-linear Analysis of Rectangular Mindlin Plates using the Finite Strip Method', Computers and Structures, Vol. 22, No. 3, (1985), PP.423 – 436.

[17] Reddy J.N., 'A simple Higher-order Theory for Laminated Composite Plates', Journal of Applied Mechanics, Vol.51, No. 745, (1984),PP.745 – 752.

[18] Gorji M., ' On Large Deflection of symmetric Composite Plates under Static Loading', Institution of Mech. Engineering, Vol. 200, (1986), PP.13 – 19.

[19] Chuen – Yuan Chia, ' Large Deflection of Unsymmetrical Laminates with Mixed Boundary Conditions ', International Journal of Non-linear Mechanics, Vol. 20, No. 4, (1985), PP.273 – 282.

[20] Voyiadjis George Z. and Baluch Mohammed H., 'Refined Theory for Thick Composite Plate', Journal of Engineering Mechanics, Vol.11, No.4, (1988), PP.671 – 687.

[21] Mottram J.T., ' A simple Non-linear Analysis of Multi-layered Rectangular Plates ', Computers and Structures, Vol. 26, No.4, (1987), PP.597 – 608.

[22] Reddy J.N., 'A penalty Plate-bending Element for the Analysis of Laminated Anisotropic Composite Plates', International Journal for Numerical Methods in Engineering, Vol.15,(1980),PP. 1187 –1206.

[23] Reddy J.N. and Chao W.C., 'Non-linear Bending of Thick Rectangular, Laminated Composite Plates', International Journal of Non-linear Mechanics, Vol.16, No. 3/4, (1981), PP.291 – 301 .

[24] Sciuva M.Di, 'Bending, Vibration and Buckling of Simply Supported Thick Multilayered Orthotropic Plates: An Evaluation of A new Displacement Model', Journal of Sound and Vibration, Vol.105, No.3, (1986), PP.425 – 442.

[25] Chuen – Yuan Chia, 'Geometrically Non-linear Behavior of Composite Plates: A review ', Applied Mechanics Reviews, Vol. 41, No .12, (1988), PP.439 – 450.

[26] Ahmed K. Noor and Burton W. Scott, ' Assessment of Shear Deformation Theories for Multilayered Composite Plates', Applied Mechanics Reviews ,Vol. 42, No .1, (1989), PP.1 – 12.

[27] Sheng H.Y. and Ye J.Q.,'A semi-analytical Finite Element for Laminated Composite Plates', Composite Structures, Vol. 57, (2002), PP.117 – 123.

[28] Kolli M. and Chandrashekhara K., 'Finite Element Analysis of Stiffened Laminated Plates under Transverse Loading', Composites Science and Tech., Vol. 56, (1996), PP.1355 – 1361.

[29] Zenkour A.M. and Fares M.E., 'Non-homogeneous Response of Cross-ply laminated Elastic Plates using A higher Order Theory', Composite Structures, Vol. 44, (1999), PP.297 – 305.

[30] Yiu – Yin Lee and Chung – Fai Ng,'Non-linear Response of Composite Plates using the Finite Element Modal Reduction Method ', Engineering Structures, Vol. 23, (2001), PP.1104 – 1114.

[31] Onsy L. Roufaeil, Thanh Tran – Cong, "Finite Strip Elements for Laminated Composite Plates with Transverse Shear Strain Discontinuities', Composite Structures, Vol. 56, (2002), PP.249 – 258.

[32] Wang J., Liew K.M, Tan M.J., and Rajendran S.,' Analysis of Rectangular Laminated Composite Plates via FSDT Mesh less Method ', International Journal of Mechanical Sciences, Vol.44, (2002), PP. 1275 –1293.

[33] Hiroyuki Matsunaga, ' Assessment of A global Higher-order Deformation Theory for Laminated Composite and Sandwich Plates', Composite Structures ,Vol. 56, (2002), PP.279 – 291.

[34] Vuksanovic Dj., 'Linear Analysis of Laminated Composite Plates using Single Layer Higher-order Discrete Models', Composite Structures ,Vol. 48, (2000), PP.205 – 211.

[35] Edward A.Sadek, 'Some Serendipity Finite Elements for the Analysis of Laminated Plates', Computers and Structures, Vol.69, (1998), PP. 37 – 51.

[36] Prabhu Madabhusi – Raman, and Julio F.Davalos, 'Static Shear Correction Factor for laminated Rectangular Beams ', Composites: Part B 27B, (1996), PP.285 – 293.

[37] Reissner E. and Stavsky Y., 'Bending and Stretching of Certain Types of Heterogeneous Aeolotropic Plates', Journal of Applied Mechanics, Vol.28, (1961), PP.402 – 408.

[38] Constance P. Yang, Charles H.Norris and Yehuda Stavsky, ' Elastic Wave Propagation in Heterogeneous Plates', International Journal of Solids and Structures, Vol.2, (1966), PP.665 – 684.

[39] Ashton J.E., 'Approximate Solutions for Unsymmetrically Laminated Plates', Journal of Composite Materials, Vol.3, (1969), PP. 189 –191.

[40] Pagano N.J., 'Exact Solutions for Rectangular Bidirectional Composites and Sandwich Plates', Journal of Composite Materials, Vol.4, (1970), PP. 20 –34.

[41] Whitney J.M.,' The Effect of Transverse Shear Deformation on the Bending of Laminated Plates ', Journal of Composite Materials, Vol.3, (1969), PP. 534 –547.

[42] Zaghloul S.A. and Kennedy J.B., 'Nonlinear Behavior of Symmetrically Laminated Plates', Journal of Applied Mechanics, Vol.42, (1975), PP.234 – 236.

[43] Mindlin R.D., 'Influence of Rotary Inertia and Shear on Flexural Motions of Isotropic Elastic Plates', Journal of Applied Mechanics, (1951), PP.31 – 38.

[44] Whitney J.M. and Pagano N.J.,' Shear Deformation in Heterogeneous Anisotropic Plates ', Journal of Applied Mechanics, Vol.4, (1970), PP.1031 – 1036.

[45] Chia C.Y. and Prabhakara M.K., 'Large Deflection of Unsymmetric Cross-ply and Angle-ply Plates', Journal of Mechanical Engineering Science, Vol.18, No.4, (1976), PP. 179 –183.

[46] Reddy J.N., 'A refined Non-linear Theory of Plates with Transverse Shear Deformation', International Journal of Solids and Structures, Vol.20, No. 9/10, (1984), PP.881 – 896.

[47] Sayman O., 'Elasto-plastic Stress Analysis in Stainless Steel Fiber Reinforced Aluminum Metal Matrix Laminated Plates Loaded Transversely', Vol.43, (1998), PP.147 – 154.

[48] Kruis J., Matous K., and Dostal Z., 'Solving Laminated Plates by Domain Decomposition', Advances in Engineering Software, Vol.33, (2002), PP.445 – 452.

[49] Hui – Shen Shen, 'Large Deflection of Composite Laminated Plates under Transverse and In-plane Loads and Resting on Elastic Foundation', Composite Structures, Vol. 45, (1999), PP.115 – 123.

[50] Ying Qing Huang, Shenglin Di, Chang Chun Wu, and Huiya Sun, 'Bending Analysis of Composite Laminated Plates using A partially Hybrid Stress Element with Interlaminar Continuity ', Computer and Structures, Vol.80, (2002), PP.403 – 410.

[51] Sailendra N.Chatterjee and Satish V.Kulkarni, 'Shear Correction Factors for Laminated Plates', AIAA Journal, Vol.17, No.5, (1979), PP.498 – 499.

[52] Cassell A.C. and Hobbs R.E., 'Numerical Stability of Dynamic Relaxation Analysis of Nonlinear Structures ', International Journal for Numerical Methods in Engineering, Vol.35, No.4, (1966), PP. 1407 –1410.

[53] Day A.S., ' An Introduction to Dynamic Relaxation ', the Engineer, Vol.219, No.5688, (1965), PP.218 – 221.

[54] David Roylance ,'Introduction to Composite Materials', Department of Materials Science and Engineering, Massachusetts Institute of Tech., Cambridge, (2000).

[55] Haisler W.E, Stricklin J.A. and F.J. Stebbins, 'Development and Evaluation of Solution Procedures for Geometric Nonlinear Analysis', AIAA Journal, Vol.10, (1972), PP.264 – 267.

[56] Aalami B., 'Large Deflection of Elastic Plates under Patch Loading ', Journal of the Structural Division, ASCE, Vol.98, No.ST 11, (1972), PP.2567 – 2586.

[57] Librescu L, Khdeir A.A., 'Analysis of symmetric cross-ply laminated elastic plates using a higher-order theory. Part I –stress and displacement ', Composite Structure, Vol.9, (1988), PP. 189 – 213.

[58] Chia C.Y., 'Nonlinear analysis of plates ', McGraw – Hill, New York, (1980), PP. 227 – 288, 379.

[59] Reddy J.N., Energy and variational methods in applied mechanics, John Wiley and Sons, New York, (1984), PP. 379 – 387.

[60] Chia C.Y., 'Finite deflection of uniformly loaded, clamped rectangular anisotropic plates ', Journal of Mechanical Engineering Science, Vol. 18, No.4,( 1976), PP. 179 – 183.

# APPENDIX (A)

# Tables

**Table A.1** DR Solution convergence results for a simply supported (SS5) square plate subjected to uniform pressure $(\bar{q}=1, h/a=0.1 \text{ and } \nu=0.3)$

| Mesh size | $\overline{w}_C$ |
|---|---|
| 2 × 2 | 0.04437 |
| 3 × 3 | 0.04592 |
| 4 × 4 | 0.04601 |
| 5 × 5 | 0.04627 |
| 6 × 6 | 0.04629 |
| 7 × 7 | 0.04638 |
| 8 × 8 | 0.04640 |

**Table A.2** Comparison of present DR, Turvey and Osman [6], and exact values of Reddy [46] small deflection results for uniformly loaded simply supported (SS5) square and rectangular plates of various thickness ratios $(\bar{q}=1, \nu=0.3)$.

| *a/b* | *h/a* | *S* | $\overline{w}_c$ | $\overline{\sigma}_1(1)$ | $\overline{\sigma}_2(1)$ | $\overline{\sigma}_6(2)$ | $\overline{\sigma}_5(3)$ | $\overline{\sigma}_4(4)$ |
|---|---|---|---|---|---|---|---|---|
| 1 | 0.20 | 1 | 0.0529 | 0.2879 | 0.2879 | -0.2035 | 0.3983 | 0.3983 |
| | | 2 | 0.0529 | 0.2879 | 0.2879 | -0.2035 | 0.3984 | 0.3984 |
| | | 3 | 0.0536 | 0.2873 | 0.2873 | -0.1946 | 0.3928 | 0.3928 |
| | 0.10 | 1 | 0.0463 | 0.2866 | 0.2866 | -0.2038 | 0.3960 | 0.3960 |
| | | 2 | 0.0463 | 0.2865 | 0.2865 | -0.2038 | 0.3990 | 0.3990 |
| | | 3 | 0.0467 | 0.2873 | 0.2873 | -0.1946 | 0.3928 | 0.3928 |
| | 0.01 | 1 | 0.0440 | 0.2853 | 0.2853 | -0.2033 | 0.3960 | 0.3960 |
| | | 2 | 0.0441 | 0.2860 | 0.2860 | -0.2039 | 0.3990 | 0.3990 |
| | | 3 | 0.0444 | 0.2873 | 0.2873 | -0.1946 | 0.3928 | 0.3928 |
| 2 | 0.20 | 1 | 0.1204 | 0.2825 | 0.6165 | -0.2952 | 0.4230 | 0.5400 |
| | | 2 | 0.1216 | 0.2840 | 0.6225 | -0.2829 | 0.4341 | 0.5410 |
| | | 3 | 0.1248 | 0.2779 | 0.6100 | -0.2769 | 0.4192 | 0.5451 |

| | | | | | | | | |
|---|---|---|---|---|---|---|---|---|
| | 0.10 | 1 | 0.1111 | 0.2819 | 0.6148 | -0.2964 | 0.4200 | 0.5412 |
| | | 2 | 0.1122 | 0.2838 | 0.6209 | -0.2843 | 0.4358 | 0.5447 |
| | | 3 | 0.1142 | 0.2779 | 0.6100 | -0.2769 | 0.4192 | 0.5451 |
| | 0.01 | 1 | 0.1080 | 0.2823 | 0.6141 | -0.2970 | 0.4200 | 0.5400 |
| | | 2 | 0.1109 | 0.2842 | 0.6212 | -0.2857 | 0.4377 | 0.5472 |
| | | 3 | 0.1106 | 0.2779 | 0.6100 | -0.2769 | 0.4192 | 0.5451 |

S (1): Present DR results

S (2): DR results of Ref. [6].

S (3): Exact results of Ref. [46].

$(1)\,x=\frac{1}{2}a\,,y=\frac{1}{2}b,z=\frac{1}{2}h;(2)x=y=0,z=\frac{1}{2}h;(3)x=0,y=\frac{1}{2}b,z=0;(4)x=\frac{1}{2}a,y=z=0$

**Table A.3** Dimensionless central deflection of a square simply supported isotropic plate (SS5) $\left(\bar{q}=1.0\quad \nu=0.3\ ,k^2=0.833\right)$

| *a/h* | Present DR* Results | 3- Node strip Ref.[31] | 2-node strip Ref.[31] | Hinton E, Huang H as stated in Ref.[31] |
|---|---|---|---|---|
| 100 | 0.00403 | 0.00406 | 0.00406 | 0.00406 |
| 10 | 0.00424 | 0.00427 | 0.00426 | 0.00425 |

**Table A.4** Comparison of present DR , Turvey and Osman [7] , and Ref.[46] center deflections of a simply supported (SS3) square orthotropic plate made of material I for different thickness ratios when subjected to uniform loading $(\bar{q}=1.0)$.

| Thickness ratio *h/a* | Uniform Load | | |
|---|---|---|---|
| | $\bar{w}_C(DR)$ present | $\bar{w}_C(DR)$ Ref. [7] | $\bar{w}_C(exact)$ Ref. [46] |
| 0.2 | 0.017914 | 0.017912 | 0.018159 |
| 0.1 | 0.09444 | 0.09441 | 0.009519 |
| 0.08 | 0.008393 | 0.008385 | 0.008442 |
| 0.05 | 0.007245 | 0.007230 | 0.007262 |
| 0.02 | 0.006617 | 0.006602 | 0.006620 |
| 0.01 | 0.006512 | 0.006512 | 0.006528 |

**Table A.5** Comparison of present DR, Ref.[7] , Ref. [46], and exact solutions Ref.[11] for a uniformly loaded simply supported (SS5) orthotropic plate made of material II when subjected to uniform loading $(\bar{q} = 1.0)$.

| *b/a* | *h/a* | *S* | $\overline{w}_C$ | $\sigma_1(1)$ | $\sigma_5(2)$ |
|---|---|---|---|---|---|
| 1 | 0.05 | 1 | 0.0306 | 0.3563 | 0.4387 |
| | | 2 | 0.0306 | 0.3562 | 0.4410 |
| | | 3 | 0.0308 | 0.3598 | 0.4351 |
| | | 4 | 0.0308 | 0.3608 | 0.5437 |
| | 0.10 | 1 | 0.0323 | 0.3533 | 0.4393 |
| | | 2 | 0.0323 | 0.3534 | 0.4395 |
| | | 3 | 0.0326 | 0.3562 | 0.4338 |
| | | 4 | 0.0325 | 0.3602 | 0.5341 |
| | 0.14 | 1 | 0.0344 | 0.3498 | 0.4367 |
| | | 2 | 0.0344 | 0.3498 | 0.4374 |
| | | 3 | 0.0347 | 0.3516 | 0.5328 |
| | | 4 | 0.0346 | 0.3596 | 0.5223 |
| 2 | 0.05 | 1 | 0.0629 | 0.6569 | 0.5606 |
| | | 2 | 0.0629 | 0.6568 | 0.5637 |
| | | 3 | 0.0636 | 0.6550 | 0.5600 |
| | | 4 | 0.0636 | 0.6567 | 0.7024 |
| | 0.10 | 1 | 0.0657 | 0.6566 | 0.5623 |
| | | 2 | 0.0657 | 0.6566 | 0.5628 |
| | | 3 | 0.0665 | 0.6538 | 0.5599 |
| | | 4 | 0.0664 | 0.6598 | 0.6927 |
| | 0.14 | 1 | 0.0692 | 0.6564 | 0.5613 |
| | | 2 | 0.0692 | 0.6564 | 0.5613 |
| | | 3 | 0.0703 | 0.6521 | 0.5597 |
| | | 4 | 0.0701 | 0.6637 | 0.6829 |

S(1): Present DR results

S(2): DR results of Ref.[7].

S(3): Finite element solution Ref.[46].

S(4): Exact solution Ref.[11].

$(1)\, x = \frac{1}{2}a,\ y = \frac{1}{2}b,\ z = \frac{1}{2}h;\quad (2)\, x = 0,\ y = \frac{1}{2}b,\ z = 0$

**Table A.6** Comparison of present DR , and finite element results Ref. [22] for [45º/-45º/45º/-45º] simply supported (SS4) square laminate made of material V and subjected to uniform loads and for different thickness ratios ($\bar{q} = 1.0$).

| *h/a* | *S* | $\bar{w}_C \times 10^3$ | $\bar{\sigma}_1(1)$ |
|---|---|---|---|
| 0.2 | 1 | 9.0809 | 0.2022 |
| | 2 | 9.0000 | 0.1951 |
| 0.10 | 1 | 4.3769 | 0.2062 |
| | 2 | 4.2000 | 0.1949 |
| 0.05 | 1 | 3.2007 | 0.2081 |
| | 2 | 3.0000 | 0.1938 |
| 0.04 | 1 | 3.0574 | 0.2090 |
| | 2 | 2.9000 | 0.1933 |
| 0.02 | 1 | 2.8371 | 0.2063 |
| | 2 | 2.8000 | 0.1912 |

S (1): Present DR results

S (3): Reddy [22] as read from graph. (1) $x = y = \frac{1}{2}a, z = \frac{1}{2}h$ .

**Table A.7** Non-dimensionalized deflections in three layer cross-ply [0º/90º/0º] simply supported (SS5) square laminates under uniform load ($\bar{q} = 1.0$)

| *a/h* | *S* | $\bar{w}_C$ |
|---|---|---|
| 2 | 1 | 0.0693 |
| | 2 | 0.0726 |
| | 3 | 0.0716 |
| 5 | 1 | 0.0224 |
| | 2 | 0.0232 |
| | 3 | 0.0235 |
| 10 | 1 | 0.0147 |
| | 2 | 0.0150 |
| | 3 | 0.0151 |

| | | |
|---|---|---|
| 20 | 1 | 0.0127 |
| | 2 | 0.0128 |
| | 3 | 0.0128 |

S (1): Present DR results linear analysis

S (2): Librescu L and Khdeir A. A [57].

S (3):A.M.Zenkour, and M.E.Fares [29] results.

**Table A.8** Comparison of present DR, Aalami and Chapman's [12] large deflection results for a simply supported (SS3) square isotropic plate subjected to uniform pressure $\left( h/a = 0.02\ , \nu = 0.3 \right)$

| $\overline{q}$ | S | $\overline{w}_c$ | $\overline{M}_1(1)$<br>$\overline{M}_2(1)$ | $\overline{N}_1(1)$<br>$\overline{N}_2(1)$ |
|---|---|---|---|---|
| 20.8 | 1 | 0.7360 | 0.7357 | 0.7852 |
| | 2 | 0.7386 | 0.7454 | 0.8278 |
| 41.6 | 1 | 1.1477 | 1.0742 | 1.8436 |
| | 2 | 1.1507 | 1.0779 | 1.9597 |
| 63.7 | 1 | 1.4467 | 1.2845 | 2.8461 |
| | 2 | 1.4499 | 1.2746 | 3.0403 |
| 97.0 | 1 | 1.7800 | 1.4915 | 4.1688 |
| | 2 | 1.7800 | 1.4575 | 4.4322 |

S (1): Present DR results (6×6 uniform mesh over quarter of the plate)

S (2): Ref.[12] results (6×6 graded mesh over quarter of the plate)

*(1)* $x = y = \frac{1}{2}a,\ z = 0.$

**Table A.9** Comparison of present DR, Aalami and Chapman's [12] large deflection results for simply supported (SS4) square isotropic plate subjected to uniform pressure $\left( h/a = 0.02\ , \nu = 0.3 \right)$

| $\overline{q}$ | $S$ | $\overline{w}_c$ | $\overline{M}_1(1)$<br>$\overline{M}_2(1)$ | $N_1(1)$<br>$N_2(1)$ | $N_1(2)$<br>$N_2(3)$ | $N_1(3)$<br>$N_2(2)$ | $N_1(4)$<br>$N_2(4)$ |
|---|---|---|---|---|---|---|---|
| 20.8 | 1 | 0.5994 | 0.6077 | 1.0775 | 0.2423 | 1.1411 | 0.1648 |
| | 2 | 0.6094 | 0.6234 | 1.0714 | 0.2097 | 1.1172 | 0.2225 |
| 41.6 | 1 | 0.8613 | 0.8418 | 2.2435 | 0.5405 | 2.4122 | 0.3177 |
| | 2 | 0.8738 | 0.8562 | 2.2711 | 0.4808 | 2.4084 | 0.4551 |
| 63.7 | 1 | 1.0434 | 0.9930 | 3.3151 | 0.8393 | 3.6014 | 0.4380 |
| | 2 | 1.0572 | 1.0114 | 3.3700 | 0.7564 | 3.6172 | 0.6538 |
| 97.0 | 1 | 1.2411 | 1.1489 | 4.7267 | 1.2604 | 5.1874 | 0.5706 |
| | 2 | 1.2454 | 1.1454 | 4.8626 | 1.1538 | 2.2747 | 0.9075 |

S(1): Present DR results (6×6 uniform mesh over quarter of the plate)

S(2) : Ref.[12] results (6×6 graded mesh over quarter of the plate)

$(1)\, x = y = \frac{1}{2}a\ , z = 0; (2) x = \frac{1}{2}a, y = z = 0; (3) x = 0, y = \frac{1}{2}a, z = 0; (4) x = y = z = 0$

**Table A.10** Comparison of present DR, Aalami and Chapman's [12] large deflection results for simply supported (SS2) square isotropic plate subjected to uniform pressure $\left( h/a = 0.02\ , \nu = 0.3 \right)$

| $\overline{q}$ | S | $\overline{w}_c$ | $\overline{M}_1(1)$<br>$\overline{M}_2(1)$ | $\overline{M}_1(3)$<br>$\overline{M}_2(2)$ | $\overline{N}_1(1)$<br>$\overline{N}_2(1)$ |
|---|---|---|---|---|---|
| 20.8 | 1 | 0.2917 | 0.4305 | -0.9841 | 0.1584 |
| | 2 | 0.2793 | 0.4516 | -1.0502 | 0.1731 |
| 41.6 | 1 | 0.5422 | 0.7789 | -1.8592 | 0.5588 |
| | 2 | 0.5292 | 0.8340 | -2.0366 | 0.6099 |
| 63.7 | 1 | 0.7653 | 1.0687 | -2.6791 | 1.1116 |
| | 2 | 0.7549 | 1.1527 | -2.9925 | 1.2179 |

| | | | | | |
|---|---|---|---|---|---|
| 97.0 | 1 | 1.0381 | 1.3939 | -3.7454 | 2.0121 |
| | 2 | 1.0315 | 1.4990 | -4.2671 | 2.2070 |

S (1): Present DR results (6×6 uniform mesh over quarter of the plate)

S (2) : Ref.[12] results (6×6 graded mesh over quarter of the plate)

$(1)\, x = y = \frac{1}{2}a\,, z = 0; (2) x = \frac{1}{2}a, y = z = 0; (3) x = 0, y = \frac{1}{2}a, z = 0$

**Table A.11** Comparison of present DR, Aalami and Chapman's [12] large deflection results for Clamped (CC3) square isotropic plate subjected to uniform pressure $(h/a = 0.02\ , \nu = 0.3)$

| $\overline{q}$ | S | $\overline{w}_c$ | $\overline{M}_1(1)$ $\overline{M}_2(1)$ | $\overline{M}_1(3)$ $\overline{M}_2(2)$ | $\overline{N}_1(1)$ $\overline{N}_2(1)$ | $\overline{N}_1(3)$ $\overline{N}_2(2)$ | $\overline{N}_1(4)$ $N_2(4)$ |
|---|---|---|---|---|---|---|---|
| 20.8 | 1 | 0.2831 | 0.4169 | -0.9531 | 0.2469 | 0.2158 | 0.0541 |
| | 2 | 0.2850 | 0.4516 | -1.0169 | 0.2473 | 0.1648 | 0.1520 |
| 41.6 | 1 | 0.5064 | 0.7296 | -1.7251 | 0.8167 | 0.7267 | 0.1766 |
| | 2 | 0.5231 | 0.8063 | -1.9313 | 0.8233 | 0.5641 | 0.5156 |
| 63.7 | 1 | 0.6909 | 0.9751 | -2.3874 | 1.5380 | 1.3929 | 0.3299 |
| | 2 | 0.7234 | 1.1056 | -2.7986 | 1.5659 | 1.0989 | 0.9982 |
| 97.0 | 1 | 0.9031 | 1.2400 | -3.1816 | 2.6446 | 2.4480 | 0.5627 |
| | 2 | 0.9540 | 1.3522 | -3.9069 | 2.7015 | 1.9689 | 1.7766 |

S(1): Present DR results (6×6 uniform mesh over quarter of the plate)

S(2) : Ref.[12] results (6×6 graded mesh over quarter of the plate)

$(1)\, x = y = \frac{1}{2}a\,, z = 0; (2) x = \frac{1}{2}a, y = z = 0; (3) x = 0, y = \frac{1}{2}a, z = 0; (4) x = y = z = 0$

**Table A.12** Comparison of present DR, Aalami and Chapman's [12] large deflection results for Clamped (CC1) square isotropic plate subjected to uniform pressure $(h/a = 0.02\ , \nu = 0.3)$

| $\overline{q}$ | S | $\overline{w}_c$ | $M_1(1)$ $M_2(1)$ | $M_1(3)$ $M_2(2)$ | $N_1(1)$ $N_2(1)$ | $N_1(2)$ $N_2(3)$ |
|---|---|---|---|---|---|---|
| 20.8 | 1 | 0.2962 | 0.4380 | -0.9993 | 0.1139 | -0.1293 |
| | 2 | 0.2920 | 0.4655 | -1.0335 | 0.1401 | -0.1731 |

| | | | | | | |
|---|---|---|---|---|---|---|
| 41.6 | 1 | 0.5643 | 0.8120 | -1.9359 | 0.4129 | -0.4280 |
| | 2 | 0.5622 | 0.8756 | -2.0255 | 0.5073 | -0.6438 |
| 63.7 | 1 | 0.8163 | 1.1375 | -2.8669 | 0.8497 | -0.8423 |
| | 2 | 0.8169 | 1.2358 | -3.0202 | 1.0440 | -1.3645 |
| 97.0 | 1 | 1.1423 | 1.5149 | -4.21744 | 1.6044 | -1.5776 |
| | 2 | 1.1401 | 1.6403 | -4.3779 | 1.9505 | -2.6832 |

S(1): Present DR results (6×6 uniform mesh over quarter of the plate)

S(2) : Ref.[12] results (6×6 graded mesh over quarter of the plate)

$(1)\,\mathrm{x} = y = \frac{1}{2}\mathrm{a}\,,\ \mathrm{z} = 0; (2) x = \frac{1}{2}a,\ y = z = 0; (3) x = 0,\ y = \frac{1}{2}a,\ z = 0$

**Table A.13** Comparison of present DR, and Rushton's [13] large deflection results for a simply supported (SS5) square isotropic plate subjected to a uniform pressure $(\nu = 0.3)$.

| $\bar{q}$ | $S$ | $\bar{w}_C$ | $\bar{\sigma}_1(1)$ |
|---|---|---|---|
| 8.2 | 1 | 0.3172 | 2.3063 |
| | 2 | 0.3176 | 2.3136 |
| | 3 | 0.291 | 2.09 |
| 29.3 | 1 | 0.7252 | 5.9556 |
| | 2 | 0.7249 | 5.9580 |
| | 3 | 0.731 | 6.25 |
| 91.6 | 1 | 1.2147 | 11.3180 |
| | 2 | 1.2147 | 11.3249 |
| | 3 | 1.22 | 11.43 |
| 293.0 | 1 | 1.8754 | 20.749 |
| | 2 | 1.8755 | 20.752 |
| | 3 | 1.87 | 20.82 |

S (1): Present DR results (*h/a* =0.02; 8 × 8 uniform mesh over quarter of the plate)

S (2): Present DR results (*h/a* =0.01; 8×8 uniform mesh over quarter of the plate)

S (3): Ref. [13] results (thin plate 8×8 uniform mesh over quarter of the plate)

$(1)\ x = y = \frac{1}{2}a\ ,\ z = \frac{1}{2}h$

**Table A.14** Comparison of present DR, and Rushton's Ref. [14] large deflection results for clamped (CC5) square isotropic plate subjected to a uniform pressure $(\nu = 0.3)$.

| $\bar{q}$ | S | $\bar{w}_C$ | $\bar{\sigma}_1(1)$ | $\bar{\sigma}_1(2)$ |
|---|---|---|---|---|
| 9.2 | 1 | 0.1288 | 1.2567 | -2.6870 |
| | 2 | 0.1310 | 1.3100 | -2.8300 |
| 36.6 | 1 | 0.4568 | 4.8353 | -9.3458 |
| | 2 | 0.488 | 5.28 | -11.290 |
| 146.5 | 1 | 1.1525 | 13.6338 | -23.9843 |
| | 2 | 1.208 | 14.1 | -35.5 |
| 586.0 | 1 | 2.1429 | 29.4982 | -45.2634 |
| | 2 | 2.24 | 29.3 | -93.8 |
| 2344.0 | 1 | 3.5780 | 63.5551 | -68.4882 |
| | 2 | 3.74 | 62.8 | -222.0 |
| 9377.0 | 1 | 5.8130 | 142.8994 | -84.3537 |
| | 2 | 6.01 | 145.1 | -481.0 |

S (1): Present DR results ($h/a$ =0.02; 8 × 8 uniform mesh over quarter of the plate)

S (2): Ref. [13] results (thin plate 8×8 uniform mesh over quarter of the plate)

$(1)\, x = y = \frac{1}{2}a\,, z = \frac{1}{2}h;\ (2)\, x = 0, y = \frac{1}{2}a,\ z = \frac{1}{2}h;\ \ (3)\, x = y = \frac{1}{2}a, z = 0$

**Table A.15** Comparison of the present DR, and Azizian and Dawe's [16] large deflection results for thin shear deformable simply supported (SS5) square isotropic plates subjected to a uniform pressure ($h/a = 0.01$, $\nu = 0.3$).

| $\bar{q}$ | S | $\bar{w}_C$ |
|---|---|---|
| 9.2 | 1 | 0.34693 |
| | 2 | 0.34677 |
| 36.6 | 1 | 0.80838 |
| | 2 | 0.81539 |
| 146.5 | 1 | 1.45232 |
| | 2 | 1.46250 |

| | | |
|---|---|---|
| 586.1 | 1 | 2.38616 |
| | 2 | 2.38820 |

S (1): Present DR results (6 × 6 uniform mesh over quarter of the plate)

S (2): Azizian and Dawe [16] results.

**Table A.16** Comparison of the present DR, and Azizian and Dawe's [16] large deflection results for moderately thick shear deformable simply supported (SS5) square isotropic plates subjected to a uniform pressure (*h/a =0.05, v =0.3*).

| $\overline{q}$ | $S$ | $\overline{w}_C$ |
|---|---|---|
| 0.92 | 1 | 0.04106 |
| | 2 | 0.04105 |
| 4.6 | 1 | 0.19493 |
| | 2 | 0.19503 |
| 6.9 | 1 | 0.27718 |
| | 2 | 0.27760 |
| 9.2 | 1 | 0.34850 |
| | 2 | 0.34938 |

S (1): Present DR results (6 × 6 uniform mesh over quarter of the plate)

S (2): Azizian and Dawe [16] results.

**Table A.17** Pressure versus center deflection comparison for a square clamped (CC 5) orthotropic plate made of material III and subjected to uniform loading (*h/a* =0.02) .

| $\overline{q}$ | $\overline{w}_C(DR)$ | $\overline{w}_C$ (DR Ref. [8] ) | $\overline{w}_C(Chia's \text{ results}[58])$ |
|---|---|---|---|
| 82.0 | 0.556 | 0.5824 | 0.53 |
| 163.0 | 0.8815 | 0.9251 | 0.90 |
| 245.0 | 1.1030 | 1.1639 | 1.16 |
| 326.0 | 1.2700 | 1.3421 | 1.33 |
| 408.0 | 1.4100 | 1.4984 | 1.50 |

DR results (5 × 5 uniform mesh over quarter of the plate) of the present study.

DR results Ref. [8] (5×5 uniform mesh over quarter of the plate).

**Table A.18** Comparison of present DR , finite element results Ref. [59], and experimental results Ref. [42] for a uniformly loaded simply supported (SS3) square orthotropic plate made of material IV ($h/a$ =0.0115).

| $\bar{q}$ | $\bar{w}_C(1)$ | $\bar{w}_C(2)$ | $\bar{w}_C(3)$ | $\bar{w}_C(4)$ |
|---|---|---|---|---|
| 17.9 | 0.5859 | 0.5858 | 0.58 | 0.58 |
| 53.6 | 1.2710 | 1.2710 | 1.30 | 1.34 |
| 71.5 | 1.4977 | 1.4977 | 1.56 | 1.59 |
| 89.3 | 1.6862 | 1.6862 | 1.74 | 1.74 |

S (1): Present DR results (5 × 5 uniform non – interlacing mesh over quarter of the plate)

S (3): Reddy's finite element results [59].

S (4): Zaghloul's and Kennedy's Ref. [42] experimental results as read from graph.

**Table A.19** Comparison of present DR, and Chia's approximate analytical results for 4 and 2-layer anti-symmetric angle-ply clamped (CC1) plates made of material V and subjected to uniform pressure.

| $\bar{q}$ | NOL* | $\bar{w}_C$ (DR) | $\bar{w}_C$ (Chia's results [60]) |
|---|---|---|---|
| 500.0 | 4 | 0.5830 | 0.58 |
| | 2 | 1.1432 | 1.24 |
| 1000.0 | 4 | 1.1273 | 1.10 |
| | 2 | 1.8500 | 2.00 |
| 1500.0 | 4 | 1.6016 | 1.53 |
| 2000.0 | 4 | 2.0113 | 1.94 |

* Denote number of layers.

Present DR results: (($h/a$ = 0.02) 5×5 uniform mesh over quarter of the plate).

Chia's results: Results read from graph [60].

**Table A. 20** Comparison of present DR, and finite element Ref. [10] center deflections of quasi-isotropic [0º/45º/-45º/90º] clamped (CC5) square plates made of material V and subjected to uniform pressure. ($h/a$ =0.1).

| $\bar{q}$ | S | $\bar{w}_C$ |
|---|---|---|
| 50.0 | 1 | 0.19 |
| | 2 | 0.14 |

| | | |
|---|---|---|
| 100.0 | 1 | 0.32 |
| | 2 | 0.27 |
| 150.0 | 1 | 0.42 |
| | 2 | 0.37 |
| 200.0 | 1 | 0.51 |
| | 2 | 0.46 |
| 250.0 | 1 | 0.57 |
| | 2 | 0.53 |

S (1): Present DR results (5 × 5 uniform mesh over quarter of the plate)

S (2): Putcha and Reddy's finite element results Ref. [10] read from graph.

**Table A.21** Comparison of present DR , and finite element results Ref.[10] for a 2and 8-layer anti-symmetric angle-ply [45º/-45º/…] clamped (CC5) square plate made of material I and subjected to uniform pressure .($h/a$ = 0.1) .

| $\bar{q}$ | $S$ | $\overline{w}_C\left(NOL=2\right)$ | $\overline{w}_C\left(NOL=8\right)$ |
|---|---|---|---|
| 50.0 | 1 | 0.2919 | 0.2033 |
| | 2 | 0.2400 | 0.2100 |
| 100.0 | 1 | 0.4727 | 0.3677 |
| | 2 | 0.3700 | 0.3800 |
| 150.0 | 1 | 0.5979 | 0.4945 |
| | 2 | 0.4600 | 0.5000 |
| 200.0 | 1 | 0.6950 | 0.5962 |
| | 2 | 0.5300 | 0.6000 |
| 250.0 | 1 | 0.7753 | 0.6812 |
| | 2 | 0.5800 | 0.6800 |

S (1): Present DR results (5 × 5 uniform mesh over quarter of the plate)

S (2): Ref. [10] results read from graph.

*NOL:* Number of layers.

**Table A.22** Deflection of the center of a two-layer anti-symmetric cross- ply simply supported in-plane fixed (SS5) strip under uniform pressure ($b/a$ =5, h/a =0.01) .

| $\bar{q}$ | $S$ | $\bar{w}_1\left[0^o/90^\circ\right]$ | $\bar{w}_2\left[90^o/0^\circ\right]$ | $\bar{w}_o\left(B_{ij}=0\right)$ | %(1) | %(2) | %(3) |
|---|---|---|---|---|---|---|---|
| | 1 | 0.6851 | 0.2516 | | 131.4 | -15.0 | 172.3 |
| 18 | 2 | 0.6824 | 0.2544 | 0.2961 | 130.5 | -14.1 | 168.2 |
| | 3 | 0.6800 | 0.2600 | | | | |
| | 1 | 0.8587 | 0.3772 | | 88.1 | -17.4 | 127.7 |
| 36 | 2 | 0.8561 | 0.3822 | 0.4565 | 87.5 | -16.3 | 124.0 |
| | 3 | 0.8400 | 0.3900 | | | | |
| | 1 | 1.0453 | 0.5387 | | 61.0 | -17.0 | 94.0 |
| 72 | 2 | 1.0443 | 0.5472 | 0.6491 | 60.9 | -15.7 | 90.8 |
| | 3 | 1.0400 | 0.5500 | | | | |
| | 1 | 1.1671 | 0.6520 | | 50.0 | -16.2 | 79.0 |
| 108 | 2 | 1.1675 | 0.6630 | 0.7781 | 50.0 | -14.8 | 76.1 |
| | 3 | 1.1500 | 0.6600 | | | | |
| | 1 | 1.2611 | 0.7418 | | 43.6 | -15.5 | 70.0 |
| 144 | 2 | 1.2629 | 0.7551 | 0.8780 | 43.8 | -14.0 | 67.2 |
| | 3 | 1.2300 | 0.7600 | | | | |
| | 1 | 1.3390 | 0.8173 | | 39.3 | -14.9 | 63.8 |
| 180 | 2 | 1.3421 | 0.8327 | 0.9609 | 39.7 | -13.3 | 61.2 |
| | 3 | 1.0300 | 0.8400 | | | | |

S (1): Present DR results

S (2): DR results Ref. [8].

S (3): Values determined from Sun and Chin's graphical results Ref. [15].

(1) : $100\times\left(\bar{w}_1-\bar{w}_o\right)/\bar{w}_o$ .

(2) : $100\times\left(\bar{w}_2-\bar{w}_o\right)/\bar{w}_o$ .

(3) : $100\times\left(\bar{w}_1-\bar{w}_2\right)/\bar{w}_2$ .

**Table A.23** Center deflection of two-layer anti-symmetric cross-ply simply supported in-plane free (SS1) plate under uniform pressure and with different aspect ratios ($h/a$ =0.01; $\bar{q}=18$).

| $b/a$ | $S$ | $\overline{w}_1\left[0^o/90^\circ\right]$ | $\overline{w}_2\left[90^o/0^\circ\right]$ | $\overline{w}_o\left(B_{ij}=0\right)$ | %(1) | %(2) | %(3) |
|---|---|---|---|---|---|---|---|
| 5.0 | 1 | 0.8691 | 0.8718 | 0.3764 | 130.9 | 131.6 | -0.3 |
| | 2 | 0.8683 | 0.8709 | 0.3764 | 129.1 | 130.2 | -0.3 |
| 4.0 | 1 | 0.8708 | 0.8758 | 0.3801 | 129.1 | 129.1 | -0.6 |
| | 2 | 0.8708 | 0.8757 | 0.3801 | 129.1 | 130.4 | -0.6 |
| 3.0 | 1 | 0.8591 | 0.8677 | 0.3883 | 121.2 | 123.5 | -1.0 |
| | 2 | 0.8593 | 0.8678 | 0.3883 | 121.3 | 123.5 | -1.0 |
| 2.5 | 1 | 0.8325 | 0.8422 | 0.3907 | 113.1 | 115.6 | -1.15 |
| | 2 | 0.8328 | 0.8424 | 0.3907 | 113.2 | 115.6 | -1.1 |
| 2.0 | 1 | 0.7707 | 0.7796 | 0.3807 | 102.4 | 104.8 | -1.14 |
| | 2 | 0.7712 | 0.7799 | 0.3807 | 102.6 | 104.9 | -1.1 |
| 1.75 | 1 | 0.7173 | 0.7248 | 0.3640 | 97.0 | 99.1 | -1.0 |
| | 2 | 0.7169 | 0.7251 | 0.3640 | 97.0 | 99.2 | -1.1 |
| 1.5 | 1 | 0.6407 | 0.6460 | 0.3335 | 92.1 | 93.7 | -0.82 |
| | 2 | 0.6407 | 0.6455 | 0.3325 | 92.7 | 94.1 | -0.70 |
| 1.25 | 1 | 0.5324 | 0.5346 | 0.2781 | 91.4 | 92.2 | -0.4 |
| | 2 | 0.5325 | 0.5347 | 0.2782 | 91.4 | 92.2 | -0.4 |
| 1.0 | 1 | 0.3797 | 0.3797 | 0.1946 | 95.1 | 95.1 | 0.0 |
| | 2 | 0.3796 | 0.3796 | 0.1949 | 94.8 | 94.8 | 0.0 |

S (1): Present DR results

S (2): DR results Ref.[8].

(1): $100\times\left(\overline{w}_1-\overline{w}_o\right)/\overline{w}_o$.

(2): $100\times\left(\overline{w}_2-\overline{w}_o\right)/\overline{w}_o$.

(3): $100\times\left(\overline{w}_1-\overline{w}_2\right)/\overline{w}_2$.

**Table A.24** Center deflection of a two-layer anti-symmetric cross-ply clamped in-plane free (CC1) plate with different aspect ratios ($h/a$ =0.01; $\bar{q}=18$) .

| *b/a* | *S* | $\overline{w}_1\left[0^o/90^\circ\right]$ | $\overline{w}_2\left[90^o/0^\circ\right]$ | $\overline{w}_o\left(B_{ij}=0\right)$ | %(1) | %(2) | %(3) |
|---|---|---|---|---|---|---|---|
| 5.0 | 1 | 0.1765 | 0.1766 | 0.0768 | 129.8 | 129.9 | 0.0 |
| | 2 | 0.1766 | 0.1767 | 0.0767 | 130.2 | 130.2 | 0.0 |
| 4.0 | 1 | 0.1770 | 0.1771 | 0.0772 | 129.3 | 129.4 | 0.0 |
| | 2 | 0.1770 | 0.1771 | 0.0770 | 129.9 | 130.0 | 0.0 |
| 3.0 | 1 | 0.1777 | 0.1780 | 0.0778 | 128.4 | 128.8 | 0.0 |
| | 2 | 0.1777 | 0.1780 | 0.0777 | 128.7 | 129.1 | 0.0 |
| 2.5 | 1 | 0.1776 | 0.1780 | 0.0782 | 127.1 | 127.6 | -0.2 |
| | 2 | 0.1776 | 0.1780 | 0.0781 | 127.4 | 127.9 | -0.2 |
| 2.0 | 1 | 0.1743 | 0.1747 | 0.0776 | 124.6 | 125.1 | -0.2 |
| | 2 | 0.1743 | 0.1747 | 0.0775 | 124.9 | 125.4 | -0.2 |
| 1.75 | 1 | 0.1686 | 0.1689 | 0.0757 | 122.7 | 123.1 | -0.2 |
| | 2 | 0.1685 | 0.1689 | 0.0755 | 123.2 | 123.7 | -0.2 |
| 1.5 | 1 | 0.1563 | 0.1565 | 0.0708 | 120.8 | 121.0 | -0.1 |
| | 2 | 0.1862 | 0.1564 | 0.0707 | 120.9 | 121.2 | -0.1 |
| 1.25 | 1 | 0.1325 | 0.1326 | 0.0606 | 118.6 | 118.8 | 0.0 |
| | 2 | 0.1324 | 0.1325 | 0.0605 | 118.8 | 119.0 | 0.0 |
| 1.0 | 1 | 0.0932 | 0.0932 | 0.0428 | 117.8 | 117.8 | 0.0 |
| | 2 | 0.0931 | 0.0931 | 0.4280 | 117.5 | 117.5 | 0.0 |

S (1): Present DR results

S (2): DR results Ref.[8].

(1):$100\times\left(\overline{\mathrm{w}}_1-\overline{\mathrm{w}}_{\mathrm{o}}\right)/\overline{\mathrm{w}}_{\mathrm{o}}$.

(2): $100\times\left(\overline{\mathrm{w}}_2-\overline{\mathrm{w}}_{\mathrm{o}}\right)/\overline{\mathrm{w}}_{\mathrm{o}}$.

(3): $100\times\left(\overline{\mathrm{w}}_1-\overline{\mathrm{w}}_2\right)/\overline{\mathrm{w}}_2$.

**Table A.25** Center deflection of two-layer anti-symmetric cross-ply clamped in -plane (CC5) rectangular plate with different aspect ratios ($h/a$ =0.01).

| $b/a$ | $S$ | $\bar{q}$ | $\bar{w}_1\left[0^o/90^\circ\right]$ | $\bar{w}_2\left[90^o/0^\circ\right]$ | $\bar{w}_o\left(B_{ij}=0\right)$ | %(1) | %(2) | %(3) |
|---|---|---|---|---|---|---|---|---|
| 5.0 | 1 | 18 | 0.1706 | 0.1706 | 0.0767 | 122.4 | 122.4 | 0.0 |
| | | 72 | 0.4945 | 0.4947 | 0.2934 | 68.5 | 68.6 | 0.0 |
| | | 180 | 0.8031 | 0.8033 | 0.6060 | 32.5 | 32.6 | 0.0 |
| | 2 | 18 | 0.1708 | 0.1708. | 0.0768 | 122.4 | 122.4 | 0.0 |
| | | 72 | 0.4947 | 0.4949 | 0.3073 | 61.0 | 61.0 | 0.0 |
| | | 180 | 0.8034 | 0.8036 | 0.7684 | 4.6 | 4.6 | 0.0 |
| 4.0 | 1 | 18 | 0.1710 | 0.1710 | 0.0770 | 122.1 | 122.1 | 0.0 |
| | | 72 | 0.4953 | 0.4953 | 0.2943 | 68.3 | 68.3 | 0.0 |
| | | 180 | 0.8037 | 0.8040 | 0.6073 | 32.3 | 32.3 | 0.0 |
| | 2 | 18 | 0.1712 | 0.1712 | 0.0771 | 122.0 | 122.0 | 0.0 |
| | | 72 | 0.4955 | 0.4957 | 0.3084 | 60.7 | 60.7 | 0.0 |
| | | 180 | 0.8040 | 0.8044 | 0.7711 | 4.3 | 4.3 | 0.0 |
| 3.0 | 1 | 18 | 0.1720 | 0.1720 | 0.0776 | 121.6 | 121.6 | 0.0 |
| | | 72 | 0.4974 | 0.4974 | 0.2967 | 67.6 | 67.6 | 0.0 |
| | | 180 | 0.8059 | 0.8065 | 0.6111 | 31.9 | 32.0 | 0.0 |
| | 2 | 18 | 0.1720 | 0.1720 | 0.0777 | 120.4 | 120.4 | 0.0 |
| | | 72 | 0.4976 | 0.4979 | 0.3110 | 60.0 | 60.0 | 0.0 |
| | | 180 | 0.8062 | 0.8068 | 0.7771 | 3.7 | 3.7 | 0.0 |
| 2.5 | 1 | 18 | 0.1722 | 0.1722 | 0.0781 | 120.5 | 120.5 | 0.0 |
| | | 72 | 0.4994 | 0.4994 | 0.2985 | 67.3 | 67.3 | 0.0 |
| | | 180 | 0.8083 | 0.8090 | 0.6150 | 31.4 | 31.5 | 0.0 |
| | 2 | 18 | 0.1723 | 0.1722 | 0.0781 | 120.6 | 120.6 | 0.0 |
| | | 72 | 0.4996 | 0.4999 | 0.3126 | 59.8 | 59.9 | 0.0 |
| | | 180 | 0.8086 | 0.8093 | 0.7802 | 3.6 | 3.7 | 0.0 |
| 2.0 | 1 | 18 | 0.1698 | 0.1698 | 0.0776 | 118.8 | 118.8 | 0.0 |
| | | 72 | 0.4997 | 0.4997 | 0.2976 | 67.9 | 67.9 | 0.0 |
| | | 180 | 0.8103 | 0.8110 | 0.6170 | 31.3 | 31.4 | 0.0 |
| | 2 | 18 | 0.1699 | 0.1697 | 0.0775 | 119.2 | 119.2 | 0.0 |
| | | 72 | 0.4999 | 0.4999 | 0.3101 | 61.2 | 61.2 | 0.0 |
| | | 180 | 0.8106 | 0.8113 | 0.7711 | 5.1 | 5.1 | 0.0 |

| | | | | | | | | |
|---|---|---|---|---|---|---|---|---|
| 1.75 | 1 | 18 | 0.1649 | 0.1649 | 0.0756 | 118.1 | 118.1 | 0.0 |
| | | 72 | 0.4947 | 0.4947 | 0.2917 | 69.6 | 69.6 | 0.0 |
| | | 180 | 0.8072 | 0.8078 | 0.6113 | 32.0 | 32.0 | 0.0 |
| | 2 | 18 | 0.1650 | 0.1648 | 0.0756 | 118.3 | 118.0 | 0.0 |
| | | 72 | 0.4949 | 0.4948 | 0.3022 | 63.8 | 63.8 | 0.0 |
| | | 180 | 0.8075 | 0.8081 | 0.7492 | 7.8 | 7.9 | 0.0 |
| 1.5 | 1 | 18 | 0.1539 | 0.1539 | 0.0708 | 117.4 | 117.4 | 0.0 |
| | | 72 | 0.4778 | 0.4778 | 0.2753 | 73.6 | 73.6 | 0.0 |
| | | 180 | 0.7918 | 0.7922 | 0.5895 | 34.3 | 34.4 | 0.0 |
| | 2 | 18 | 0.1539 | 0.1537 | 0.0707 | 117.7 | 117.7 | 0.0 |
| | | 72 | 0.4780 | 0.4778 | 0.2828 | 69.0 | 69.0 | 0.0 |
| | | 180 | 0.7921 | 0.7925 | 0.6993 | 13.3 | 13.3 | 0.0 |
| 1.25 | 1 | 18 | 0.1313 | 0.1313 | 0.0605 | 117.0 | 117.0 | 0.0 |
| | | 72 | 0.4330 | 0.4330 | 0.2383 | 81.7 | 81.7 | 0.0 |
| | | 180 | 0.7430 | 0.7432 | 0.5301 | 40.2 | 40.2 | 0.0 |
| | 2 | 18 | 0.1314 | 0.1312 | 0.0605 | 117.2 | 116.9 | 0.0 |
| | | 72 | 0.4331 | 0.4330 | 0.2420 | 79.0 | 79.0 | 0.0 |
| | | 180 | 0.7432 | 0.7434 | 0.5992 | 24.0 | 24.1 | 0.0 |
| 1.0 | 1 | 18 | 0.0927 | 0.0927 | 0.0428 | 116.6 | 116.6 | 0.0 |
| | | 72 | 0.3347 | 0.3347 | 0.1702 | 96.7 | 96.7 | 0.0 |
| | | 180 | 0.6207 | 0.6207 | 0.4012 | 54.7 | 54.7 | 0.0 |
| | 2 | 18 | 0.0928 | 0.0928 | 0.0428 | 116.8 | 116.8 | 0.0 |
| | | 72 | 0.3348 | 0.3348 | 0.1711 | 95.7 | 95.7 | 0.0 |
| | | 180 | 0.6210 | 0.6210 | 0.4261 | 45.7 | 45.7 | 0.0 |

S (1): Present DR results

S (2): DR results Ref. [8].

%(1): $100\times(\overline{w}_1-\overline{w}_o)/\overline{w}_o$.

%(2): $100\times(\overline{w}_2-\overline{w}_o)/\overline{w}_o$.

%(3): $100\times(\overline{w}_1-\overline{w}_2)/\overline{w}_2$.

**Table A.26** Comparison of the present DR method and M.Kolli and K.chandrashekhara [28] large deformation results for simply supported (SS5) four layer symmetric rectangular laminates of cross-ply [0º/90º/90º/0º] and angle-ply [45º/-45º/-45º/45º] subjected to uniform pressure . ($b/a = 2$, $a/h = 20$, $\nu = 0.3$).

| $\bar{q}$ | $S$ | $\overline{w}_C$ | |
|---|---|---|---|
| | | 0º/90º/90º/0º | 45/-45/-45/45 |
| 11.432 | 1 | 0.15 | 0.23 |
| | 2 | 0.15 | 0.25 |

S (1): present DR results.

S (2): results of Ref. [28].

**Table A.27** Variation of central deflection $\overline{w_c}$ with load, $\bar{q}$ of thin (h/a = 0.02) and thick (h/a =0.2) isotropic plates of simply supported (SS5) condition $(\nu = 0.3)$.

| $\bar{q}$ | S | $\overline{w_c}$ | |
|---|---|---|---|
| | | h/a =0.02 | h/a = 0.2 |
| 20 | 1 | 0.8856 | 1.0635 |
| | 2 | 0.5846 | 0.6159 |
| 40 | 1 | 1.7708 | 2.1271 |
| | 2 | 0.8432 | 0.8626 |
| 60 | 1 | 2.6562 | 3.1906 |
| | 2 | 1.0138 | 1.0262 |
| 80 | 1 | 3.5416 | 4.2542 |
| | 2 | 1.1447 | 1.1526 |
| 100 | 1 | 4.4270 | 5.3177 |
| | 2 | 1.2527 | 1.2573 |
| 120 | 1 | 5.3125 | 6.3812 |
| | 2 | 1.3455 | 1.3478 |
| 140 | 1 | 6.1979 | 7.4448 |
| | 2 | 1.4275 | 1.4279 |
| 160 | 1 | 7.0833 | 8.5083 |
| | 2 | 1.5012 | 1.5001 |
| 180 | 1 | 7.9685 | 9.578 |
| | 2 | 1.5685 | 1.5662 |
| 200 | 1 | 8.8541 | 10.6354 |
| | 2 | 1.6306 | 1.6274 |

S (1): *Linear*

S (2): *Nonlinear*

**Table A.28** A comparison of the non-dimensionalized center deflections Vs. side to thickness ratio of a four layered anti-symmetric cross-ply [0º/90º/0º/90º] and angle-ply [45º/-45º/45º/-45º] square laminates under uniform lateral load ($\bar{q}$ =1.0)

| *a/h* | $\overline{w_c}$ | | | |
|---|---|---|---|---|
| | SS1 | | CC1 | |
| | [0º/90º/0º/90º] | [45º/-45º/45º/-45º] | [0º/90º/0º/90º] | [45º/-45º/45º/-45º] |
| 10 | 0.0148 | 0.0115 | 0.0045 | 0.0048 |
| 15 | 0.0138 | 0.0102 | 0.0035 | 0.0037 |
| 20 | 0.0134 | 0.0097 | 0.0032 | 0.0032 |
| 25 | 0.0133 | 0.0095 | 0.0030 | 0.0030 |
| 30 | 0.0132 | 0.0094 | 0.0029 | 0.0029 |
| 35 | 0.0131 | 0.0093 | 0.0029 | 0.0029 |
| 40 | 0.0131 | 0.0092 | 0.0028 | 0.0028 |
| 50 | 0.0130 | 0.0092 | 0.0028 | 0.0028 |
| 80 | 0.0130 | 0.0091 | 0.0027 | 0.0027 |
| 100 | 0.0130 | 0.0091 | 0.0027 | 0.0027 |

**Table A.29** A comparison of the non-dimensionalized center deflections vs. side to thickness ratio of a four layered anti-symmetric cross-ply [0º/90º/0º/90º] and angle-ply [45º/-45º/45º/-45º] square laminates under uniform lateral load. ($\bar{q}$ =200.0)

| *a/h* | $\overline{w_c}$ | | | |
|---|---|---|---|---|
| | SS1 | | CC1 | |
| | [0º/90º/0º/90º] | [45º/-45º/45º/-45º] | [0º/90º/0º/90º] | [45º/-45º/45º/-45º] |
| 10 | 1.8682 | 1.6788 | 0.8488 | 0.8874 |
| 15 | 1.8027 | 1.5700 | 0.6842 | 0.7152 |
| 20 | 1.7792 | 1.5144 | 0.6225 | 0.6447 |
| 25 | 1.7682 | 1.4860 | 0.5932 | 0.6092 |
| 30 | 1.7622 | 1.4697 | 0.5771 | 0.5889 |
| 35 | 1.7585 | 1.4595 | 05673 | 05763 |
| 40 | 1.7562 | 1.4528 | 0.5609 | 0.5679 |
| 50 | 1.7534 | 1.4446 | 0.5534 | 0.5578 |
| 80 | 1.7504 | 1.4356 | 0.5451 | 0.5467 |
| 100 | 1.7497 | 1.4335 | 05432 | 0.5440 |

**Table A.30** Number of layers effect on a simply supported (SS5) anti-symmetric cross-ply [$(0^o/90^o)_n$] square plate under uniformly distributed loads. ($h/a$ = 0.1)

| $\bar{q}$ | $\overline{w_c}$ | | | | |
|---|---|---|---|---|---|
| | $[0^o/90^o]$ | $[0^o/90^o]_2$ | $[0^o/90^o]_3$ | $[0^o/90^o]_4$ | $[0^o/90^o]_8$ |
| 20 | 0.2953 | 0.2278 | 0.2250 | 0.2241 | 0.2232 |
| 40 | 0.4323 | 0.3769 | 0.3728 | 0.3714 | 0.3702 |
| 60 | 0.5287 | 0.4807 | 0.4758 | 0.4742 | 0.4727 |
| 80 | 0.6057 | 0.5605 | 0.5551 | 0.5533 | 0.5517 |
| 100 | 0.6725 | 0.6258 | 0.6201 | 0.6182 | 0.6165 |
| 120 | 0.7294 | 0.6815 | 0.6756 | 0.6736 | 0.6718 |
| 140 | 0.7791 | 0.7304 | 0.7242 | 0.7221 | 0.7202 |
| 160 | 0.8236 | 0.7740 | 0.7676 | 0.7655 | 0.7636 |
| 180 | 0.8639 | 0.8136 | 0.8071 | 0.8049 | 0.8029 |
| 200 | 0.9009 | 0.8500 | 0.8433 | 0.8411 | 0.8390 |

*Subscripted values 2, 3, 4, and 8: No. of the arrangements of a two layered laminate.*

**Table A.31** Number of layers effect on a simply supported (SS5) anti-symmetric angle-ply [$(45^o/-45^o)_n$] square plate under uniformly distributed loads. ($h/a$ = 0.1)

| $\bar{q}$ | $\overline{w_c}$ | | | | |
|---|---|---|---|---|---|
| | $[0^o/90^o]$ | $[0^o/90^o]_2$ | $[0^o/90^o]_3$ | $[0^o/90^o]_4$ | $[0^o/90^o]_8$ |
| 20 | 0.2160 | 0.1637 | 0.1583 | 0.1565 | 0.1549 |
| 40 | 0.3715 | 0.3009 | 0.2926 | 0.2899 | 0.2875 |
| 60 | 0.4841 | 0.4103 | 0.4010 | 0.3979 | 0.3951 |
| 80 | 0.5721 | 0.4993 | 0.4897 | 0.4865 | 0.4835 |
| 100 | 0.6446 | 0.5740 | 0.5644 | 0.5611 | 0.5582 |
| 120 | 0.7067 | 0.6384 | 0.6289 | 0.6257 | 0.6228 |
| 140 | 0.7612 | 0.6953 | 0.6859 | 0.6827 | 0.6798 |
| 160 | 0.8101 | 0.7462 | 0.7370 | 0.7339 | 0.7310 |
| 180 | 0.8544 | 0.7924 | 0.7834 | 0.7804 | 0.7775 |
| 200 | 0.8952 | 0.8349 | 0.8260 | 0.8231 | 0.8203 |

*Subscripted values 2, 3, 4, and 8: No. of the arrangements of a two layered laminate.*

**Table A.32** Effect of material anisotropy on the non-dimensionalized center deflections of a four layered symmetric cross-ply and angle-ply clamped laminates (CC5) under uniform lateral load ($\bar{q}$=100.0, *h/a* = 0.1)

| $E_1/E_2$ | $\overline{w_c}$ | |
|---|---|---|
| | [0º/90º/90º/0º] | [45º/-45º/-45º/45º] |
| 2 | 0.8211 | 0.8318 |
| 4 | 0.6574 | 0.6882 |
| 6 | 0.5631 | 0.6006 |
| 8 | 0.5015 | 0.5408 |
| 10 | 0.4580 | 0.4970 |
| 12 | 0.4254 | 0.4633 |
| 14 | 0.4000 | 0.4364 |
| 20 | 0.3485 | 0.3804 |
| 25 | 0.3210 | 0.3498 |
| 30 | 0.3010 | 0.3273 |
| 35 | 0.2876 | 0.3099 |
| 40 | 0.2732 | 0.2959 |
| 45 | 0.2631 | 0.2845 |
| 50 | 0.2545 | 0.2748 |

**Table A.33** Effect of material anisotropy on the non-dimensionalized center deflections of a four layered symmetric cross-ply and angle-ply simply supported laminates (SS5) under uniform lateral load ($\bar{q}$=100.0, *h/a* = 0.1)

| $E_1/E_2$ | $\overline{w_c}$ | |
|---|---|---|
| | [0º/90º/90º/0º] | [45º/-45º/-45º/45º] |
| 2 | 1.1114 | 1.1128 |
| 4 | 0.9424 | 0.9397 |
| 6 | 0.8362 | 0.8272 |
| 8 | 0.7610 | 0.7466 |
| 10 | 0.7041 | 0.6851 |
| 12 | 0.6589 | 0.6362 |
| 14 | 0.6218 | 0.5962 |
| 20 | 0.5410 | 0.5098 |
| 25 | 0.4944 | 0.4609 |
| 30 | 0.4589 | 0.4242 |
| 35 | 0.4306 | 0.3955 |
| 40 | 0.4076 | 0.3724 |
| 45 | 0.3883 | 0.3534 |
| 50 | 0.3718 | 0.3374 |

**Table A.34** Effects of fiber orientation θ on the deflection of a simply supported square plate ($\bar{q}$ = 120.0, *h/a* = 0.1)

| θ | $\overline{w_c}$ | | | |
|---|---|---|---|---|
| | SS2 | SS3 | SS4 | SS5 |
| 0 | 1.3706 | 1.2346 | 0.6511 | 0.6513 |
| 5 | 1.3671 | 1.2274 | 0.6655 | 0.6537 |
| 10 | 1.3560 | 1.2074 | 0.7011 | 0.6606 |
| 15 | 1.3359 | 1.1769 | 0.7434 | 0.6713 |
| 20 | 1.3070 | 1.1366 | 0.7805 | 0.6843 |
| 25 | 1.2752 | 1.0876 | 0.8060 | 0.6979 |
| 30 | 1.2438 | 1.0321 | 0.8173 | 0.7101 |
| 35 | 1.2129 | 0.9745 | 0.8161 | 0.7194 |
| 40 | 1.1898 | 0.9259 | 0.8089 | 0.7249 |
| 45 | 1.1815 | 0.9056 | 0.8049 | 0.7267 |
| 50 | 1.1898 | 0.9259 | 0.8089 | 0.7249 |
| 55 | 1.2129 | 0.9745 | 0.8161 | 0.7194 |
| 60 | 1.2438 | 1.0321 | 0.8173 | 0.7101 |
| 65 | 1.2752 | 1.0876 | 0.8060 | 0.6979 |
| 70 | 1.3070 | 1.1366 | 0.7805 | 0.6843 |
| 75 | 1.3359 | 1.1769 | 0.7434 | 0.6713 |
| 80 | 1.3560 | 1.2074 | 0.7011 | 0.6606 |
| 85 | 1.3671 | 1.2274 | 0.6655 | 0.6537 |
| 90 | 1.3706 | 1.2346 | 0.6511 | 0.6513 |

**Table A.35 Effects** of fiber orientation θ on the deflection of a clamped square plate ($\bar{q}$ = 120.0, *h/a* = 0.1)

| θ | $\overline{w_c}$ | | | | |
|---|---|---|---|---|---|
| | CC1 | CC2 | CC3 | CC4 | CC5 |
| 0 | 0.5895 | 0.5815 | 0.4713 | 0.4709 | 0.4708 |
| 5 | 0.5920 | 0.5835 | 0.4789 | 0.4778 | 0.4730 |
| 10 | 0.5995 | 0.5896 | 0.4985 | 0.4952 | 0.4793 |
| 15 | 0.6110 | 0.5992 | 0.5242 | 0.5173 | 0.4895 |
| 20 | 0.6254 | 0.6106 | 0.5514 | 0.5400 | 0.5027 |
| 25 | 0.6419 | 0.6212 | 0.5764 | 0.5606 | 0.5178 |
| 30 | 0.6584 | 0.6279 | 0.5960 | 0.5769 | 0.5331 |
| 35 | 0.6712 | 0.6280 | 0.6078 | 0.5871 | 0.5467 |
| 40 | 0.6788 | 0.6223 | 0.6118 | 0.5908 | 0.5561 |
| 45 | 0.6813 | 0.6183 | 0.6122 | 0.5913 | 0.5594 |
| 50 | 0.6788 | 0.6223 | 0.6118 | 0.5908 | 0.5561 |
| 55 | 0.6712 | 0.6280 | 0.6078 | 0.5871 | 0.5467 |
| 60 | 0.6584 | 0.6279 | 0.5960 | 0.5769 | 0.5331 |
| 65 | 0.6419 | 0.6212 | 0.5764 | 0.5606 | 0.5178 |

| | | | | | |
|---|---|---|---|---|---|
| 70 | 0.6254 | 0.6106 | 0.5514 | 0.5400 | 0.5027 |
| 75 | 0.6110 | 0.5992 | 0.5242 | 0.5173 | 0.4895 |
| 80 | 0.5995 | 0.5896 | 0.4985 | 0.4952 | 0.4793 |
| 85 | 0.5920 | 0.5835 | 0.4789 | 0.4778 | 0.4730 |
| 90 | 0.5895 | 0.5815 | 0.4713 | 0.4709 | 0.4708 |

**Table A.36** Variation of central deflection $\overline{w_c}$ with a high pressure range $\bar{q}$ of a simply supported (SS4) four-layered anti-symmetric square plate of the arrangement $[\theta^o/-\theta^o/\theta^o/-\theta^o]$ with different orientations (h/a =0.2) .

| $\bar{q}$ | $\overline{w_c}$ | | | |
|---|---|---|---|---|
| | θ= 0° or 90° | θ= 15° or 75° | θ = 30° or 60° | θ= 45° |
| 20 | 0.2922 | 0.2799 | 0.2568 | 0.2466 |
| 40 | 0.4268 | 0.4209 | 0.4098 | 0.4039 |
| 60 | 0.5150 | 0.5141 | 0.5141 | 0.5135 |
| 80 | 0.5826 | 0.5853 | 0.5943 | 0.5984 |
| 100 | 0.6382 | 0.6438 | 0.6603 | 0.6685 |
| 120 | 0.6859 | 0.6940 | 0.7169 | 0.7286 |
| 140 | 0.7281 | 0.7382 | 0.7667 | 0.7816 |
| 160 | 0.7660 | 0.7779 | 0.8114 | 0.8292 |
| 180 | 0.8007 | 0.8141 | 0.8521 | 0.8725 |
| 190 | 0.8170 | 0.8311 | 0.8712 | 0.8929 |
| 200 | 0.8326 | 0.8475 | 0.8896 | 0.9124 |

**Table A.37** Variation of central deflection $\overline{w_c}$ with a high pressure range $\bar{q}$ of clamped (CC3) four-layered anti-symmetric square plate of the arrangement $[\theta^o/-\theta^o/\theta^o/-\theta^o]$ with different orientations (h/a =0.2).

| $\bar{q}$ | $\overline{w_c}$ | | | |
|---|---|---|---|---|
| | θ= 0° or 90° | θ= 15° or 75° | θ= 30° or 60° | θ= 45° |
| 20 | 0.2136 | 0.2125 | 0.2064 | 0.2003 |
| 40 | 0.3521 | 0.3553 | 0.3572 | 0.3531 |
| 60 | 0.4478 | 0.4550 | 0.4667 | 0.4668 |
| 80 | 0.5211 | 0.5317 | 0.5521 | 0.5564 |
| 100 | 0.5812 | 0.5946 | 0.6224 | 0.6307 |
| 120 | 0.6324 | 0.6483 | 0.6826 | 0.6944 |
| 140 | 0.6774 | 0.6954 | 0.7355 | 0.7505 |
| 160 | 0.7177 | 0.7376 | 0.7828 | 0.8007 |
| 180 | 0.7543 | 0.7759 | 0.8257 | 0.8464 |
| 200 | 0.7880 | 0.8111 | 0.8652 | 0.8883 |

**Table A.38** Central deflection of a two layer anti-symmetric cross-ply simply supported in-plane fixed (SS5) rectangular plate under uniform pressure ($b/a$ = 5.0, $h/a$ = 0.1)

| $\bar{q}$ | $\overline{w_1}$ [0°/90°] | $\overline{w_2}$ [90°/0°] | $\overline{w_0}$ ($B_{ij}$ =0) | %S(1) | %S(2) | %S(3) |
|---|---|---|---|---|---|---|
| 20 | 0.7051 | 0.2860 | 0.3387 | 108.2 | -15.6 | 146.5 |
| 25 | 0.7599 | 0.3260 | 0.3879 | 95.9 | -16.0 | 133.1 |
| 30 | 0.8052 | 0.3616 | 0.4303 | 87.1 | -16.0 | 122.9 |
| 35 | 0.8442 | 0.3931 | 0.4677 | 80.5 | -16.0 | 114.8 |
| 40 | 0.8787 | 0.4221 | 0.5013 | 75.3 | -15.8 | 108.2 |
| 50 | 0.9380 | 0.4738 | 0.5599 | 67.5 | -15.4 | 98.0 |
| 60 | 0.9884 | 0.5191 | 0.6103 | 62.0 | -14.9 | 90.4 |
| 70 | 1.0325 | 0.5597 | 0.6546 | 57.7 | -14.5 | 84.5 |
| 80 | 1.0721 | 0.5966 | 0.6945 | 54.4 | -14.1 | 79.7 |
| 100 | 1.1412 | 0.6620 | 0.7641 | 49.4 | -13.4 | 72.4 |
| 120 | 1.2007 | 0.7192 | 0.8241 | 45.7 | -12.7 | 66.9 |
| 140 | 1.2534 | 0.7702 | 0.8772 | 42.9 | -12.2 | 62.7 |
| 160 | 1.3009 | 0.8166 | 0.9250 | 40.6 | -11.7 | 59.5 |
| 180 | 1.3444 | 0.8592 | 0.9686 | 39.8 | -11.3 | 65.5 |
| 200 | 1.3846 | 0.8988 | 1.0089 | 37.2 | -10.9 | 54.1 |

S(1):$100 \times (\overline{w_1} - \overline{w_0})/\overline{w_0}$

S(2):$100 \times (\overline{w_2} - \overline{w_0})/\overline{w_0}$

S(3):$100 \times (\overline{w_1} - \overline{w_2})/\overline{w_2}$

**Table A.39** Central deflection of a two layer anti-symmetric angle-ply simply supported in-plane fixed (SS5) rectangular plate under uniform pressure ($b/a$ = 5.0, $h/a$ = 0.1 )

| $\bar{q}$ | $\overline{w_1}$ [45°/-45°] = $\overline{w_2}$ [-45°/45°] | $\overline{w_0}$ ($B_{ij}$ =0) | %S(1)= %S(2) | %S(3) |
|---|---|---|---|---|
| 20 | 0.4788 | 0.4503 | 6.3 | 0.0 |
| 25 | 0.5348 | 0.5082 | 5.2 | 0.0 |
| 30 | 0.5827 | 0.5578 | 4.5 | 0.0 |
| 35 | 0.6250 | 0.6013 | 3.9 | 0.0 |
| 40 | 0.6629 | 0.6404 | 3.5 | 0.0 |
| 50 | 0.7292 | 0.7084 | 2.9 | 0.0 |
| 60 | 0.7863 | 0.7669 | 2.5 | 0.0 |
| 70 | 0.8367 | 0.8184 | 2.2 | 0.0 |
| 80 | 0.8821 | 0.8648 | 2.0 | 0.0 |
| 100 | 0.9618 | 0.9459 | 1.7 | 0.0 |
| 120 | 1.0308 | 1.0160 | 1.5 | 0.0 |
| 140 | 1.0919 | 1.0780 | 1.3 | 0.0 |

| | | | | |
|---|---|---|---|---|
| 160 | 1.1472 | 1.1340 | 1.2 | 0.0 |
| 180 | 1.1978 | 1.1852 | 1.1 | 0.0 |
| 200 | 1.2445 | 1.2324 | 1.0 | 0.0 |

S(1):$100 \times (\overline{w_1} - \overline{w_0})/\overline{w_0}$

S(2):$100 \times (\overline{w_2} - \overline{w_0})/\overline{w_0}$

S(3):$100 \times (\overline{w_1} - \overline{w_2})/\overline{w_2}$

**Table A.40** Central deflection of a two layer anti-symmetric cross-ply and angle-ply simply supported in-plane fixed (SS5) rectangular plate under uniform pressure and with different aspect ratios ( $h/a$ = 0.1, $\overline{q}$ =200.0)

| $b/a$ | $\overline{w}$ | |
|---|---|---|
| | [0º/90$^0$] | [45º/-45$^0$] |
| 5.00 | 1.3846 | 1.2445 |
| 4.00 | 1.3848 | 1.2448 |
| 3.00 | 1.3854 | 1.2431 |
| 2.50 | 1.3838 | 1.2370 |
| 2.00 | 1.3679 | 1.2145 |
| 1.90 | 1.3594 | 1.2055 |
| 1.80 | 1.3473 | 1.1940 |
| 1.75 | 1.3395 | 1.1871 |
| 1.70 | 1.3303 | 1.1793 |
| 1.60 | 1.3067 | 1.1606 |
| 1.55 | 1.2919 | 1.1494 |
| 1.50 | 1.2745 | 1.1369 |
| 1.45 | 1.2544 | 1.1227 |
| 1.40 | 1.2311 | 1.1069 |
| 1.35 | 1.2044 | 1.0891 |
| 1.30 | 1.1740 | 1.0693 |
| 1.25 | 1.1394 | 1.0471 |
| 1.20 | 1.1006 | 1.0225 |
| 1.00 | 0.9009 | 0.8952 |

**Table A.41** Variations of center deflection $\overline{w_c}$ with load, $\overline{q}$ of simply supported (SS1) and (SS5), and clamped (CC5) thin isotropic plates ($h/a$ = 0.02, $v$ = 0.3)

| $\overline{q}$ | $\overline{w_c}$ | | |
|---|---|---|---|
| | SS1 | SS5 | CC5 |
| 10 | 0.4763 | 0.3688 | 0.1301 |
| 20 | 0.8582 | 0.5846 | 0.2576 |
| 30 | 1.1647 | 0.7310 | 0.3754 |
| 40 | 1.4192 | 0.8200 | 0.4803 |
| 50 | 1.6382 | 0.9351 | 0.5728 |

| | | | |
|---|---|---|---|
| 60 | 1.8318 | 1.0138 | 0.6548 |
| 70 | 2.0065 | 1.0828 | 0.7281 |
| 80 | 2.1662 | 1.1447 | 0.7943 |
| 90 | 2.3210 | 1.2010 | 0.8546 |
| 100 | 2.4692 | 1.2527 | 0.9101 |

**Table A.42** Variation of central deflection $\overline{w_c}$ with pressure $\bar{q}$ of a simply supported (SS2) four-layered anti-symmetric and symmetric cross-ply and angle-ply square plate ($h/a$ = 0.1)

| $\bar{q}$ | $\overline{w_c}$ | | | |
|---|---|---|---|---|
| | [0º/ 90º/0º/ 90º] | [0º/ 90º/90º/ 0º] | [45º/ -45º/45º/ -45º] | [45º/ -45º/-45º/ 45º] |
| 10 | 0.1410 | 0.1299 | 0.0900 | 0.0934 |
| 20 | 0.2792 | 0.2577 | 0.1794 | 0.1862 |
| 30 | 0.4142 | 0.3814 | 0.26278 | 0.2777 |
| 40 | 0.5382 | 0.4999 | 0.3548 | 0.3674 |
| 50 | 0.6570 | 0.6126 | 0.4399 | 0.4548 |
| 60 | 0.7685 | 0.7192 | 0.5229 | 0.5398 |
| 70 | 0.8730 | 0.8200 | 0.6038 | 0.6221 |
| 80 | 0.9713 | 0.9154 | 0.6824 | 0.7016 |
| 90 | 1.0637 | 1.0057 | 0.7587 | 0.7785 |
| 100 | 1.1511 | 1.0915 | 0.8327 | 0.8528 |

**Table A.43** Variation of central deflection $\overline{w_c}$ with pressure $\bar{q}$ of clamped (CC2) four-layered anti-symmetric and symmetric cross-ply and angle-ply square plate ($h/a$ = 0.1)

| $\bar{q}$ | $\overline{w_c}$ | | | |
|---|---|---|---|---|
| | [0º/ 90º/0º/ 90º] | [0º/ 90º/90º/ 0º] | [45º/ -45º/45º/ -45º] | [45º/ -45º/-45º/ 45º] |
| 10 | 0.0450 | 0.0457 | 0.0478 | 0.0499 |
| 20 | 0.0900 | 0.0913 | 0.0954 | 0.0997 |
| 30 | 0.1349 | 0.1368 | 0.1426 | 0.1489 |
| 40 | 0.1797 | 0.1822 | 0.1891 | 0.1971 |
| 50 | 0.2243 | 0.2274 | 0.2346 | 0.2441 |
| 60 | 0.2686 | 0.2724 | 0.2787 | 0.2895 |
| 70 | 0.3126 | 0.3169 | 0.3214 | 0.3331 |
| 80 | 0.3563 | 0.3611 | 0.3625 | 0.3749 |
| 90 | 0.3995 | 0.4048 | 0.4021 | 0.4149 |
| 100 | 0.4422 | 0.4479 | 0.4400 | 0.4532 |

# Appendix (B)
# Graphs

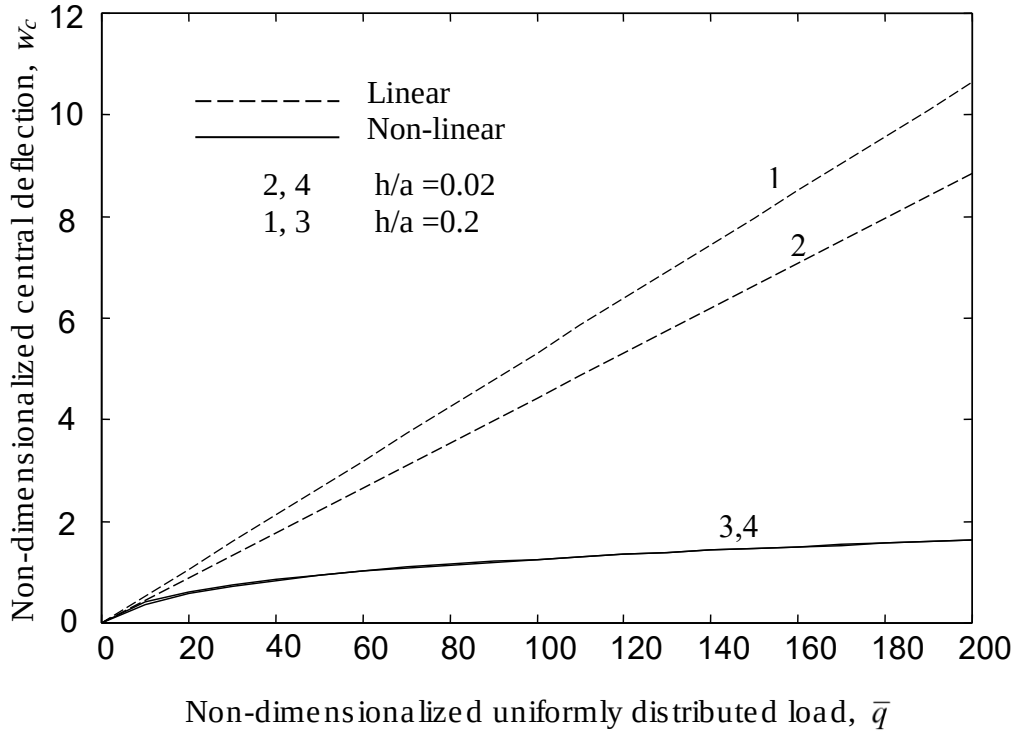


**Fig. B.1** Variation of central deflection, $\overline{w}_c$ with load, $\bar{q}$ of thin (h/a =0.02) and thick (h/a =0.2) simply supported (SS5) square isotropic plate.

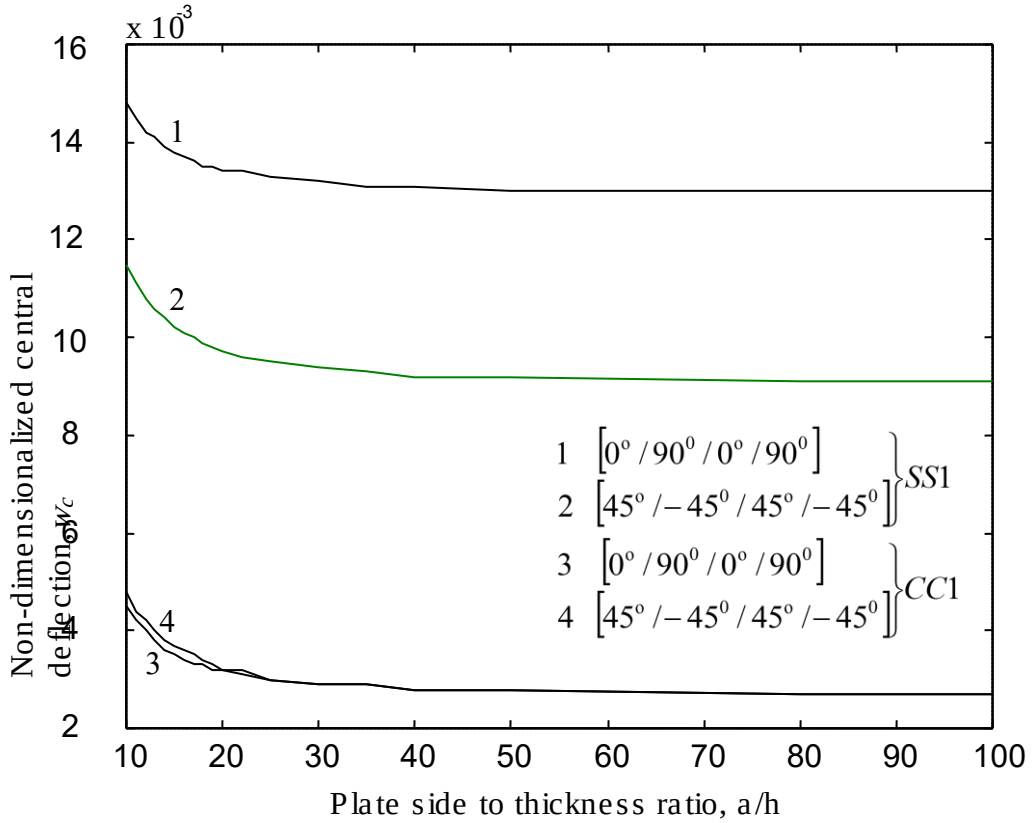


**Fig. B.2** A comparison of center deflections versus side to thickness ratio of anti-symmetric cross-ply and angle-ply square laminates under uniform lateral load ( $\bar{q}$ =1.0 ).

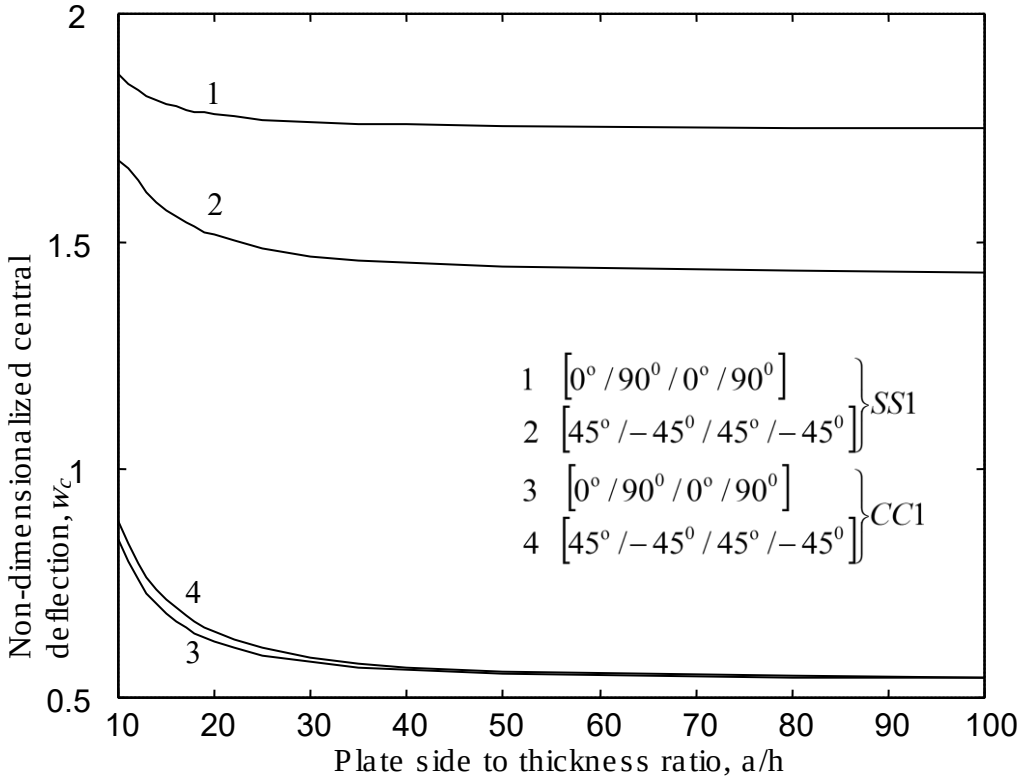


**Fig. B.3** A comparison of center deflections versus side to thickness ratio of anti-symmetric cross-ply and angle-ply square laminates under uniform lateral load ($\bar{q}$ =200.0).

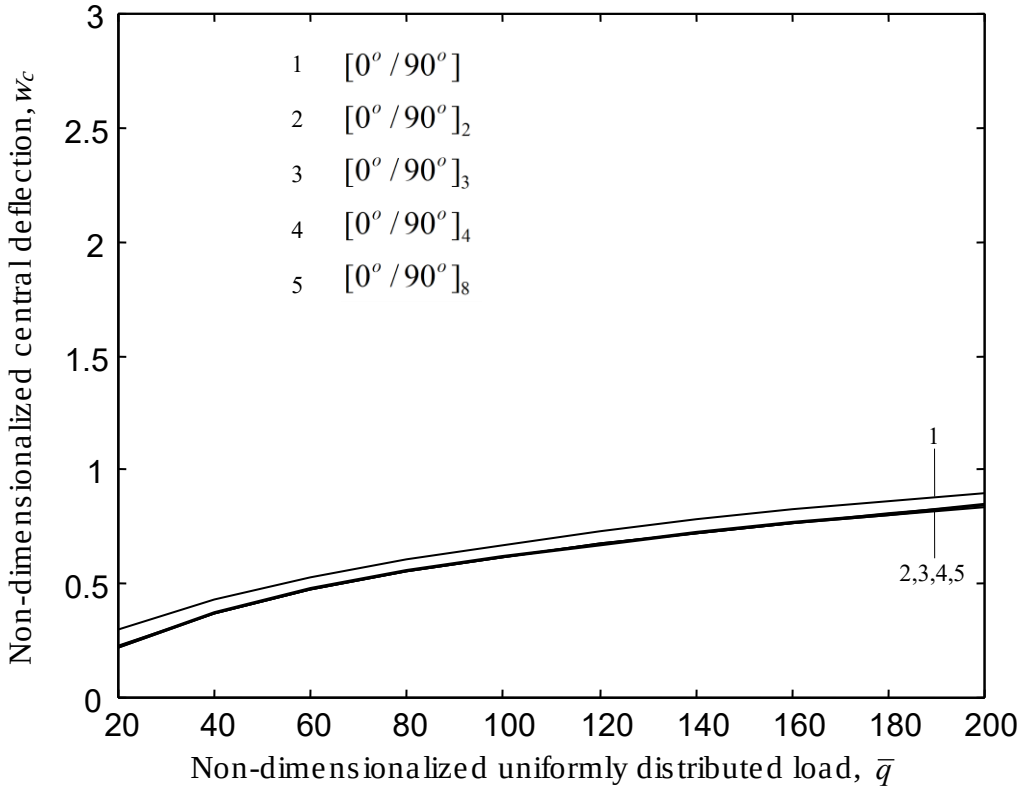


**Fig. B.4** Number of layers effect on a simply supported (SS5) antisymmetric cross-ply [$(0^o/90^o)_n$] square plate under uniformly distributed loads ( $h/a$ = 0.1).

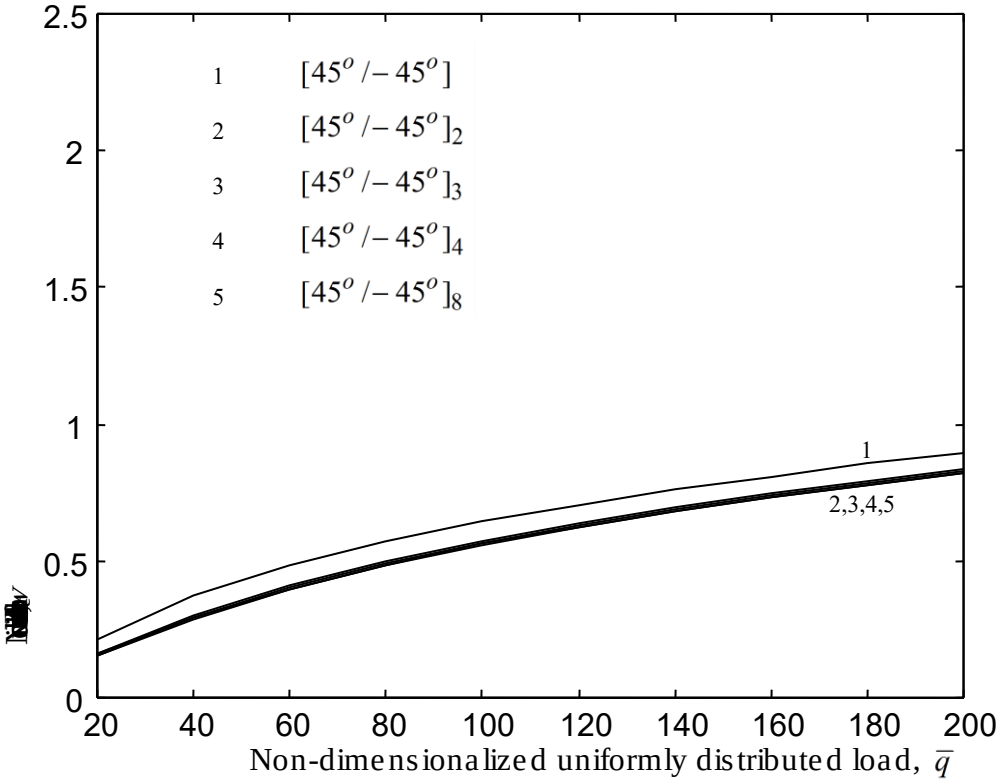


**Fig. B.5** Number of layers effect on a simply supported (SS5) antisymmetric a angle-ply [$(45^o / -45^o)_n$] square plate under uniformly distributed loads ($h/a$ = 0.1).

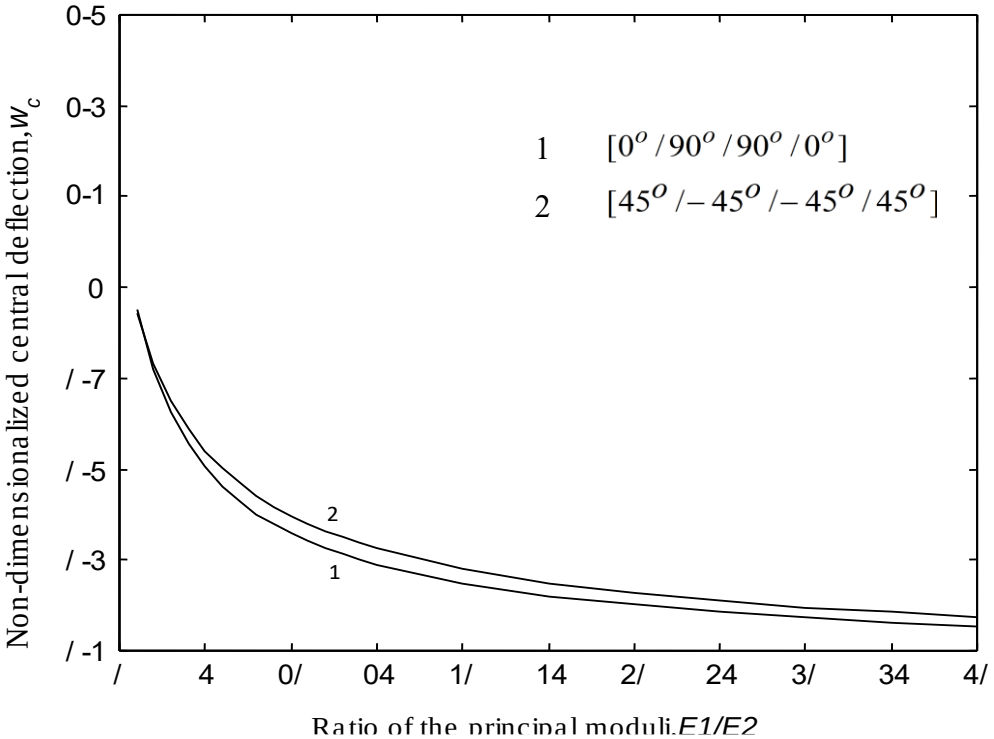


**Fig. B.6** Effect of material anisotropy on the non-dimensionalized Centre deflections of a four layered symmetric cross-ply and angle-ply clamped laminates (CC5) under uniform lateral load ($\bar{q}$ = 100.0, $h/a$ = 0.1).

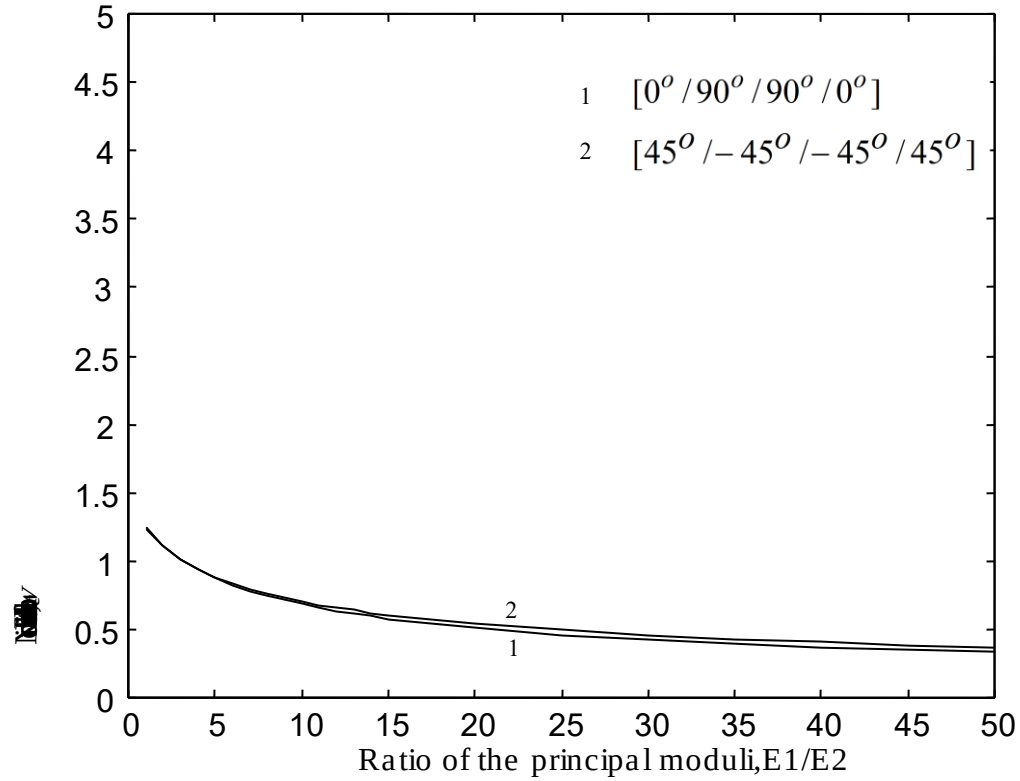


**Fig. B.7** Effect of material anisotropy on the non-dimensionalized center deflections of a four layered symmetric cross-ply and angle-ply simply supported laminates (SS5) under uniform lateral load ($\bar{q}$ = 100.0, *h/a* = 0.1).

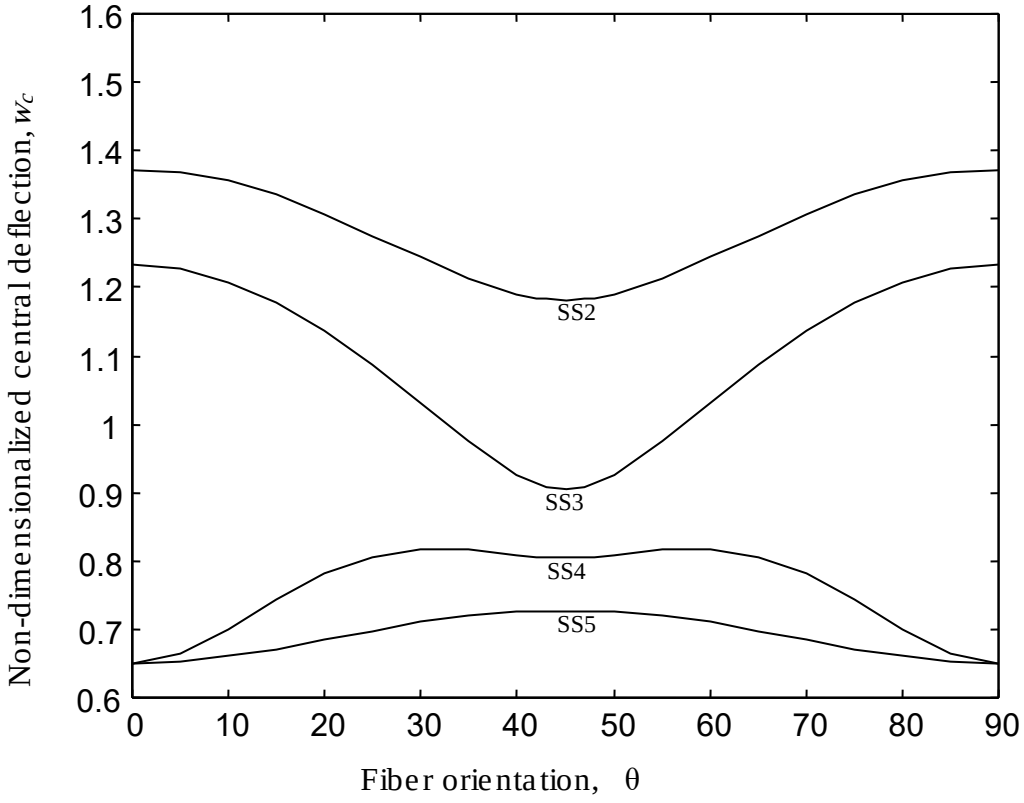


**Fig. B.8** Effects of fiber orientation, θ on the deflection of a simply supported square plate ($\bar{q}$ = 120.0, *h/a* = 0.1).

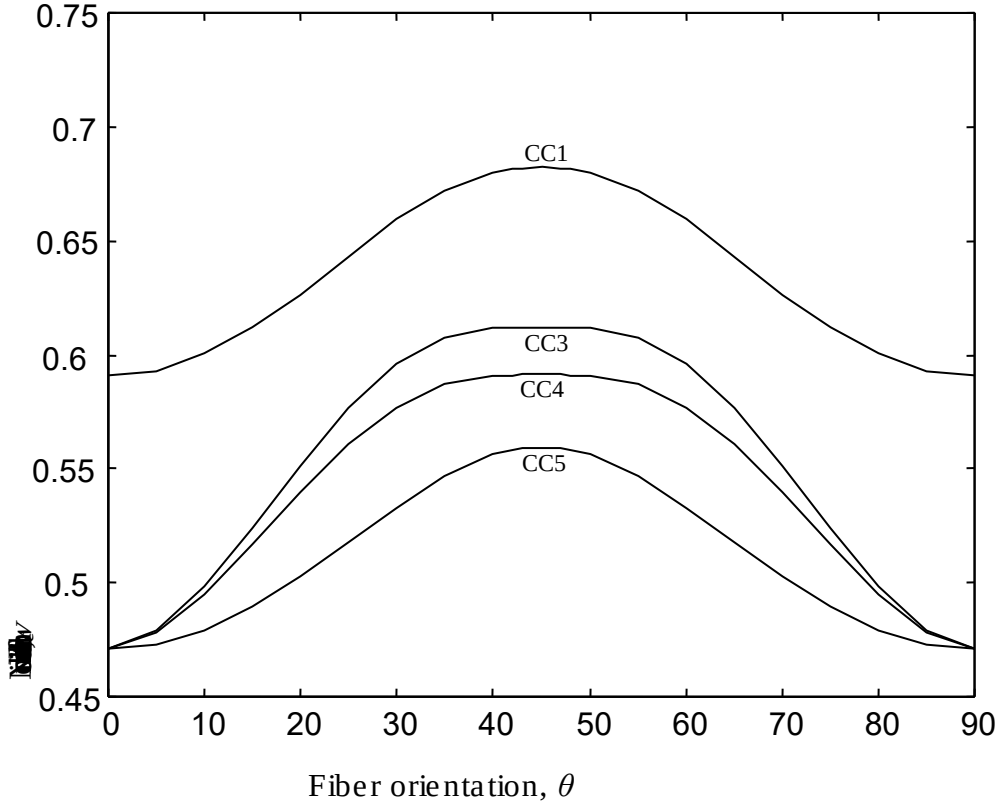


**Fig. B.9** Effects of fiber orientation, θ on the deflection of a clamped square plate ($\bar{q}$ =120.0, *h/a* = 0.1).

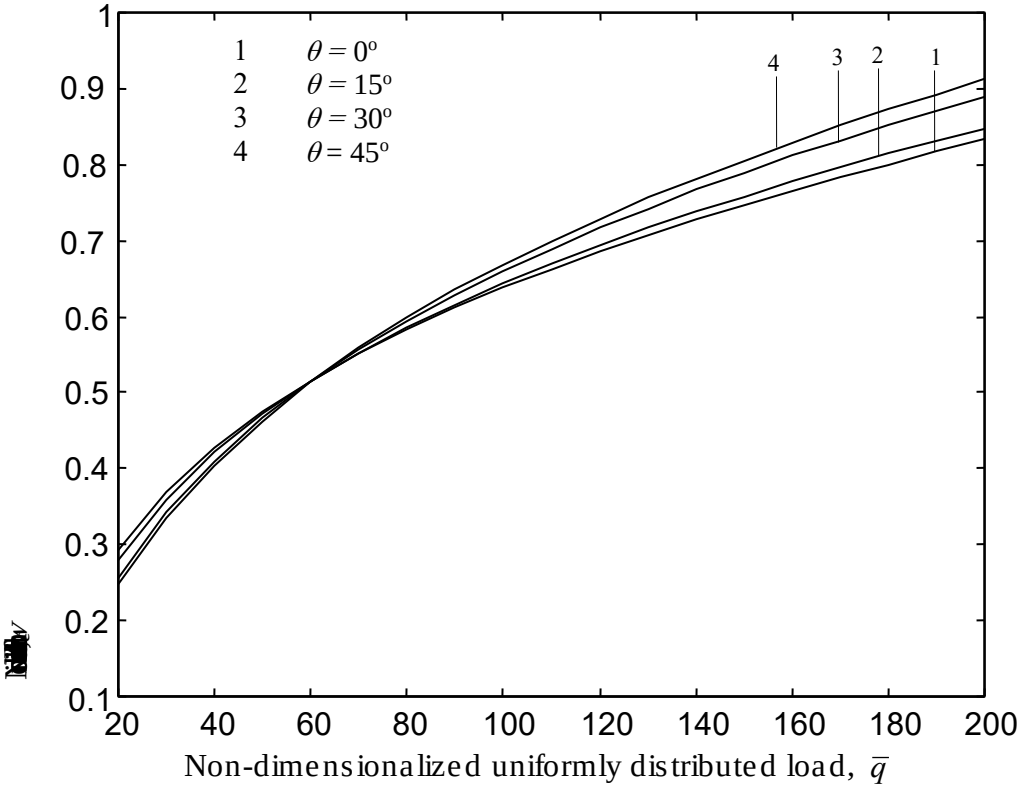


**Fig. B.10** Variation of central deflection, $\bar{w}_c$ with pressure, $\bar{q}$ of simply supported (SS4) antisymmetric square plate with different orientations (h/a =0.2)

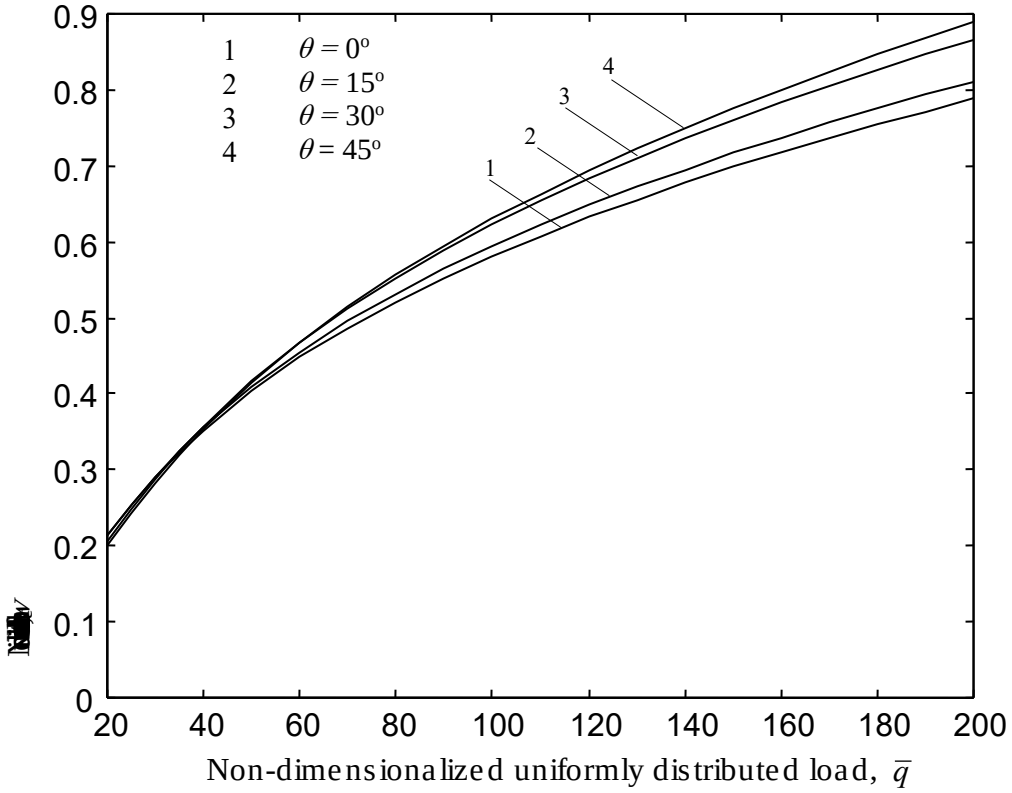


**Fig. B.11** Variation of central deflection, $\overline{w}_c$ with pressure, $\overline{q}$ of clamped (CC3) antisymmetric square plate with different orientations (h/a = 0.2).

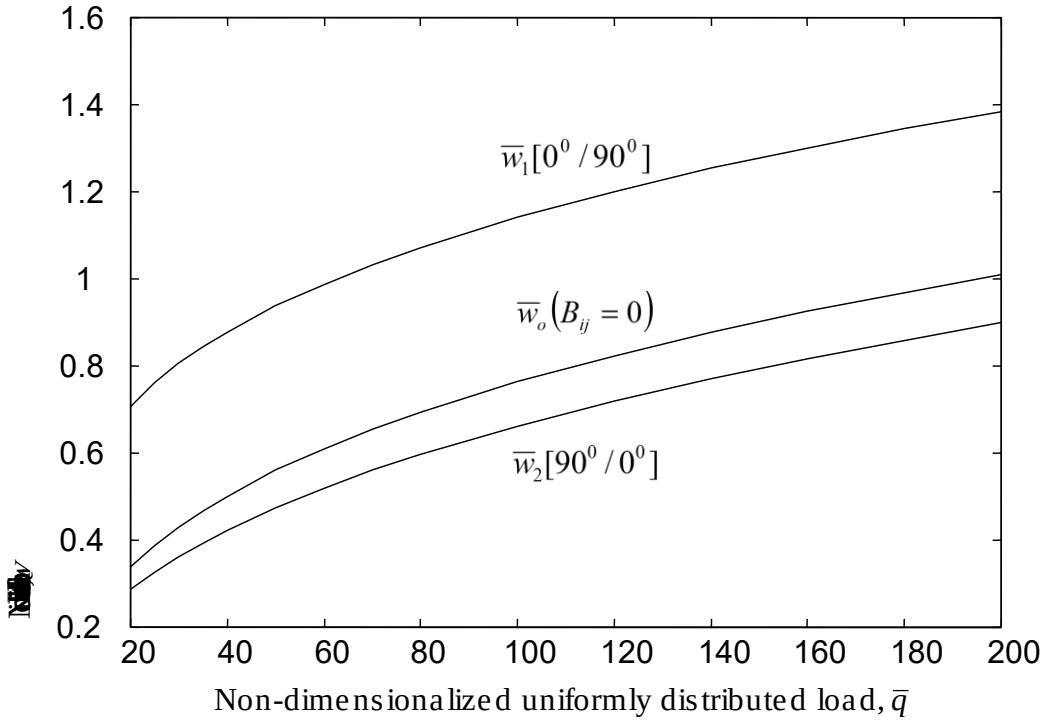


**Fig. B.12** Central deflection of a two layer antisymmetric cross-ply simply supported (SS5) rectangular plate under uniform pressure (*b/a* = 5.0, *h/a* = 0.1).

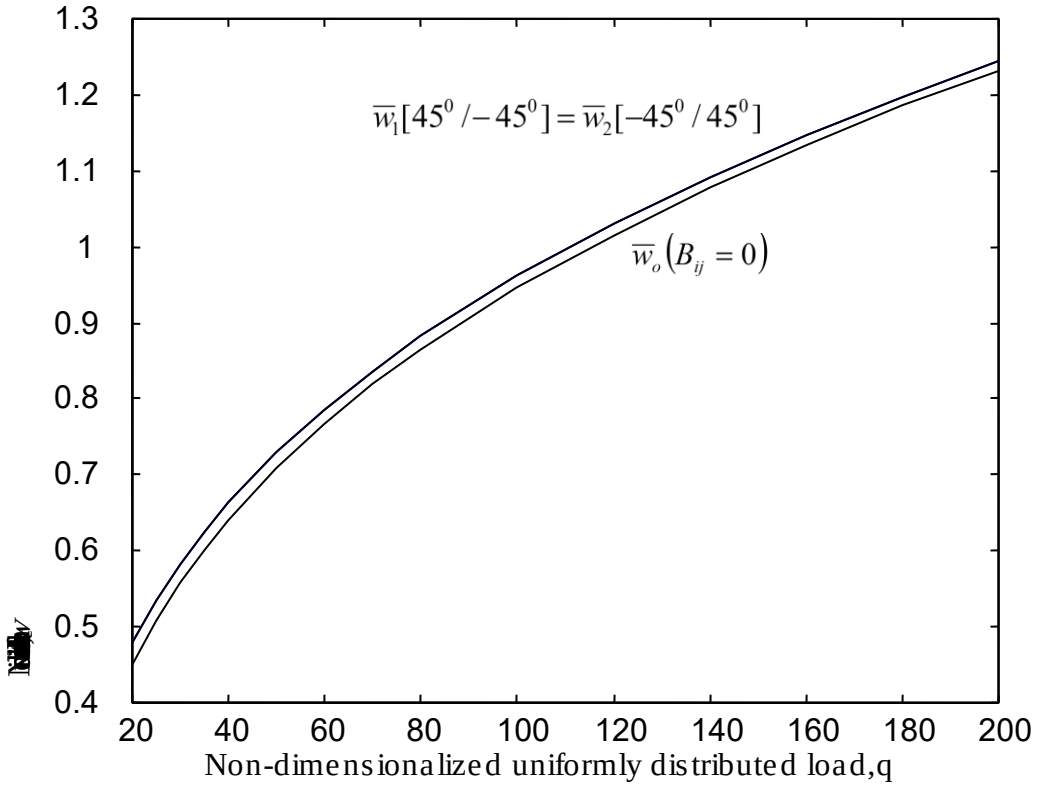


**Fig. B.13** Central deflection of a two layer antisymmetric angle-ply simply supported (SS5) rectangular plate under uniform pressure (*b/a* = 5.0, *h/a* = 0.1).

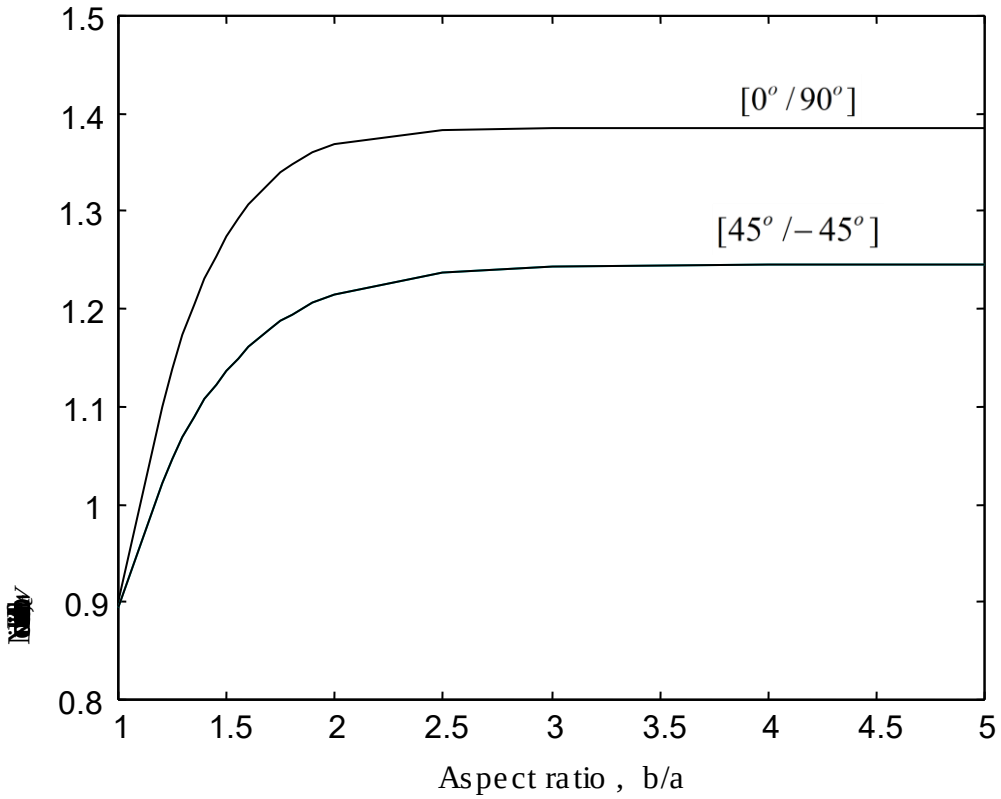


**Fig. B.14** Central deflection of a two layer antisymmetric cross-ply and angle-ply simply supported (SS5) rectangular plate under uniform pressure and with different aspect ratios (*h/a* = 0.1, $\bar{q}$ = 200.0).

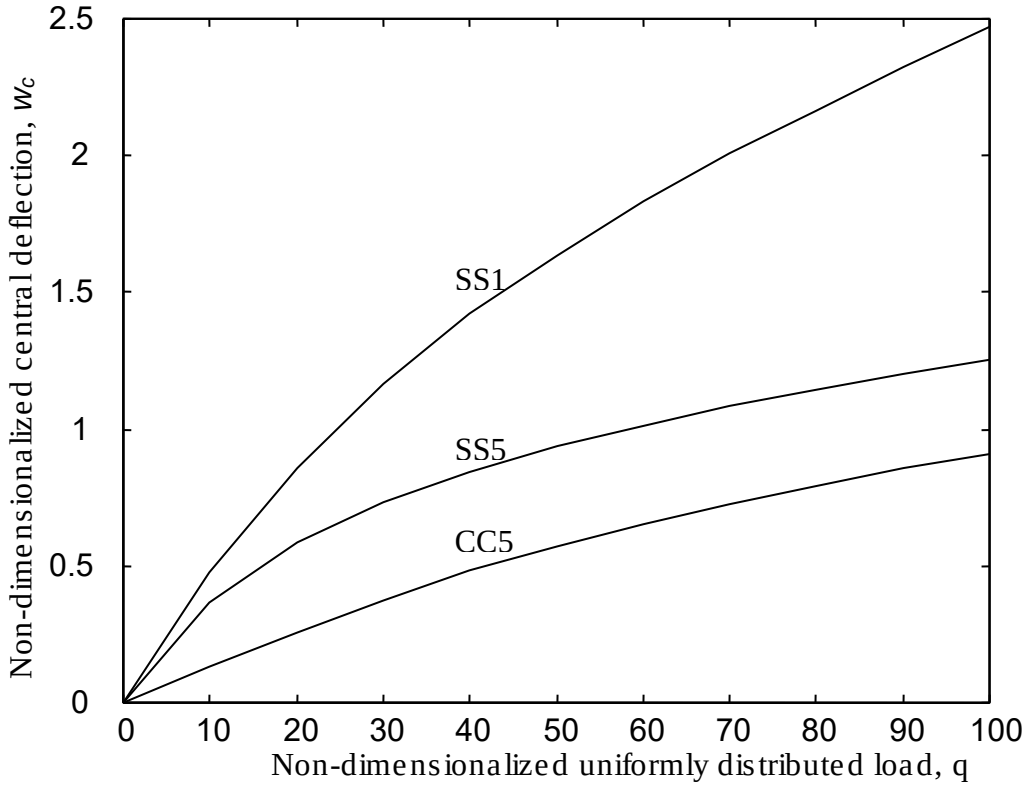


**Fig. B.15** Variations of central deflection, $\overline{w}_c$ with load, $\overline{q}$ of thin (h/a =0.02) isotropic simply supported (SS1) and (SS5), and clamped (CC5) conditions ($\nu$ = 0.3).

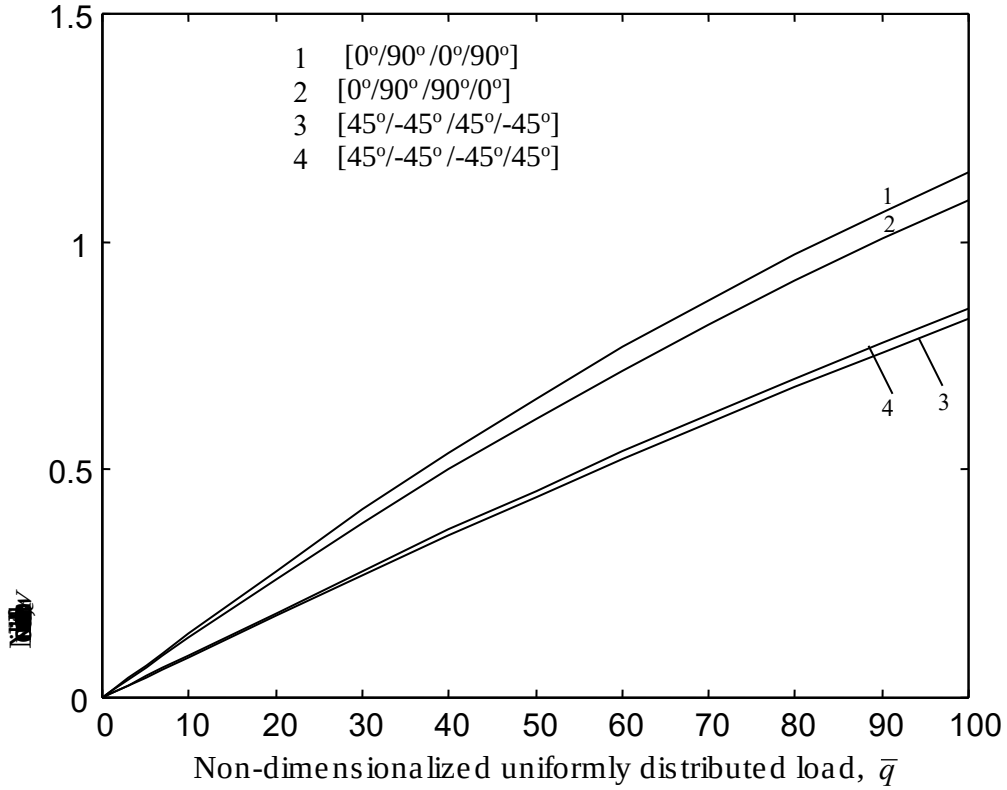


**Fig. B.16** Variation of $\overline{w}_c$ with pressure, $\overline{q}$ of simply supported (SS2) 4-layered anti-symmetric and symmetric cross-ply and angle-ply square laminate ($h/a$ = 0.1).

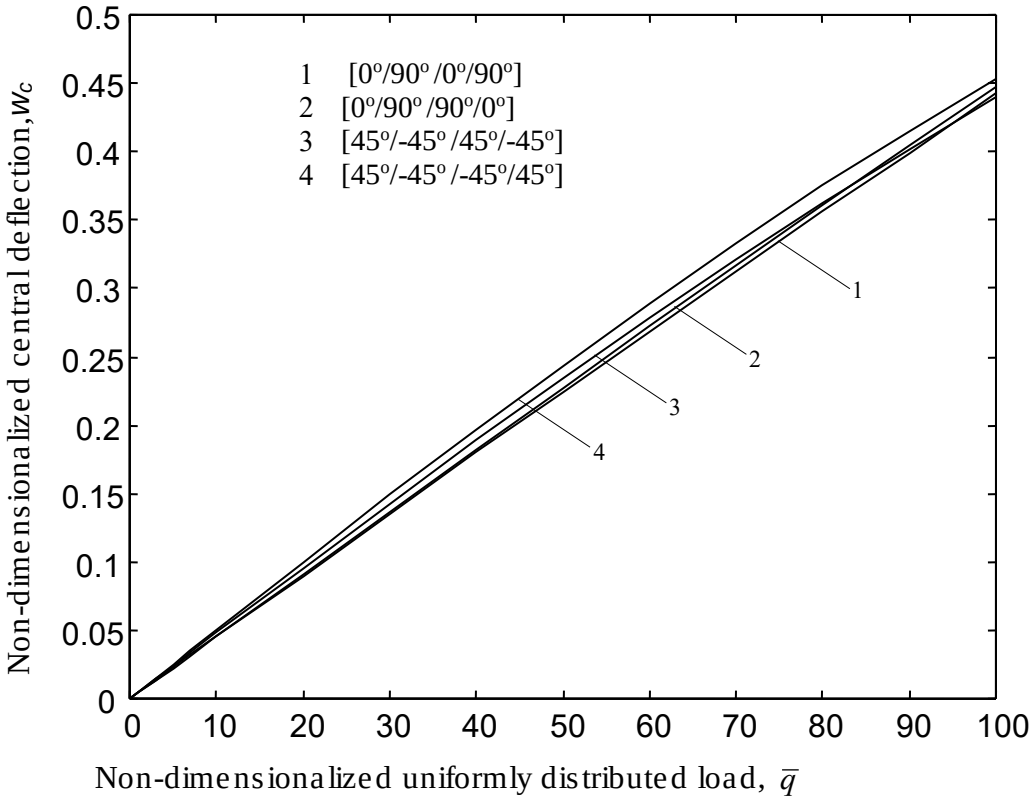


**Fig. B.17** Variation of central deflection, $\overline{w}_c$ with pressure, $\bar{q}$ of clamped (CC2) 4-layered anti-symmetric and symmetric cross-ply and angle-ply square laminate ($h/a$ = 0.1).

# Appendix (C)

# Boundary conditions

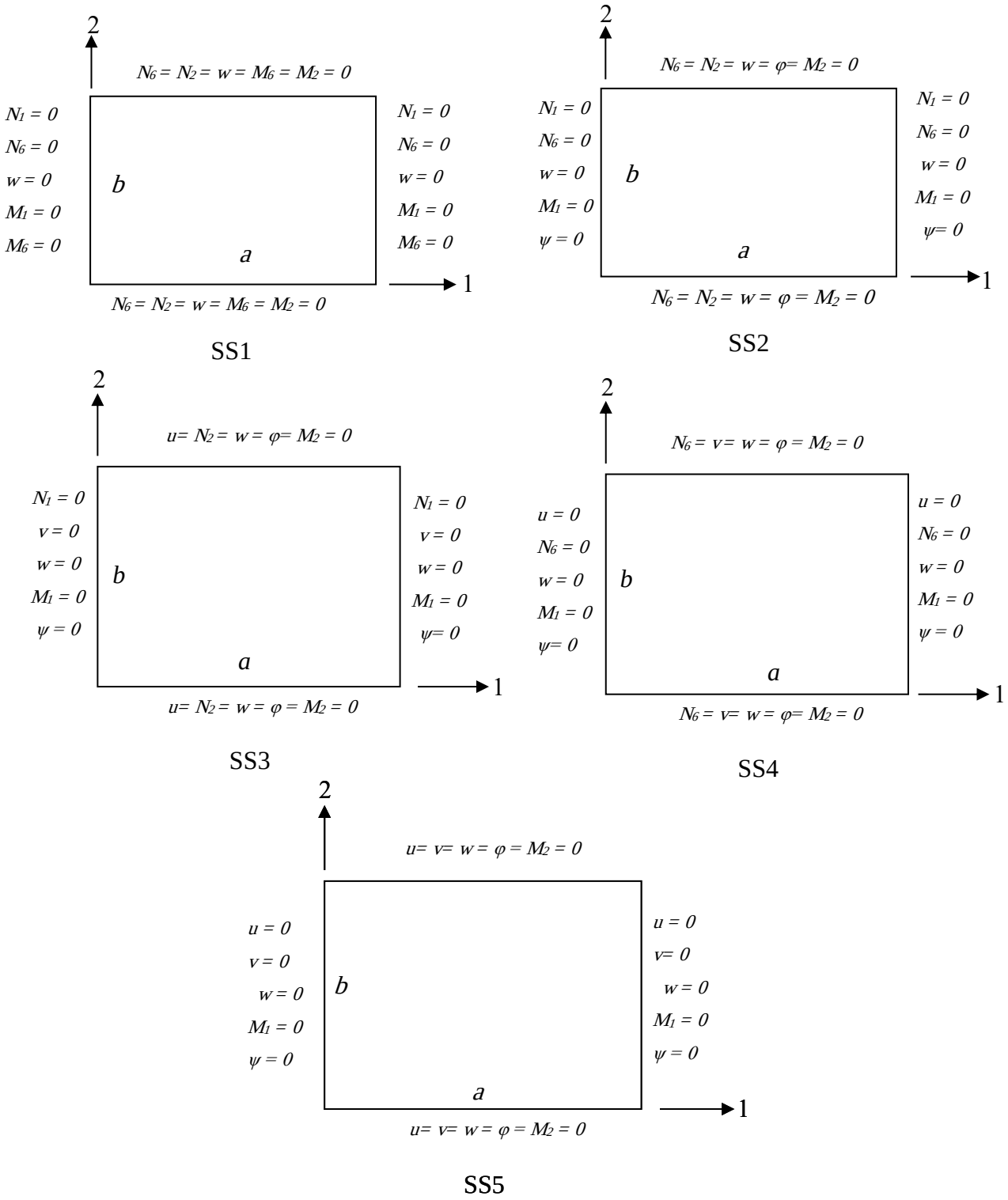


**Fig. C.1 Simply supported boundary conditions**

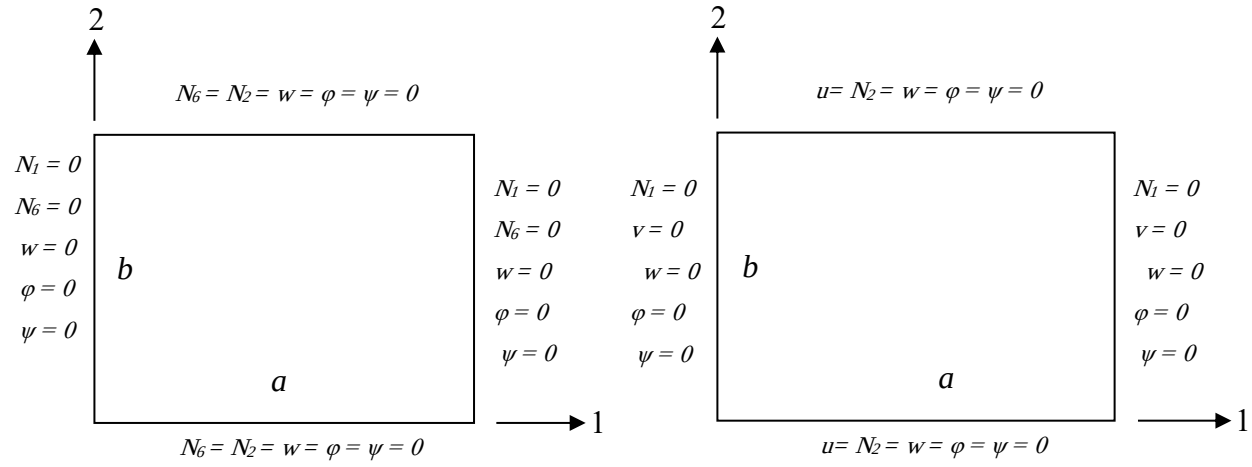


CC1




CC2

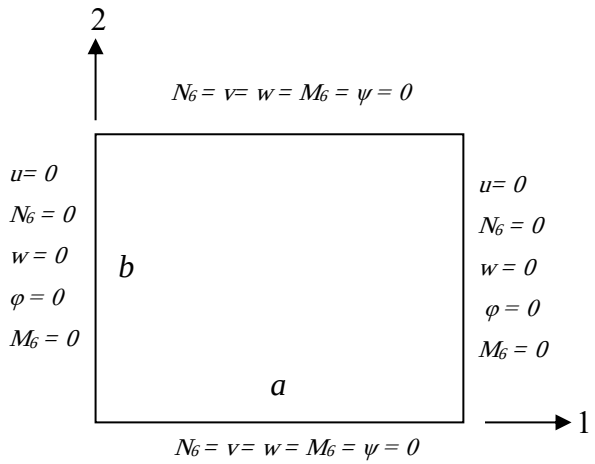


CC3

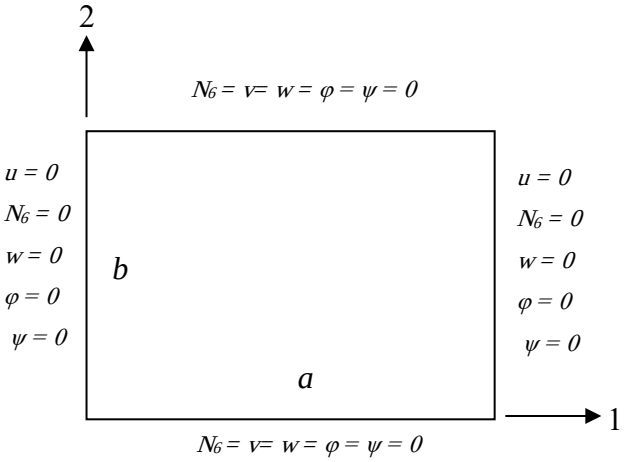


CC4

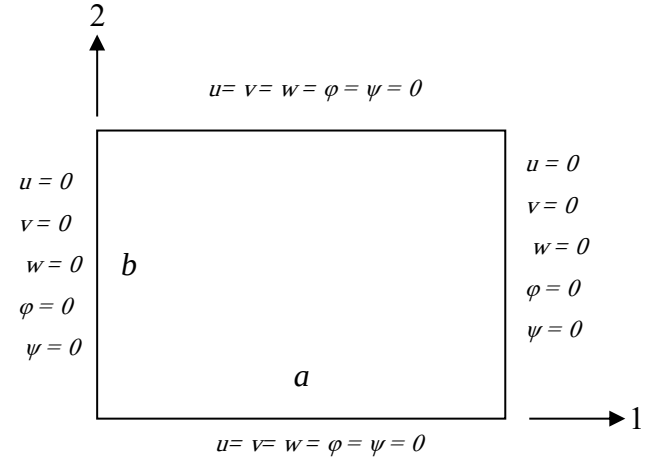


CC5

**Fig. C.2 Clamped boundary conditions**

# Appendix (D)

# Estimation of the fictitious densities

The following fictitious densities have been derived using the procedure proposed by Cassel and Hobbs [52].

With reference to Fig.3.2:

$$\rho_u(i,j)=0.25\left\{\frac{1}{2\Delta x}\left[\overline{N}_1(i+1,j)+\overline{N}_1(i-1,j)\right]+\frac{1}{2\Delta y}\left[\overline{N}_6(i,j+1)+\overline{N}_6(i,j-1)\right]\right\} \tag{D.1}$$

$$\rho_v(i,j)=0.25\left\{\frac{1}{2\Delta x}\left[\overline{N}_6(i+1,j)+\overline{N}_6(i-1,j)\right]+\frac{1}{2\Delta y}\left[\overline{N}_2(i,j+1)+\overline{N}_2(i,j-1)\right]\right\} \tag{D.2}$$

$$\begin{aligned}\rho_w(i,j)=0.25\Bigg\{&\left(\frac{a}{h}\right)^2\left(\frac{\overline{Q}_1}{\Delta x}+\frac{\overline{Q}_2}{\Delta y}\right)+\frac{4}{\Delta y^2}\left|N_2(i,j)\right|+\frac{4}{\Delta x^2}\left|N_1(i,j)\right|\\&+\frac{2}{\Delta x\Delta y}\left|N_6(i,j)\right|+\frac{\overline{N}_1(i,j)}{\Delta x^2}\left|w(i+1,j)-2w(i,j)+w(i-1,j)\right|\\&+\frac{\overline{N}_2(i,j)}{\Delta y^2}\left|w(i,j+1)-2w(i,j)+w(i,j-1)\right|\\&+\frac{\overline{N}_6(i,j)}{2\Delta x\Delta y}\left|w(i+1,j+1)-w(i-1,j+1)+w(i-1,j-1)-w(i+1,j-1)\right|\Bigg\}\end{aligned} \tag{D.3}$$

$$\begin{aligned}\rho_\phi(i,j)=0.25\Bigg\{&\frac{1}{2\Delta x}\left[\overline{M}_1(i+1,j)+\overline{M}_1(i-1,j)\right]\\&+\frac{1}{2\Delta y}\left[\overline{M}_6(i,j+1)+\overline{M}_6(i,j-1)\right]+\left(\frac{a}{h}\right)^2\overline{Q}_1(i,j)\Bigg\}\end{aligned} \tag{D.4}$$

$$\begin{aligned}\rho_\Psi(i,j)=0.25\Bigg\{&\frac{1}{2\Delta x}\left[\overline{M}_6(i+1,j)+\overline{M}_6(i-1,j)\right]\\&+\frac{1}{2\Delta y}\left[\overline{M}_2(i,j+1)+\overline{M}_2(i,j-1)\right]+\left(\frac{a}{h}\right)^2\overline{Q}_2(i,j)\Bigg\}\end{aligned} \tag{D.5}$$

Where the over lined quantities are given by:

$$\begin{aligned}\overline{N}_1(i,j)=&\frac{1}{\Delta x}\left(A_{11}+A_{16}\right)+\frac{1}{\Delta y}\left(A_{12}+A_{16}\right)+\frac{4}{\Delta x^2}B_{11}+\frac{4}{\Delta y^2}B_{12}+\frac{2}{\Delta x\Delta y}B_{16}\\&+A_{11}l_1+A_{12}l_2+A_{16}l_3\end{aligned}$$

$$\begin{aligned}\overline{N}_2(i,j)=&\frac{1}{\Delta x}\left(A_{12}+A_{26}\right)+\frac{1}{\Delta y}\left(A_{22}+A_{26}\right)+\frac{4}{\Delta x^2}B_{12}+\frac{4}{\Delta y^2}B_{22}+\frac{2}{\Delta x\Delta y}B_{26}\\&+A_{12}l_1+A_{22}l_2+A_{26}l_3\end{aligned}$$

$$\overline{N}_6(i,j)=\frac{1}{\Delta x}\left(A_{16}+A_{66}\right)+\frac{1}{\Delta y}\left(A_{26}+A_{66}\right)+\frac{4}{\Delta x^2}B_{16}+\frac{4}{\Delta y^2}B_{26}+\frac{2}{\Delta x\Delta y}B_{66}$$
$$+A_{16}l_1+A_{26}l_2+A_{66}l_3$$
$$\overline{M}_1(i,j)=\frac{1}{\Delta x}\left(B_{11}+B_{16}\right)+\frac{1}{\Delta y}\left(B_{12}+B_{16}\right)+\frac{4}{\Delta x^2}D_{11}+\frac{4}{\Delta y^2}D_{12}+\frac{2}{\Delta x\Delta y}D_{16}$$
$$+B_{11}l_1+B_{12}l_2+B_{16}l_3$$

$$\overline{M}_2(i,j)=\frac{1}{\Delta x}\left(B_{12}+B_{26}\right)+\frac{1}{\Delta y}\left(B_{22}+B_{26}\right)+\frac{4}{\Delta x^2}D_{12}+\frac{4}{\Delta y^2}D_{22}+\frac{2}{\Delta x\Delta y}D_{26}$$
$$+B_{12}l_1+B_{22}l_2+B_{26}l_3$$

$$\overline{M}_6(i,j)=\frac{1}{\Delta x}\left(B_{16}+B_{66}\right)+\frac{1}{\Delta y}\left(B_{26}+B_{66}\right)+\frac{4}{\Delta x^2}D_{16}+\frac{4}{\Delta y^2}D_{26}+\frac{2}{\Delta x\Delta y}D_{66}$$
$$+B_{16}l_1+B_{26}l_2+B_{66}l_3$$

$$\overline{Q}_1(i,j)=A_{45}\left(\frac{1}{\Delta y}+1\right)+A_{55}\left(\frac{1}{\Delta x}+1\right)$$

$$\overline{Q}_2(i,j)=A_{44}\left(\frac{1}{\Delta y}+1\right)+A_{45}\left(\frac{1}{\Delta x}+1\right)$$

And $l_1$, $l_2$ and $l_3$ are as follows:

$$l_1=\frac{1}{2\Delta x^2}\left|w(i+1,j)-w(i-1,j)\right|$$

$$l_2=\frac{1}{2\Delta y^2}\left|w(i,j+1)-w(i,j-1)\right|$$

$$l_3=\frac{1}{2\Delta x\Delta y}\left[\left|w(i+1,j)-w(i-1,j)\right|+\left|w(i,j+1)-w(i,j-1)\right|\right]$$